Università degli Studi di Firenze

DOTTORATO DI RICERCA IN
SCIENZE CHIMICHE

CICLO XXV

Coordinatore Prof. Andrea Goti

Surface plasmon resonance imaging for the detection of single nucleotide polymorphisms

Settore Scientifico Disciplinare CHIM/01

Dottorando
Maria Laura Ermini

Tutore
Prof. Maria Minunni

Anni 2010/2012

"Satisfaction does not come from the achievement of the goal but from what was learnt during the path."

Outline

In my three years of study I worked for implementing a Surface Plasmon Resonance imaging (SPRi) biosensor for improving its analytical performances in DNA-based sensing. In particular, the work was developed on two different fronts:

- The application of the biosensor was studied for the determination of single nucleotide polymorphisms (SNPs) with the ultimate goal of developing a system applicable for molecular diagnostics, directly on clinical samples, such as blood. To achieve this, the study was divided into several steps:

    1. A rational method based on computational evaluations was found for selecting probes and it was tested about the ability to predict the performance of DNA sequences as probes for the analysis SPRi. Thank to this method, it was possible a rational design of the assay for the application to the determination of SNPs.
    2. Various steps for the optimization of experimental condition and sequence characteristics were studied and the final biosensor asset for SNPs was established with synthetics oligonucleotides.

3. The developed strategy was successfully applied to real samples.

   First, it was possible to perform the direct detection (label-free) of a specific sequence present in a properly treated sample of genomic DNA. Then the strategy for the determination of SNPs was applied to samples of human genomic DNA from blood, previously amplified using an unconventional approach, different from the PCR. The sample was enriched by the random amplification of the whole genome (WGA) and it was subsequently applied on the sensor, allowing, with success, the determination of the type of base was present in the sample in the polymorphic site under investigation.

Behind this,

- the influence of nanoparticles (NPs) on SPRi system has been studied with the aim of improving the sensitivity. To obtain this result, NPs have been applied with the aim of obtaining plasmonic coupling with the surface; their behavior was compared to NPs with different plasmonic properties, size and characteristics.

  Two different approaches were studied:

  1. NPs were immobilized directly on the gold layer of the chip and further functionalized with DNA probe. Nanostructured surfaces were studied by SEM and AFM. The hybridization signals with the complementary sequence were evaluated. In particular the signal from nanostructured surfaces were compared to that from probes immobilized directly on gold and an improvement of the signal has been detected in certain conditions.
  2. NPs were used as signal enhancers, functionalized with DNA probes, in a sandwich-like assay. In this case, conventional

chips were modified with the DNA probe to hybridize a longer sequence, complementary to it at one end. Further a second probe, complementary at the other end, was used, eventually modified with NPs. NPs of different materials and shapes have been functionalized with this secondary probe, a sequence complementary at the other DNA extremity; the signal coming from this latter hybridization reaction was evaluated. An improvement in sensor performance, in terms of SPR signal, was recorded when used NPs able to resonate with plasmons of the surface.

In both cases the main system analytical performances, *i.e.* specificity, sensitivity, reproducibility, were studied and evaluated.

List of related papers

1. **M. L. Ermini**, S. Scarano, R. Bini, M. Banchelli, D. Berti, M. Mascini and M. Minunni, "A Rational Approach in Probe Design for Nucleic Acid-Based Biosensing", *Biosens. Bioelectron.*, **26**(12), 4785-4790 (2011).

2. **M. L. Ermini**, S. Mariani, S. Scarano and M. Minunni, "Direct Detection of Genomic DNA by Surface Plasmon Resonance Imaging: an Optimized Approach", *Biosens. Bioelectron.*, **40**(1), 193-199 (2012).

3. **M. L. Ermini**, S. Mariani, S. Scarano, D. Campa, R. Barale and M. Minunni, "Single Nucleotide Polymorphism Detection by Optical DNA-Based Sensing Coupled to Whole Genomic Amplification", *Anal. Bioanal. Chem.*, In press.

4. S. Mariani, **M. L. Ermini**, S. Scarano, F. Bellissima, D. Berti, M. Bonini and M. Minunni, "Nanotechnology Coupled to Biosensing: Looking for Improved Analytical Performances with Application to DNA-Based Sensing", Submitted to *J. Phys. Chem. C.*

5. **M. L. Ermini** *et al.*, "DNA Functionalized Nanoparticles for Surface Plasmon Resonance Signal Improvement". In preparation for *Adv. Funct. Mater.*

PROCEEDINGS

1. **M. L. Ermini**, S. Mariani, F. Bellissima, S. Scarano, M. Bonini and M. Minunni. "Coupling Nanotechnology to Optical Affinity Sensing: the Case of Surface Plasmon Resonance Imaging for DNA Detection". Proceedings of the 1^{st} Convegno Nazionale Sensori "Innovazione, Attualità e Prospettive", Rome, Italy, 15^{th}-17^{th} February 2012.

2. S. Scarano, **M. L. Ermini**, M. Mascini and M. Minunni, "Surface Plasmon Resonance Imaging for Affinity-Based Sensing: an Analytical Approach", Proceedings of the International Conference "Biophotonics 2011", Parma, Italy, 8^{th}-11^{th} June 2011.

3. **M. L. Ermini**, S. Scarano and M. Minunni, "Surface Nanostructuring for Surface Plasmon Resonance Imaging", Proceedings of the International Conference "Biophotonics 2011", Parma, Italy, 8^{th}-11^{th} June 2011.

Contents

1 Introduction

1.1 Surface Plasmon Resonance (SPR): Principle and Applications to Biosensing

The surface plasmon phenomenon was first recognized for optical sensing in the 1980s, used to study metal surfaces and to detect gases[1]. Then, in subsequent years it has been exploited for studying organized biomolecules multi-layers on metal surfaces[2] and numerous surface plasmon resonance (SPR) sensors have been reported[3]. Surface plasmon resonance phenomenon is widely applied as transduction principle in DNA biosensing, also for clinical diagnostic. SPR instrumentation results to be a very useful tool for DNA analysis thank to the possibility to perform real time analysis permitting to obtain fast responses. Surface plasmon resonance also has been applied combined with mass spectroscopy[4] to specifically identify compounds interacting with immobilized biomolecules after surface complex dissociation, and more recently also to find enzymes inhibitors. First, direct interactions with an immobilized enzyme is detected with SPR, then inhibition of the enzymatic action is analyzed by MS[4].

SPR imaging in particular results to be a versatile asset thank to the

possibility to work in multi-array format and to record in real time an image of the biosensor reacting surface[3]. This permit to clearly establish if unspecific interaction occur, *i.e.* control in real time reference areas and blank spots.

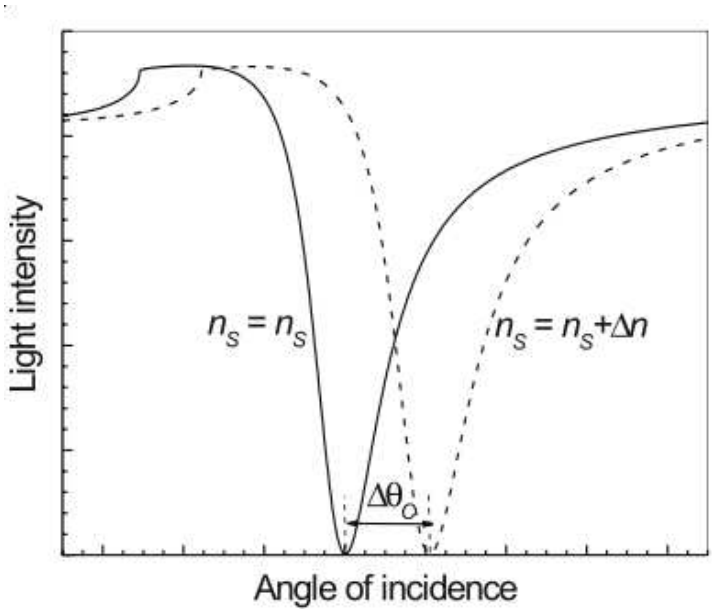

Figure 1.1: Theoretical plasmon curves plotting reflected light intensity *vs.* angle of incidence. A variation in refractive index of the medium at the gold interface causes a shift in the resonance angle[5].

For being simple, a SPR biosensor uses evanescent waves to investigate changes on the surface that occur in presence of analytes. In the Kretschmann geometry of the ATR (attenuated total reflectance) method, a high refractive index prism is covered with a thin metal film and the incident light is reflected or absorbed by the metal surface; no refraction occurs. The refractive index of the prism is higher than the refractive index of the gold so that light passed through prism reaches the metal film with the suitable characteristics to excite surface plasmons. The angle of incidence modulates the component of incident light that contributes to the evanescent wave. Thus, for a certain wavelength

the resonance condition is satisfied for a single angle of incidence, the resonant angle. When light hits the metal at this angle, a minimum of the intensity of reflected light and a maximum in the energy converted in plasmons are reached.

Plotting intensity of reflected light *vs.* the angle of incidence, the plasmon curve is obtained (Fig. 1.1). Usually it is recorded from the modified surface, with receptor immobilized. In measurements based on intensity modulation, the instrument is set to reveal light at the angle where curve has maximum slope, *i.e.* the angle where the variation of reflectivity is the highest for changes in resonance angle.

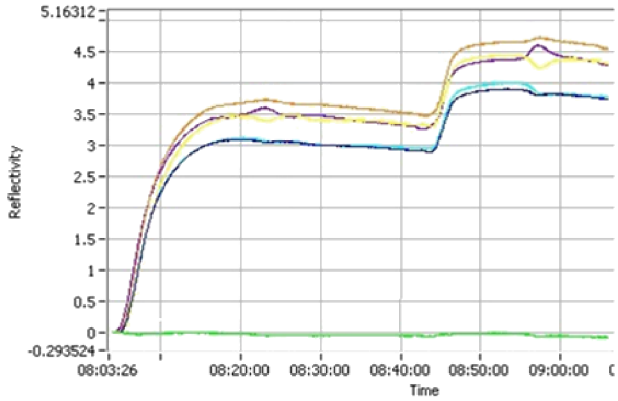

Figure 1.2: Sensorgrams recorded from sandwich-like assay using NPs. A 250 nM solution of an 84-mer sequence is first hybridized with an immobilized probe. Further it interacts with a secondary probe functionalized with silver NPs (flow 6 μl/min).

When the surface undergoes to modifications, the refractive index at the interface changes, producing an alteration of the resonance condition and a shift of the resonance angle. Thus, for a fixed angle, interactions with the receptor immobilized on the surface can be followed recording the variation of reflected light.

The signal that is considered for the measurements in an SPR biosensor

is the reflectivity variation percent versus time, reported in the sensorgram. An SPR sensorgram of a typical bio-interaction usually consists of different stages. The base line (only receptor immobilized on metal on which flows a running solution) can be recorded, and then when the analyte solution comes in contact with the receptor an association step begins. The biomolecules interact and a dynamic equilibrium state is reached, the concentration of free analyte remains constant. When the running solution flows again on the surface, dissociation step occurs: the free analyte concentration is stepped down to zero and only bound molecules remain on the surface. An example of SPR response is shown in Fig. 1.2.

1.2 Surface Plasmon Resonance imaging

SPR imaging (SPRi), also called "SPR microscopy" exploits the characteristics of SPR sensing and, in addition, gives the possibility to visualize, follow and analyze the sensing surface. SPRi represents a promising tool in biosensing thank to its highly versatility as sensing platform. SPRi has been reported for a variety of affinity systems, including DNA/DNA, DNA-binding protein, RNA aptamers/protein, antibody-antigen and carbohydrate/protein[3;6].

SPRi technology enables monitoring affinity interactions in real-time, following the SPR signal and, in the same time, recording by a CCD camera images of the chip. Different receptor can be immobilized at the same time on one chip in a multi-array asset allowing simultaneous analysis of many interactions. In this work surface functionalization was performed with the same procedure previously reported[3;7]. For each SPRi experiment here reported, the immobilization of different probes on the same gold biochip was accomplished by the use of a PDMS (polydimethylsiloxane) mask (Fig. 1.3). It permits to delimit up to 30 microwells for thiolated probe deposition on chip surface.

The possibility to exploit images analysis represents an important feature of the SPRi technology. In fact, the possibility to see in real time the sensing surface permits to gain information about surface characteristics, *i.e.* receptor deposition homogeneity, interacting areas, and on the other hand is of help in many practical aspects like presence on air bubbles or salt deposit. Thus, furthermore it's possible to control, during all the measurement time, areas where the probe is active and also to control the quality of the array. In particular, the differential image (Fig. 1.4) can be strategic for a good experiment: the modifications occurring on the biosensor surface in a certain range of time are considered simultaneously and added second after second.

Software processes these data and renders the modifications in a color

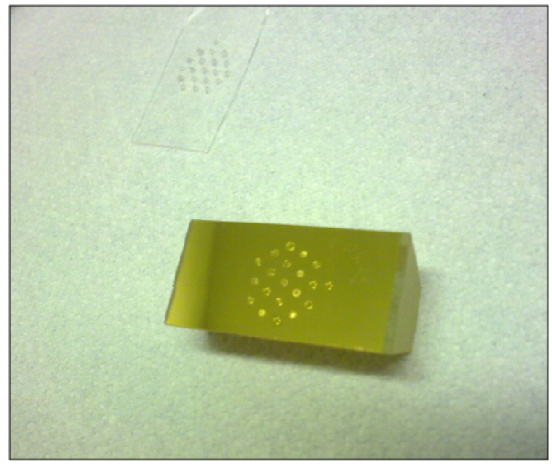

Figure 1.3: Gold chip after probes immobilization step and PDMS mask removed after this treatment.

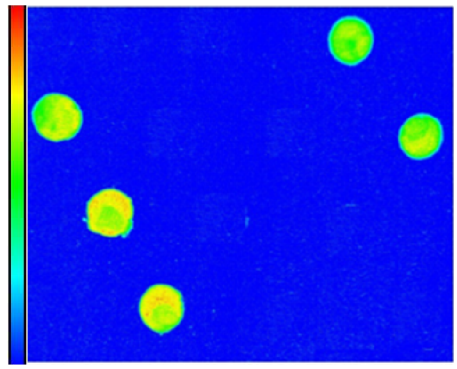

Figure 1.4: Differential image recorded from sandwich-like assay using NPs. A 250 nM solution of an 84-mer sequence, captured on biosensor surface, interacted with a secondary probe functionalized with silver NPs (flow 6 μl/min). Bright areas in differential image correspond to spots where hybridization reaction occurred.

scale, allowing the operator to clearly follow the biointeraction in real-time (Fig. 1.4). SPRi technique results to be suitable for designing affinity biosensors because of its versatility and sensitivity. Using a multi-array system it is possible to simultaneously detect different tar-

gets, allowing fast measurements, saving time and reagents.

For this work the instrument SPRi-Lab$^+$ from Horiba Scientific was used (Fig. 1.5). The instrument is made by different components, with different functionalities. The opto-mechanical part consists of a LED source that emits visible light (635 nm).

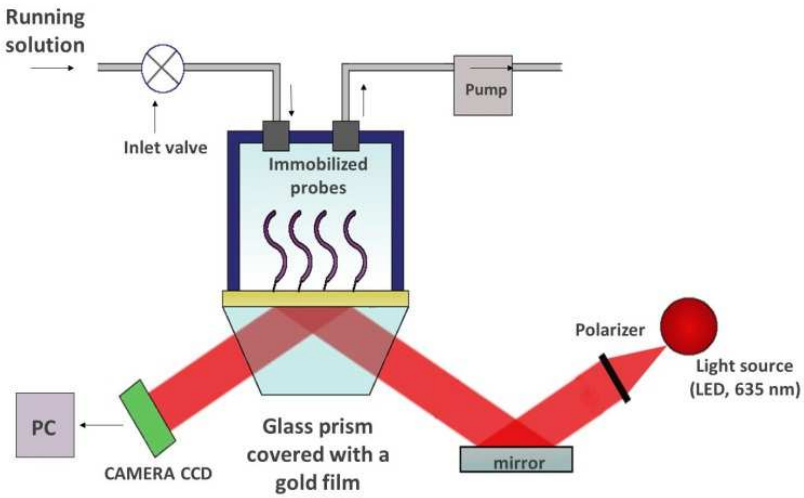

Figure 1.5: Schematic representation of SPRi instrument used for the work.

The optical asset is as follows: light passes through a polarizer, and then is reflected by a mirror on the prism, the SPRi-Biochip, where probes are immobilized. This is the biosensor core, where hybridizations reactions occur and where is focuses our study, involving chip modification by nanostructures using nanoparticles (NPs). The reflected light, reaches a CCD camera that transmits the converted signal to a PC. The prism is mounted on a support that is pushed on a cell by a piston. The flow cell is constituted by a plastic support, connected with a fluidic system.

Working solution, hybridization buffer, is aspired passing through PEEK

tubes (Restek Corporation, 1/16" OD x 0.01" ID) and, it comes to a valve (Rheodyne). The valve has a loop inject system that can permit insertion of samples into tubing system. The loop's volume is 50 μl, sample injected in excess is sent to waste. The valve outlet tube carries the solution into the flow cell. A computer is interfaced with the instrument for signal recording by dedicated software, provided by Horiba Scientific, which displays both SPR signal and real-time images.

1.3 Surface Plasmon Resonance and Single Nucleotide Polymorphism

Human genome is characterized by DNA variability, particularly in some regions. Differences in nucleotides sequences of one or more bases are found in genes among members of the same population. If the frequency of one of these variations is lower than 1 per cent, it is usually called mutation, if higher it can be classified as polymorphism. It is common to refer to polymorphisms as a variants in DNA sequence that generally do not cause debilitating disease, on the other hand, many severe diseases are related to DNA mutations. Polymorphisms can have no effect on the metabolism of the member but simply be involved in the development of certain characteristic traits, delineating the aspect of the member such as height and hair color. Anyway these definitions can not be applied rigorously. A rare disease in one population can become a polymorphism in another, if it confers an advantage and increases in frequency. A polymorphism that involves only one nucleotide in the gene sequence is called Single Nucleotide Polymorphism (SNP). The study and the determination of SNPs are of impact for what concerns clinical diagnostic, being involved in many diseases and critical biological metabolisms[8].

In many cases SNPs can be related with drug response and toxicity: if the involved gene codes for an enzyme or a transporter, the activity of the protein can be limited or inhibited. This can turn into a reduced capacity of the involved biological process to absorb the drug, lowering its pharmacological effect on the patient. The effect of the SNP on the coded protein can even bring to the impossibility to metabolize the drug, enhancing the toxicity for the patient[8].

The SNPs that occur in the human genome are widely studied and nowadays many of them are characterized and associated with the effect on the human body[8]. As explanation it is possible to cite many works and

review that refer about clinical effect of SNPs. For drug response, the common SNP is found in glutathione S-transferase P1 or xereoderma pigmentosum group D enzyme for the activity of oxaliplatin. Some SNPs are related to anticancer drugs activity, like thiopurine methyltransferase and dihydropyrimidine dehydrogenase[9]. It was reported that different ethnic groups can show differences in pain perception associated to OPRM1 A118G SNP[10]. Premature coronary artery disease and myocardial infarction are related by a SNPs in the thrombospondin gene that cause marked effects of these SNPs on the structures and functions of the protein[11].

The possibility to screen the genome of a patient to characterize the identity of SNPs is a target of relevance that eventually can help in clinical diagnostic. The final aim is to achieve personalized medicine, with tailored therapies. To go in this direction, the patient should be characterized in its genetic fingerprint. Thus molecular diagnostic analysis is increasing of interest. Fast analytical approaches allowing molecular analysis are thus welcome and among others biosensors play an important role. In fact in personalized medicine, the very final aim is the patients characterization at molecular level, achieved using low cost and fast analytical approaches, possibly using best side or bench instrumentation located in clinical cabinet or in centralized laboratory in hospitals.

Different strategies for SNPs detection are reported in literature, aiming to develop a reliable detection method for real application to routine measurements in real matrix, such as biological specimens. In the detection of SNPs, the analytical problem can be finally reduced in the identification of the base *i.e.* A, T, G, and C, present at a precise and defined position along the whole human genome. To approach this SNPs recognition, studies in this field often converge in affinity studies of DNA duplex, consisting in hybridized probe, immobilized on chip surface, with sequences added in solutions. It should be noticed that

fully matched hybrids and mismatching hybrids present different stabilities, so differences in bases of the different sequences can derived by revealing the signal given from hybridization studies. Thus fully matching and mismatching sequences can be identified.

In literature, many DNA-based sensor approaches have been developed to achieve SNPs recognition using various transduction methods, like electrochemical[12] using nanoparticles and PNA[13] cyclic voltammetry and chronocoulometry[14], differential pulse voltammetry[15], surface acoustic wave[16], impedance spectroscopy[17], Raman spectroscopy[18]. Different strategies were developed in early years for detecting SNPs on a SPR platform involving proteins, denaturing agent, nanoparticles or PNA for the SNPs discrimination (see Table 1.1).

Sometime the SNPs study was accompanied by the use of proteins.

Proteins were applied assigning them mainly two different roles: 1) mass enhancers, exploiting their dimension and thus considering as discriminating factor the lower stability of the heteroduplex respect to fully matching hybrid; 2) otherwise directly as discriminating factor, for the characteristic interaction with DNA.

In the first case, one interesting example was reported by Šípová *et al.*[19]. They realized an assay based on streptavidin–oligonucleotide (SON) complexes attached to the target and then injected in the sensor in a single step for detection of single nucleotide mismatch in a short synthetic analogue of TP53 sequence that is frequently mutated in germ line cancer. After some optimization steps about probe design and temperature it was showed that the SON complexes could amplify signal detection of about 14 times respect to direct detection (with no protein). Oligonucleotides could be detected at concentrations as low as 40 pM, discriminating fully matching targets from those containing one mismatch simply comparing their affinities (Fig. 1.6).

Author	Year	Recognition method	Principle
Šípová *et al.*	2010	Streptavidin oligonucleotide complexes	Streptavidin–oligonucleotide (SON) complexes attached to the target and then injected in the sensor in a single step.
Babic *et al.*	1996	MutS protein	MutS has the greatest affinity for the G-G heteroduplex with different affinities: G-T, A-C, A-A, T-T, G-G, A-G, C-T, C-C.
Gotoh *et al.*	1997	MutS protein incubated with ATP	Unspecific interaction between the protein and the fully matching hybrid on the sensor could be lowered to zero employing MutS with ATP
Wilson *et al.*	2005	MutS	MutS coupled to single stand binding protein reduced the unspecificity.
Nakano *et al.*	2011	MutS	Probe density was tuned in order to have an interacting substrate suitable for the size protein.
Su *et al.*	2005	MutS	Information about MutS-DNA complex.
Li *et al.*	2006	Taq DNA ligase and NPs	The enzyme catalyzed covalent bonds formation between ssDNA for fully matching target, then revealed with DNA functionalized NPs.
Sato *et al.*	2006	Gold NPs	At high salt concentrations (>0.5M NaCl), fully matched duplexes with blunt ends induced aggregation on NPs treated surface. In presence of a SNP, no aggregation was recorded.
D'Agata *et al.*	2008	PNA probes and Gold NPs for signal enhancement	Sandwich strategy on PNA probes and SNPs reveling with NPs.
D'Agata *et al.*	2011	PNA probes and Gold NPs for signal enhancement	On genomic DNA isolated from patients, sandwich strategy on PNA probes and SNPs reveling with NPs.
Lao *et al.*	2009	PNA probes	In presence of a denaturing agent the hybrids containing mismatches can selectively be destabilized.
Corradini *et al.*	2004	PNA (chiral boxes)	Modified PNA with chiral chains with greatly improved mismatch recognition ability respect to PNA.
Ananthanawat *et al.*	2010	Pyrrolidinyl PNA bearing a d-prolyl-2-aminocyclopentanecarboxylic acid backbone, acpcPNA	The acpcPNA sowed the highest mismatch discrimination efficiency than DNA or PNA.
Nakatani *et al.*	2001	Ligands of naphthyridine family	Ligands of naphthyridine family that specifically bound to the guanine–guanine mismatch
Milkani *et al.*	2010	Label-free	Comparison between fully match and single mismatch in different position on target sequence.
Song *et al.*	2002	Label-free	High-resolution SPR incorporated with a bi-cell photodiode detector combined with a flow injection device (LOD=54 fM)

Table 1.1

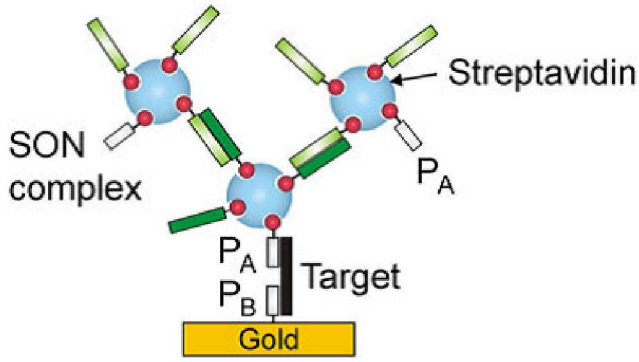

Figure 1.6: Assay based on streptavidin–oligonucleotide (SON) complexes: capture of SON–target complex by the DNA probes immobilized on the sensor surface[19].

For what concerns the second role cited above, a different approach was often reported for SNPs discrimination, not considering the DNA-DNA affinity but employing the ability of a the protein to behave differently in presence of a mismatch. In particular, the MutS protein was frequently applied for direct mismatching detection with SPR biosensor[20;21;22;23;24;25]. MutS, from a biological point of view, is involved in the methyl-directed MutHLS mismatch repair pathway[26], a strand-specific pathway that find and repair base-pair mismatches or DNA regions containing short deletions or insertions[27]. Thus, MutS not only associates with heteroduplexes DNA, identifying the presence of mismatch, but the main characteristic of this protein that makes its suitable for the SNP detection is the ability to bind all eight possible single-base mismatches with varying affinities[28].

One of the first reported attempt with SPR is about analyzing MutS affinity for various types of mismatches of a 30-mers sequence[23]. The biotinylated complementary probe was immobilized on the sensor and let hybridized with 30-mers target sequence, and then MutS was flow on the heteroduplex. They demonstrated that the SPR biosensor is able to provide direct information regarding the nature of the MutS-DNA association. MutS binding was greatest to a G-G mismatch, followed

by G-T > A-A > C-T, A-C. Binding to A-G, T-T and C-C mispairs was marginally higher than that seen between MutS and homoduplex DNA.

From this work, many were oriented to enhance the signal form specific interactions when applying MutS in a SPR biosensor[20;21;22;23;24;25] (Fig. 1.7).

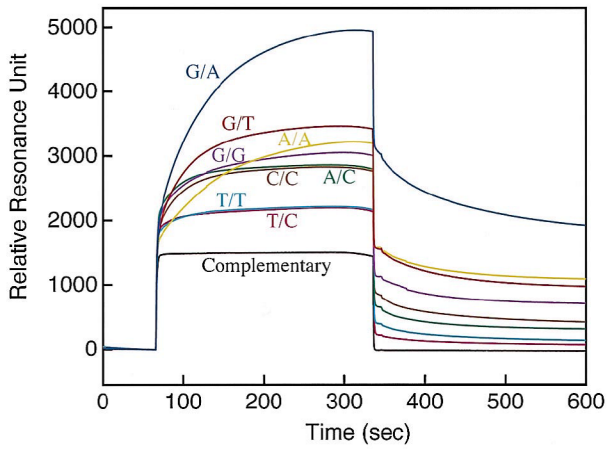

Figure 1.7: Detection of all eight possible mismatches. Complementary and eight possible mismatched dsDNA were immobilized on a sensor chip surface and then exposed to SSB. ATP-treated MutS was applied to the sensor chip surface and binding was monitored in resonance units. MutS did not bind to complementary dsDNA, however, MutS did bind all eight possible mismatched pairs[24].

It is known[29] that ATP influences the state of a MutS-mismatch complex, modulating the specificity of MutS to bind mismatched DNA. From this, Gotoh *et al.*[24] studied the influence of ATP on MutS specificity. ATP-pretreated MutS was applied over immobilized homoduplex and heteroduplex DNA. They demonstrated that the unspecific interaction between the protein and the fully matching hybrid on the sensor could be lowered to zero employing MutS pretreated with ATP, preventing the binding of MutS to complementary dsDNA. Furthermore, they

minimized also the unspecific binding of MutS to immobilized ssDNA (not affecting the binding of MutS to mismatched and complementary dsDNA) by a treatment of immobilized probes with single-strand binding protein (SSB). SSB is a protein identified in organisms from viruses to humans, where it binds selectively to single-stranded DNA in order to prevent the annealing of DNA, to avoid digestion by nuclease and to allow functions of enzymes on single strands. The main characteristic of this protein, *i.e.* to bind only to single chains of oligonucleotides, is peculiar and can be of advantage in biosensor analysis.

As well as the case reported above[24], Wilson *et al.*[20] employed SSB in combination with MutS for the detection of a mismatch with SPR. In particular they confirmed that the application of SSB prior to MutS should not affect its ability to bind to mismatches, but would prevent non-specific binding of MutS to DNA probes and chain ends. Furthermore it was showed that SSB alone could give information about the presence of a mismatch because there was a clear difference in SSB binding on matching or mismatching DNA. SSB gave a higher signal when a mismatch is present, because of the lower affinity for the immobilized DNA probes.

Interesting considerations arose from this work about the surface mismatch density in relation to MutS SPR signal. This topic was recently developed by Nakano *et al.*[22]. They demonstrated by SPR measurements that MutS binding was significantly influenced by the amount of interacting DNA on the chip. They prepared substrate density-controlled DNA chip exposing the immobilized DNA probes to a mix of complementary target of two different lengths. After, the free extremities of the longer target were hybridized with single nucleotide mismatching sequence, to subsequently interact with MutS. Thus, they found that in order to obtain accurate kinetic measurements for the SNPs detection, the density on the surface had to be tuned, *i.e.* the substrate had to be built in order to guarantee a distance between the

DNA substrates greater than the size of the protein.

SPR biosensors for its affordability and for the good results achieved in SNPs detections with MutS, was further used in parallel with other transduction principals as control. For example, Su *et al.*[25] employed a quartz crystal microbalance (QCM) and an SPR device for the study of MutS binding with DNA containing a single Thymine-Guanine (T-G) mismatch. The combined SPR and QCM data allow providing information on the structural properties of the DNA and MutS/DNA complexes.

Finally, a very original approach for SNP genotyping was reported by Li *et al.*[30] with the use of a protein, in particular of an enzyme surface ligation chemistry coupled to NPs enhanced SPR detection. Taq DNA ligase was used, an enzyme that catalyze covalent bonds formation between ssDNA only when the single chains are perfectly complementary. In this work, targets (longer than probes) and Taq DNA ligase were simultaneously introduced on immobilized probes (Fig. 1.8). Both match and mismatch hybrid formed, but only the fully complementary hybrids were metabolized by the enzyme. In this case the protein, *i.e.* Taq DNA ligase, did not recognize the kind of genotype directly, but its activity was strictly correlated with the presence of a SNP. In presence of a matching target, *i.e.* no SNP, the result was an elongation of the probe, on the other hand, if there is a SNPs, no elongation occur. The probe was subsequently regenerated and the extended part was finally revealed by reaction with the complementary DNA sequence. Thus, a signal from this secondary hybridization meant that the sample analyzed was fully complementary to probe immobilized. If no signal was recorded, a mismatch was present in the double helix (Fig. 1.8). Combining arrays with different probes immobilized and analyzing the data obtained from this strategy it was possible to identify the nature of the SNPs.

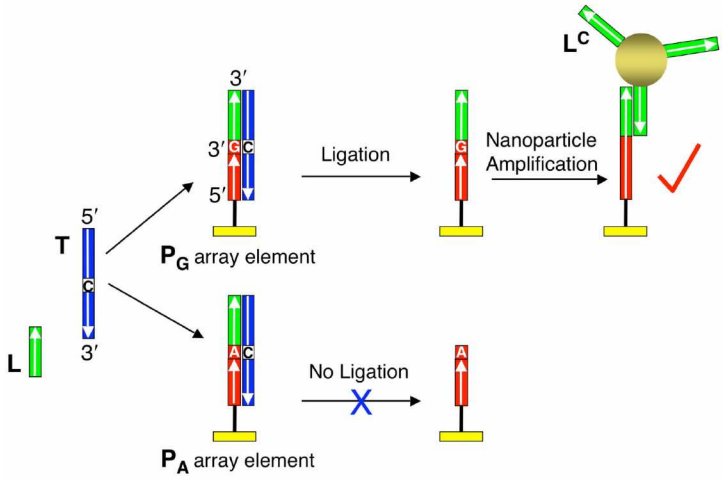

Figure 1.8: Schematic representation of the SNP genotyping method based on a combination of surface ligation chemistry and nanoparticle enhanced SPRi. Two array elements with different DNA probes are shown. The array probes (PA and PG) differ only by the last nucleotide at their 3′ ends. When target DNA (T), ligation probe DNA (L) and *Taq* DNA ligase are simultaneously introduced to the array, surface duplexes form at both array elements. However, ligation only occurs if the duplex is perfectly complementary. After denaturation, the perfectly matched PG is extended with the L sequence while PA returns to its original state. The presence of L is then detected by the hybridization adsorption of gold nanoparticles modified with oligonucleotides (LC) complementary to L[30].

The strand for the secondary hybridization was here functionalized with NPs in order to achieve a detection of target concentration down to a concentration of 1 pM, thus here nanoparticles were used for SNPs detection signal improvement. This was not the only attempt coupling Nps to the SNPs detection. A very original experiment was performed by Sato *et al.*[31], demonstrating the successful application of SPR imaging technique to the DNA sensing. They used a mixed solution of gold NPs functionalized with the probe sequence and the target sequence (label free). Surface was pretreated with gold nanoparticles, aggregating on it. No probe was immobilized on the SPR biochip but the hybridiza-

tion reaction with target took place in solution, directly in contact with the SPR sensing surface. At high salt concentrations (>0.5 M NaCl), fully matched duplexes with blunt ends induced aggregation on NPs treated surface (the LOD was 32 nM). In presence of a SNP, no aggregation was recorded.

In this case NPs are crucial in discriminating the presence of a SNP, being directly involved in the main process that permits the discernment. More often NPs are employed in combination with SPR biosensors for signal enhancement. For what concerns SNPs discriminations, D'Agata *et al.*[32;33], following a sandwich strategy, used gold Nps to improve signal from the target hybridization (synthetic[32] and genomic DNA isolated from patients[33]) to make possible the reveling of mismatch presence at concentrations down to 2.6 aM.

A role in developing SNPs detecting system is played by the probe to be used in the immobilization on the chip surface. In SPRi, in recent work, for the immobilized probe, involved in the primary hybridization with the fully matched and mismatched target, D'Agata *et al.*[32;33], used peptide nucleic acids (PNA) probes. PNA, first introduced by Nielsen *et al.*[34] and first reported combined to SPR for single nucleotide mismatches by Feriotto *et al.*[35], is a nucleic acid chain that mimics DNA but with the sugar-phosphate backbone replaced by a polyamide chain composed of N-aminoethylglycine. It was demonstrated by Lao *et al.*[36] that the hybridization conditions for SNP discrimination need to be separately optimized for PNA and DNA probes, as a consequence of their distinct properties. As stringency control strategy for single base mismatch discrimination, a denaturant, *i.e.* formamide was added in hybridization buffer. Adding hybridization suppressors like denaturing agent in working buffer, the hybrids containing mismatches can selectively be destabilized, resulting in successful discrimination of a single base mutation. In these conditions, the stability of PNA/DNA hybrids was greatly affected by the presence of a single base mismatch, thus

as a consequence, PNA showed higher mismatch discrimination efficiency than the DNA probe. For this reason PNA can be very useful for biosensor development for SNPs detection and many reported about different applications in SNPs detection[35;36;37;38;39]. In addition to examples reported above, a particular and very interesting application is about chiral boxes[37]. These were constituted by PNA chains containing an insert of three chiral monomers based on D-lysine. This structure was demonstrated to be able to recognize complementary DNA oligonucleotides with sequence selectivity higher than the corresponding achiral PNA, and in particular showed greatly improved mismatch recognition ability. Thus, it is possible to affirm that chiral PNAs can be very high selective probes in DNA recognition of SNPs.

Another application of modified PNA in SPR based SNPs detection was reported recently by Ananthanawat *et al.*[39]. They used as probe a 13-mer pyrrolidinyl peptide nucleic acid sequence bearing a d-prolyl-2-aminocyclopentanecarboxylic acid backbone, called acpcPNA. Its performances in terms of specificity to detect the mismatch in target DNA (1 μM) were evaluated and compared to the same ability of DNA and conventional peptide nucleic acid (aegPNA). The acpcPNA showed the highest mismatch discrimination efficiency between fully matched DNA and single mismatching targets, indicating that introducing suitable modification to PNA chain could be of advantage, emphasizing its peculiar characteristics in term of SNPs mismatch discrimination.

As reported so far, the most frequent approach for SNPs detection in SPR based biosensor was to immobilize a sequence on the SPR sensor surface and the discrimination was performed with different approach after the target hybridization. About this, the work of Nakatani *et al.*[40] resulted particular and differentiates from others because the discriminating molecule was immobilized on the surface. They designed and synthesized ligands of naphthyridine family that specifically bound to the guanine (G)–guanine mismatch, one of the possible SNPs. They

demonstrated that the G-G mismatch is significantly stabilized when two naphthyridine intercalators simultaneously bind to both G bases within the base stacks of the DNA duplex. In subsequent years[41] they developed a SPR sensor assay system to detect not only G–G but expected to be useful for detecting all mismatches in duplex DNA using different intercalating molecules shown to stabilize specific mismatched base pairs by selective binding. Three mismatch-binding ligand (naphthyridine dimers), were simultaneously immobilized onto a SPR sensor chip and let react with DNA duplexes containing a single-base mismatch during the SPR assay and used for the detection of target mismatched base pairs in 10 nM DNA samples (Fig 1.9).

The principle on which this latter approach is based comes from the assumption that the bulged nucleotide base has no complementary base to form a hydrogen-bonding pair, making the site susceptible to drug intercalation; a ligand would produce a highly organized and stable complex with the bulged DNA. For the different base pairs present in the mismatch site, different affinities are expected for the mismatch-binding ligands, the number of hydrogen-bonding groups complementary to the bulged base is different.

After all these different strategies, also label free approaches were successfully tested for single base mismatch recognition.

Milkani *et al.*[42] reports about a label free approach on synthetic 21-mers oligonucleotides aimed to study the influence of the mismatch position along the double helix on the interactions. They compared the SPRi signal for three targets differing only in the position of the non-complementary base. In their experimental asset, comparison was performed between $3'$ end, $5'$ end, and middle mismatches on the target DNA oligonucleotide and the effect of buffer concentration, flow rate, and temperature was studied with regard to the detection of single nucleotide mismatches using SPR. The observed response for the $5'$

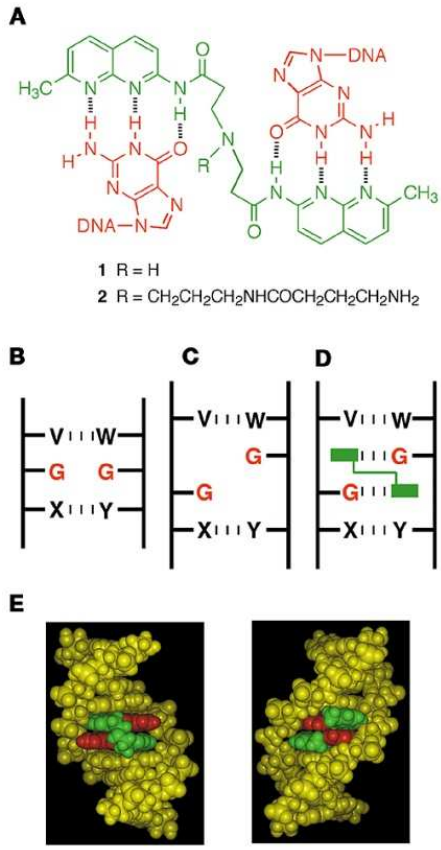

Figure 1.9: (A) Structures of naphthyridine dimers 1 and 2 (green), and hydrogen-bonding pattern to guanine (red). (B) An illustration of duplex containing a G-G mismatch. V, W, X, and Y can be any nucleotide bases. (C) Hypothetical structure of the G-G mismatch regarded as two consecutive guanine bulges. Both G bases have no complementary base to form a hydrogen-bonding pair. (D) A proposed binding model for ligand 1 to the G-G mismatch. Naphthyridine moieties of ligand 1 (shown with green boxes) intercalate into the GV and GY steps and produce hydrogen bonds to two guanines. (E) Molecular models of the simulated complex of ligand 1 (colored green) and DNA containing the G-G mismatch (colored red) viewed from the major groove side (left) and the minor groove side (right)[40].

mismatch (distal end) was similar to the fully matching strand one and single mismatches at the proximal end of the probe result in a less efficient hybridization of target to probe compared to the distal end, which is closer to the solution. Song *et al.*[43] used a high-resolution SPR incorporated with a bi-cell photodiode detector combined with a flow injection device. The influence of a mismatch on SPR signal was evaluated on a target of 47-mers (30-mer probe). With their instrumental asset the detection limit without any label was 54 fM, higher compared to other common SPR system and the selectivity is very good, the duplex with single mismatch can be recognized for the smaller affinity respect to fully complementary target.

The strategy reviewed here all are related to single nucleotide polymorphisms detection using a SPR platform. Different secondary interactions are often reported for the mismatch detection like protein specific for SNPs or protein like streptavidin, intercalating agent or enzymes or nanoparticles. Various label free approaches were also described, all on synthetics DNA sequence. From this, the main aim is to develop a strategy with a minimum number of steps that can be specific and, more important, that can be applicable to real samples analysis. This was the topic toward this work was oriented.

1.4 Surface Plasmon Resonance and Nanoparticles for Signal Enhancement

Scientists have shown tremendous interest in a variety of applications of NPs ranging from efficient catalysis to improved methods for diagnostics and the treatment of diseases. For what concerns biosensor analysis, NPs have a main role in signal enhancement using different transduction principles[44;45;46;47;48;49;50;51;52;53]. NPs were reported to be useful for enhancing performance of PCR[52;53], or in surface enhanced Raman spectroscopy[49;51].

The enormous signal enhancement associated with the use of nanomaterial provides the basis for ultrasensitive detection of biomarkers or similar. In general, the use of NPs can help to achieve signal amplification by several orders of magnitude and lower detection limits. The improvement of SPR analytical performances for a DNA biosensor is a goal in developing innovative devices, especially for clinical applications. In recent years many works were oriented to exploit their characteristics for biosensing[44;45;54;55;56;57;58] and on SPR platform[6;46;47].

NPs possess typical properties, different from macro-materials or micromaterials in terms of chemical and physical characteristics, surface area and reactivity. Due to their size they can show effects that are only present in nano-sized materials[59;60;61]. Many properties of NPs arise from their large surface-area-to-volume ratio and the spatial confinement of electrons, phonons, and electric fields in and around these particles.

The high ratio between surface area and volume drive to their particular reactivity and catalytic effect, and their large interacting area (1 kg of particles of 1 mm^3 has the same surface area as 1 mg of particles of 1 nm^3) permits to have a very small system but with a great potential in

terms of number of interactions.

Biomolecule-NPs hybrid systems combine the recognition and biocatalytic properties of biomolecules with the unique electronic, optical, and catalytic features of NPs[56;57]. This can bring to composite materials with new functionalities, allowing the development of new biosensors and system of recognitions with improved sensitivity compared to traditional method.

Acting on size, shape, material and functionalization it is possible to tune NPs features, making these particles very versatile to be applied in various system, *e.g.* in biosensing. It is possible to find synthesis conditions that are able to produce the nanoparticle that can be suitable for a certain application and to explore a wide range of possibilities.

As noble metals, NPs show a strong visible absorption due to the collective oscillation of electrons in conductive band, called plasmon effect. This is the phenomenon that gives color to colloidal NPs suspension and that characterize NPs electronic properties.

The improvement of detection sensitivities and limits of detection are constant goals in biosensing research and open up possibilities in expanding the types of analytes detectable by SPR and therefore the ability to utilize the unique characteristics of SPR sensing. A commonly suggested mechanism of improvement in NP-based SPR sensing devices is coupling between the LSPR of NPs and the propagating SPR of Au films, resulting in a greater SPR incident angle shift[62].

In my work NPs features are investigated for SPR signal enhancement. Two detection formats are discussed as well as methods of NP incorporation in SPRi sensor. The signal amplification was searched and obtained both by using NPs for nanostructuring biochip surface and by functionalizing them with sequence, in a DNA sandwich-like assay. In both studies, two kinds of NPs were selected and applied in order

to evaluate different effects: surface area improving, mass enhancement and surface plasmon coupling. All these feature can give a contribute to SPR signal improvement, but it was found that comparing signal from different structure studied and NPs features, the coupling between NPs plasmon and surface plasmon, resulted to be a requirement in order to have improved performance in SPRi sensing (see Section 3.2).

2

The aim

In this scenario the aim of my research project was to develop an original SPRi biosensor that could directly detect SNPs, first studying and verifying a model system on synthetics targets. The assay was optimized in each step, from probe design to experimental conditions and further applied to clinical relevant samples, *i.e.* human DNA extracted from blood (*i.e.* Lymphocytes).

Moreover, in parallel, the possibility to enhance the sensitivity of SPRi DNA-sensing was studied using nanoparticles. This was investigated using surface nanostructuration in order to couple plasmons of NPs and of gold chip surface and/or to, using NPs for secondary hybridization signal enhancement. NPs differing in material and shape were used and improvement of the system was found in both approaches studied.

3 Experimental part

3.1 Single Nucleotide Polymorphism Detection

3.1.1 *In Silico* Probe Design

The first aspect considered for the development of a SPRi based biosensor specific for SNP detection was to define a rational criterion to select DNA probe sequence for genome analyzing. The aim was, first, to find a method for evaluating *ex ante* the performances of the receptor to be used on the biosensor, thus in this paper the method was verified.

A computer program was chosen for selecting probe sequences specific for the detection of a target gene. The program, taking into account different aspects related to probe characteristics and gene target proprieties, estimates probe performances, through nearest-neighbor calculations, permitting an accurate choice of the receptors to be used in the DNA-based sensor.

In order to verify this procedure as a suitable tool for SPRi sensing, five probes were selected with different estimated performances. Each probe was tested on the SPRi biosensor and signal intensities for the same target concentration were compared to computational results. The strategic importance of probe design was confirmed experimentally, since the

SPRi output resulted from hybridization of the target with the different selected probes, carrying different "theoretical" score from *in silico* evaluation, was heavily affected by probe choice. Excellent agreement was found between calculated and experimental performances, suggesting that the use of *in silico* probe evaluation can be a correct and useful tool in DNA-based sensor design. From these results, the *in silico* probe design will be further applied to other target sequences and biosensing platforms, used in this study.

This part of my research was reported here:

M. L. Ermini, S. Scarano, R. Bini, M. Banchelli, D. Berti, M. Mascini and M. Minunni, "A Rational Approach in Probe Design for Nucleic Acid-Based Biosensing", *Biosens. Bioelectron.*, **26**(12), 4785-4790 (2011)

Biosensors and Bioelectronics 26 (2011) 4785–4790

Contents lists available at ScienceDirect

Biosensors and Bioelectronics

journal homepage: www.elsevier.com/locate/bios

A rational approach in probe design for nucleic acid-based biosensing

M.L. Ermini [a], S. Scarano [a], R. Bini [a], M. Banchelli [a,b], D. Berti [a,b], M. Mascini [a], M. Minunni [a,*]

[a] Dipartimento di Chimica "Ugo Schiff", Università degli Studi di Firenze, Via della Lastruccia 13, 50019, Sesto F.no (FI), Italy
[b] CSGI, Università degli Studi di Firenze, Via della Lastruccia 13, 50019, Sesto F.no (FI), Italy

ARTICLE INFO

Article history:
Received 21 March 2011
Received in revised form 16 May 2011
Accepted 7 June 2011
Available online 12 June 2011

Keywords:
DNA
Probe design
DNA biosensor
Surface Plasmon Resonance imaging
Optical biosensor

ABSTRACT

Development of nucleic acid-based sensing attracts the interest of many researchers in the field of both basic and applied research in chemistry. Major factors for the fabrication of a successful nucleic acid sensor include the design of probes for target sequence hybridization and their immobilization on the chip surface. Here we demonstrate that a rational choice of bioprobes has important impact on the sensor's analytical performances. Computational evaluations, by a simple and freely available program, successfully led to the design of the best probes for a given target, with direct application to nucleic acid-based sensing. We developed here an optimized and reproducible strategy for *in silico* probe design supported by optical transduction experiments. In particular Surface Plasmon Resonance imaging (SPRi), at the forefront of optical sensing, was used here as proof of principle. Five probes were selected, immobilized on gold chip surfaces by widely consolidated thiol chemistry and tested to validate the computational model. Using SPRi as the transducting component, real-time and label free analysis was performed, taking the *Homo sapiens* actin beta (ACTB) gene fragment as model system in nucleic acid detection. The experimental sensor behavior was further studied by evaluating the strength of the secondary structure of probes using melting experiments. Dedicated software was also used to evaluate probes' folding, to support our criteria. The SPRi experimental results fully validate the computational evaluations, revealing this approach highly promising as a useful tool to design biosensor probes with optimized performances.

1. Introduction

Nucleic acid sensing has always been an active field in chemical research. In particular, DNA sensing has been applied to a variety of analytical problems from clinical diagnostic to food and environmental analysis. Different transduction principles are evaluated, using both label and label-free approaches (D'Orazio, 2003; Scarano et al., 2010; Teles and Fonseca, 2008; Tothill, 2009). The aim of these approaches is the selective detection of target sequences at DNA or RNA level (Lucarelli et al., 2008). In the case of point mutation detection, with relevance in molecular clinical diagnostic, the sensors are designed to discriminate between sequences differing only by one base (Dell'Atti et al., 2006; Healey et al., 1997; Sato et al., 2003; Wilson et al., 2005). These devices have opened up new possibilities for cheap, fast, real time and eventually label free detection of analytes (Scarano et al., 2010 and references therein; Sendroiu et al., 2011; Halpern et al., 2011; Gifford et al., 2010; Chen et al., 2010). In DNA-based biosensor development, key steps are: the surface immobilization chemistry, which should prevent unspecific adsorption in order to lower background noise, and the probe design, responsible of the system selectivity. Different immobilization chemistries are now available for probe immobilization (Brockman et al., 1999; Caruso et al., 1997; Mannelli et al., 2005; Smith et al., 2001), despite much research in nucleic acid-based sensing being published, little work has been dedicated to strategies for probe design and the effect of its selectivity on the sensor analytical performances. Generally, the complementary sequence to the target analyte (a gene, a fragment or a short oligonucleotide) is first considered during the choice of probe. The probe length is generally set ranging from 15 to 20 bases, with one end usually linked to a functional group to be exploited for the immobilization chemistry. For example, biotinylated probes are used in surface functionalization involving streptavidin; thiolated probes (Kukanskis et al., 1999; Mannelli et al., 2005) are required for direct probe coupling to gold surfaces via Self Assembled Monolayer (SAM) formation (Allara and Nuzzo, 1983). Another criterion taken into account in probe selection is the C–G base content (three hydrogen bonds vs. two with A–T pairing); preferred composition varies from at least 40% to 60% (Powdrill, 2003) to stabilize the hybrid on the surface. Finally, to facilitate surface hybridization, it is

* Corresponding author. Tel.: +39 0554573314; fax: +39 0554573384.
E-mail address: maria.minunni@unifi.it (M. Minunni).

0956-5663/$ – see front matter © 2011 Elsevier B.V. All rights reserved.
doi:10.1016/j.bios.2011.06.004

Table 1
Probe and target sequences.

Probe 1: 101–120	5′-SH-$(CH_2)_6$-AGCGGAGCAGGAAAAGAGGA-3′
Probe 2: 5–24	5′-SH-$(CH_2)_6$-CCCTGTAAGGGAGCTTTCGG-3′
Probe 3: 138–157	5′-SH-$(CH_2)_6$-GTGAGGGGCAGGGAGGAGCT-3′
Probe 4: 150–169	5′-SH-$(CH_2)_6$-GAGCAGCCTGGGGTGAGGGG-3′
Probe 5: 145–164	5′-SH-$(CH_2)_6$-GCCTGGGGTGAGGGGCAGGG-3′
Target	5′-AGCTCCGAAAGCTCCCTTACAGGGCAAAGTTCCCAAGCACAGAAGAGAACCTGTTCACTTCTCCCCTGCTCGGCCCGCCCCCTGGCCAGGCACCTC-TACTTCCTCTTTTCCTGCTCCGCTGCTTGCTTTCTCTCTTCAGCTCCTCCCTGCCCCTCACCCCAGGCTGCTCGGCCACCTCCAACCTGCCACCTGAGGACA-CCCAGGCAGTCACTCATTCAACAGCGAGG-3′

important to avoid probe hybridization on regions that can assume conformations and may obscure the binding site of interest, i.e. by formation of secondary structures such as hairpins or loops.

Although very interesting works are present in literature related to DNA-based sensing and probe selection (Tomiuk and Hofmann, 2001; Kaderali and Schliep, 2002; Letowski et al., 2004; Lucarelli et al., 2008; Li and Stormo, 2001; Mulle et al., 2010; Tedeschi et al., 2005; Rahmann, 2003; Wang and Seed, 2003) there is a need for standardized strategies for rational probe design, that could be assessed for its validity before using the probes, avoiding the waste of money and time.

This work aims to develop an optimized and reproducible strategy for probe design for nucleic acid-based sensing. We here consider a computational assisted approach for probe design, based on a free available software. The *in silico* selection was validated by experiments conducted using optical transduction for DNA-sensing development. In particular Surface Plasmon Resonance imaging (SPRi) was used as proof of principle. In this case, the conventional SPR is coupled to a micro-array format through the introduction of a Charge-Coupled Device (CCD) as its detector system instead of a diode arrays. SPRi is at the forefront of optical sensing, allowing real-time and label free simultaneous measurements multi-analyte. In SPRi, probes are tethered on a chip gold surface in array format.

In this study, it was demonstrated that "smart" probe design for DNA-sensing significantly improves the sensor's analytical performances for DNA–DNA hybridization measurements that were coupled with a computational assisted approach (Wernersson et al., 2007). The idea we support is that it is possible to design a probe specific for target sequence using a predictive model, based on *in silico* computations, to rationalize chip design for DNA-sensing application to improve analytical sensor performances. The pool of probes sorted by the program, is scored on the base of key parameters.

As model system, we validated computational results obtained on actin beta (ACTB) gene fragment belonging to *Homo sapiens* by assaying a pool of selected probe sequences by SPRi. To better understand computational probe selection and experimental sensor behavior, melting experiments were performed by UV spectrophotometry. DNA self-complementariety of selected probes were evaluated in solution and then compared with the folding obtained with Mfold free software (Wernersson et al., 2007).

Our work demonstrated how rational design of nucleic probes with application DNA sensing can lead to improved analytical performances. This is, to the best of our knowledge, the first attempt in rational probe design with validation of probe selection, using *in silico* approach coupled to SPRi transduction. The theoretical model is confirmed by experimental testing, introducing new perspectives in the application of nucleic acid detection.

2. Materials and methods

2.1. In silico design of DNA probes

Probes' design based on free software OligoWiz 2.0 (Wernersson et al., 2007). To obtain the specific probes, first the sequence of interest, i.e. target analyte, inserted. Then the list of possible probes to be immobilized on the chip surface is provided. The program identifies complementary sequences on the basis of five parameters before producing a final ranking of the identified probes defined as: Cross-hybridization, DeltaTm, Folding, Position and Low-complexity.

In this study, the 20-mer probes selection process was applied to a 227 mer fragment of the *Homo sapiens* beta actin (ACTB) on chromosome 7 (from position 896 to 1123 of the gene sequence). Scores were calculated by the program for each probe exploiting the nearest neighbor algorithm (Buser, 1983), taking into account the characteristics of neighboring nucleotides (identity and orientation) to evaluate the free energy involved in the stability of the base pairing. The score was expressed in a range between 0 (wretched probe) and 1 (excellent probe), based on the five parameters mentioned before.

The outcome of the program finally consists of a set of scored probes. From the ranked probes, we selected five sequences, one with the best scores, one the worst scored and three with intermediate score. The following weighting of the scores was applied in our evaluation: Cross-hyb: 0.0%; DeltaTm: 70.2%; Folding: 17.5%; Position: 0.0%; Low-complexity: 12.3%.

2.2. Buffers and reagents

Thiolated DNA probes were anchored on the biochip gold surface by diluting them to a concentration of 10 μM in Immobilization Solution (IS): 1 M KH_2PO_4 (Merck, Italy), pH 3.8. To passivate gold, aqueous solution of 1 μM 11-mercapto-1-undecanol (MU) and 1 μM 6-mercapto-1-hexanol (MCH) were used. Hybridization Solution (HS) for SPRi measurements used was as follows: 300 mM NaCl, 0.02 M Na_2HPO_4, 0.1 mM EDTA, pH 7.4, 0.05% (w/v) of TWEEN® 20 (Polyethylene glycol sorbitan monolaurate). 100 mM HCl solution was used to regenerate the biochip surface, after each measurement cycle. PDMS (Sylgard 184 Silicone Elastomer Kit, Dow Corning, UK) was used for the micro-welled mask preparation. Unless otherwise stated, reagents were purchased from Sigma–Aldrich (Milan, Italy).

All solutions were prepared in MilliQ water (Millipore Corporation, MA, USA) and filtered using vacuum filter cups (Millipore E express plus, 0.22 μm) and syringe filters (Puradisc, cellulose acetate, 0.2 μm from Whatman GmbH, Dassel, Germany).

5′-Thiol modified probes and complementary unmodified targets were purchased from Eurofins MWG Operon (Ebersberg, Germany). The relative sequences and positions on the target sequence are reported in Table 1.

2.3. SPRi instrumentation

For this work probes' hybridization efficiency was tested using a Surface Plasmon Resonance imaging instrument Lab+-SPRi (Genoptics-Horiba Scientific, Orsay, France) integrated with a microfluidic system (PEEK tubing, Restek corporation, 1/16 in. OD × 0.01 in. ID; Rheodyne valve, loop injection system, 50 μl loop volume) where flux is generated by a peristaltic pump (Miniplus 3, Gilson) using accurate tubing from Elkay, orange/black, 0.015 cm^3/min.

Under total internal reflection condition, a polarized light beam passes through the prism, hits the gold layer and it is reflected to a CCD camera. Under certain conditions depending on incidence angle, gold free electrons can absorb incident light photons, resulting in resonant oscillation and generating surface plasmon waves. Modifications occurring at the chip surface, i.e. hybridization between DNA probes and target sequences can induce changes of resonance conditions due to a change in refraction index of surface. The variation of intensity of reflected light at a fixed angle was monitored by a CCD camera. A dedicated software (SPRiview L3.1.2), provided by the producer, enabled monitoring in real-time, the biomolecular interactions both by SPR signals (sensorgrams) and digital images (i.e. changes in reflected light). This instrumentation set up was also reported previously (Scarano et al., 2010).

2.4. Probes immobilization on SPRi biochip surface

DNA probes were immobilized in array format on SF-10 glass prisms coated with gold (50 nm-thick) (SPRi-Biochips™, Genoptics-Horiba Scientific, Orsay, France) using a dedicated PDMS mask for precise deposition of receptors, coupled to manual spotting procedure (Scarano et al., 2010). The PDMS film acted as micro-welled support on the gold surface. Each micro-well on chip was filled with 0.8 μl of thiolated probe solution (10 μM in IS). The selected probes were deposited on chip surface by exploiting the affinity between sulphur and gold, creating at least three spots for each probe. Two spots were used as reference surfaces (IS only).

The chip was placed into a moist chamber and vacuumed for 20 min and then left into the chamber for 12 h. During this time, the probes were anchored to the gold, forming a self-assembled monolayer (SAM). Before use, the chip surface was subjected to a passivation step, dipping the prism in the thiols mixture for 24 h. The surface was then washed with water and inserted in instrument's flow cell.

2.5. SPRi measurements

During each measurement, biochip surface was kept under a constant flow of HS (6 μl/min, 11 μl flow cell internal volume 11 μl). Calibration curves with synthetic oligonucleotides were obtained by injecting 100 μl of synthetic fully complementary targets at different known concentrations in the valve. The injection loop was 50 μl, thus volume in excess was used to wash off air bubbles or impurities from the loop assuring its complete filling. The target reaches the flow cell about 4 min after valve opening, leading to observed hybridization reaction (target-probe pairing) that lasted for about 10 min. Then the surface was washed by the HS flow, removing eventual excess of analyte from surface. Sensorgrams corresponding to hybridization binding were recorded in real time, plotting the reflectivity variation percent ($\Delta R\%$) against time. SPR signal was obtained by subtracting intensity of reflected light before injection, from the steady signal after the washing step. The differential image of the chip surface is generated by the software which recorded the reflected light variation during the experiment (from sample injection to washing step). Surface regeneration is achieved by dissociating the double-stranded DNA (dsDNA) complex on the surface with the regeneration solution (24 μl/min for 1 min), allowing probes to be available for subsequent analysis.

SPR signals were sampled on selected Regions of Interest (ROIs) of the array. For each immobilized spot, 3 circular ROIs with a radius of 70 μm were defined. Calibration curves were obtained with synthetic complementary oligonucleotides for the immobilized from 2 to 500 nM range. Each solution was prepared by diluting stock solutions of synthetic targets in HS. All measurements were performed at room temperature.

Table 2
Scores for each considered probe.

Probe	Total score	DeltaTm	Folding	Low complexity
1	0.936	0.963	1.000	0.692
2	0.936	0.952	1.000	0.692
3	0.725	0.674	1.000	0.621
4	0.500	0.338	1.000	0.709
5	0.255	0.000	0.996	653

2.6. Thermal denaturation/renaturation spectrophotometric measurements

Possible secondary structures on DNA probes sequences were investigated by melting experiments conducted on UV–VIS spectrophotometer Cary® 100 Bio (Varian, Inc.), interfaced with a computer by a dedicated software (Cary Win UV). Data analysis and fitting was performed using QtiPlot 0.9.7.13.

4 μM HS solution of each probe was subjected to four scans in temperature in a range between 25 °C and 80 °C (data interval 0.5 °C, scanning rate 1 °C/min) and relative melting profiles acquired (260 nm). Possible self-pairing structures were estimated by Mfold software (Zuker, 2003) simulating experimental conditions (25° C; 0.34 M Na^+).

3. Results and discussion

In this study a computational approach for probe selection in DNA-based sensing was performed using OligoWiz (Wernersson et al., 2007) and then experimentally validated. After identifying a pool of probes with different scores, among them, five different probes were selected (corresponding parameters summarized in Table 2). These five thiolated probes were immobilized on gold chip in an array format and relative interactions with complementary sequences were analyzed, using SPRi transduction.

3.1. Setting of critical parameters

Cross-hybridization, DeltaTm, Folding, Position, and Low-complexity are the key parameters that OligoWiz combines to obtain the total score for each probe sequence. These parameters can be tuned based on experimental conditions of the analysis. This was done by defining a specific weight (expressed as percentage contribution) for each parameter considered. For instance, relative priority should be assigned to Cross-hybridization and Position parameter to reduce unspecific interactions between probe and possible interfering sequences present in genomic DNA samples. However, in our analysis we studied on purpose a model system, using only synthetics targets in order to reduce background effects and underlying the direct role of the specific probe characteristic, i.e. the bases sequence which influences significantly its secondary structure and thus its Tm.

This evaluation was strictly based on the aim of this work, which was to study a model using the simplest experimental conditions so that the analytical performances of the biosensor depend only on the specific characteristics of the probes. Cross-hybridization score has to considered in the analysis of samples containing possible interfering sequences, i.e. amplified or genomic DNA, that can affect the biosensor selectivity, absent in this case study. Since fully complementary targets were used for our purposes, 0% value for the Cross-hybridization score was imposed to correspond to the absence of any interfering contribution from complex matrix. For this reason, in the considered case study Cross-hybridization score different from 0% would not produce a realistic evaluation.

A higher priority, instead should be granted to the DeltaTm score, that appear to be very impactful for a good prediction in

this study. This parameter considers the distribution of the melting temperatures (Tm) for all possible probes; low DeltaTm score for a certain probe sequence indicates a high deviation of its Tm from the average Tm. In SPRi, DNA probes work simultaneously in an array format and, therefore, at the same temperature. Ideally, Tm relative to target-probes duplexes should be very similar, so that the affinities of base pairing recognition are comparable under the same experimental conditions. This would ensure high homogeneity during the hybridization process of all probe sequences. DeltaTm was weighted at 70.2% for all reported experiments.

This value was selected in order to make DeltaTm contribution higher than the remaining two parameters (low complexity and folding). In other words by assigning 0% to Position and Cross-hybridization, we increased the relative priority of DeltaTm to compensate.

The formation of secondary structures on the probe sequence is also an important parameter in probe design. OligoWiz assigns a poor Folding score to sequences subjected to a folding, strong enough to the extent that it interferes with target hybridization, by calculating the free energy potential of the strongest structures. Folding parameter was weighted at 17.5% for all reported experiments. The folding weight given was selected based on advice by the program developer, i.e. to keep low values for folding. The physico-chemical evaluation considered here only accounts for the energy involved in secondary structure intramolecular base pairing. However, as demonstrated in this paper, further evaluations involving loop position with respect to chip surface were also important in the estimation of the influence on the folding.

Finally, Low complexity parameter assigns high-scored values to probe sequences displaying a high degree of complexity in the primary nucleotide sequence, and thus its weight contributes to enhance the specificity of probe. Low complexity parameter was weighted at 12.3% for all reported experiments, as standardized by the program developer.

3.2. Computational design of probes

Once the probe length (20 mers) was defined, the program output indicated the calculated scores relative to the sequences in the different positions on the target DNA.

Suitable positions on target sequence for high-scored probes are displayed in red (Wernersson et al., 2007), whereas low-scored probes, with expected low performances in hybridizing target are colored in gray. Evaluating probes distribution along the target sequence, we can have an idea of the value of the different considered parameters, by walking on the target sequence (see Fig. S1). For example, Low complexity score in our case, oscillates between 0.9 and 0.6 shows that this parameter does not fluctuate dramatically. Thus, it has little influence over the total score. Cross-hybridization score varies, along whole sequence, between the maximum and minimum (1–0) value, identifying certain sequences, expected to be very selective (1–9, 112–115) and other probes with less specificity for the target. Folding score does not vary significantly along the sequence. It has about maximum values in all positions except few regions, where the value is still relatively high. This behavior could be due to the fact that intra-molecular paring involves fewer bases than complementary hybridization with target sequence.

For the considered beta-actin sequence (227 bases), only few regions are suitable for probe mapping, and only 10 possible sequences displayed show scores higher than 0.8. Among these high-scored probes, we selected two probe sequences with equal score of 0.936 to be tested experimentally for computational approach validation, mapping position 5–24 (Probe 2) and position 101–120 (Probe 1).

Three more probes, namely Probes 3, 4 and 5, with decreasing scores from 0.725 down to 0.255, were also selected and are

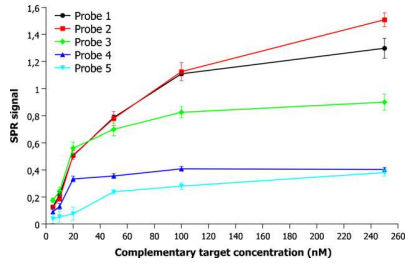

Fig. 1. SPRi calibration for the selected five probes. The reflectivity different percentage is reported for each probe vs. the target concentration in a range between 2 μM and 250 μM.

reported in Table 1. Table 2 summarized the total scores and the values resulting from the software calculations for the parameters of the selected probes.

The selected five probes were then experimentally tested by SPRi to evaluate the validity of computational approach used.

3.3. Validation of DNA probes by SPRi transduction

The five probes selected were immobilized on the same chip surface and tested for their ability to bind to the complementary sequences.

Thiolated probes were coupled to gold surface in an array format, and remaining gold surface was then passivated using mixed thiols at different length (see Section 2). Complementary targets were injected separately in concentration range from 2 nM to 250 nM and binding signals were recorded as percent variation of intensity of reflected light $\Delta R\%$. In Fig. 1 calibration curves obtained for the five selected probes were shown. In agreement with OligoWiz calculations, calibration curves display different behaviors, demonstrating that probes follow the *in silico* predictions. Calculated scores results thus correlated with SPRi responses obtained from calibration curves. In particular, best-scored probes (Probes 1 and 2) show highest signals for all the tested concentrations; Probe 3 (score 0.725) gave intermediate signals between high and low scored probes and Probes 5 and 4 displayed the worst results. This behavior is clearly shown in Fig. 2 where scores compared with SPRi responses recorded at 100 nM target concentration, within the dynamic range of the biosensor.

3.4. Melting experiments

The strength of possible secondary structures on probes was experimentally evaluated by UV melting experiments (Eryazici et al., 2010). Folding and unfolding behavior of each probe sequence in solution was studied as temperature function. The number of bases involved in secondary structures and their melting temperatures could give an idea about the strength of the conformation of a given probe at the given temperature on the chip. In DNA-based sensing, this information is strategic for estimating the potential intermolecular folding of the selected probe on the chip at given working temperature. The lower the melting temperature, the higher is the number of unpaired bases at the working temperature. Also the hyperchromic effect for each probe considered, i.e. the variation of the intensity of absorbed light. The solution employed in melting experiments thus the same as applied in SPRi-based experiments. Melting profiles are reported in Fig. 4. Probe 1, one of the two best scored, does not show any melting curve,

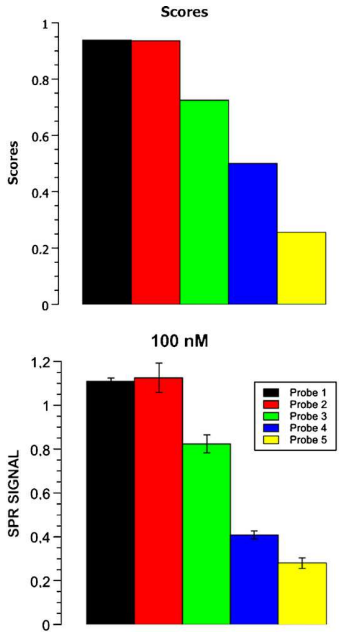

Fig. 2. SPR signals for the selected probes for the target concentration 100 nM (upward) and comparison with compared to calculated scores (down).

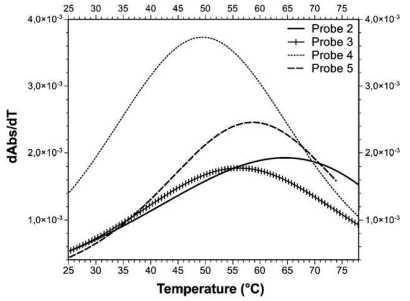

Fig. 4. Derivative curves of melting profiles are shown for each probe. Probe 1 is the only one that does not fold into a secondary structure, thus no melting curve was recorded.

meaning that, in the considered temperature range, its sequence remained unfolded. However, Probe 2, with the same score as Probe 1, displayed a melting curve characterized by an intense hyperchromic effect and the highest melting temperature (64 °C) among the considered probes. Probe 4 results the probe with lowest melting temperature (49 °C) but with hyperchromic effect similar to Probe 2. Probe 3 and Probe 5 curves profiles show intermediate melting temperature, 56 °C and 59 °C respectively. Considering the hyperchromic effect, Probe 3 and Probe 5 also showed intermediate values.

In Fig. 3 the estimated secondary structures and melting profiles for the selected probes were reported. In particular, estimated structure for Probe 2 showed four bases involved in the loop, at the 5′ end, in close proximity to sensing surface. This secondary structure results to be one of the most stable with respect to the others, as deduced from melting profiles (i.e. from hyperchromic effect) and from data obtained with Mfold software (Zuker, 2003). Free energy of Probe 2 loop is comparable to Probe 5, the worst scored probe.

It appeared that the location of these secondary structures occurring along the probe was important. In contrast to Probe 2, all the other three probes, had folding in region closer to 3′ end, which was more exposed to solution. This folding orientation may influence the hybrid formation at the sensor surface, between the probe and its complementary sequence in solution. This evaluation suggested that the relative position of the loops on probes should be considered in the computational evaluation. It could be useful to

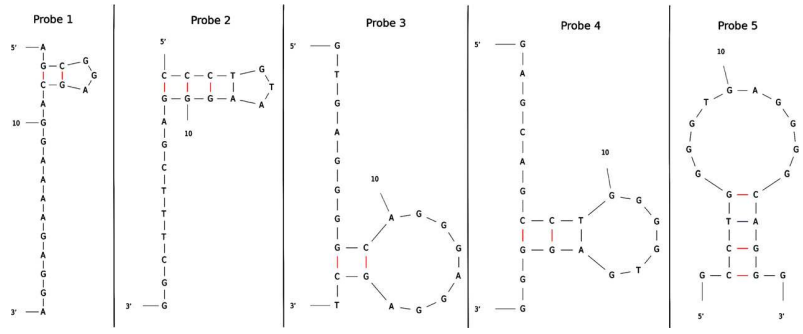

Fig. 3. Probes folding simulated with Mfold (Zuker, 2003) in order to mimic experimental conditions (DNA at 25 °C, [Na^+] = 0.34 M).

be able to manipulate this aspect by including a new factor among the parameters weighted in the program.

However, it was thus apparent that neither hyperchromic effect nor melting temperature of the loop alone is enough to predict the probe behavior. If we consider the probe solely on the basis of the intensity of the hyperchromic effect or melting temperature, we would not have insightful informations about the hybridization characteristics of probes on the sensor. This supported the idea that only a combination of suitable parameters, integrated using a rational design, can provide complete description of the phenomenon; in our case, we showed that a computational assisted tool such as OligoWiz (Wernersson et al., 2007), could take into account the different parameters involved for optimizing probe design in nucleic acid-based sensing.

Probe design is a delicate step in sensor development and to the best of our knowledge this is the first reporting about rationalization of probe selection in DNA-based sensing. This effort aimed to standardize the different steps in designing model probes for nucleic acid based sensing in order to go further in analytical system performances, in line with previously reported work on signal sampling and data management standardization (Scarano et al., 2010).

The approach has a non-restricted validity and can eventually be applied to different transduction principles. The reported method can also be used to select probes as secondary sequences, to hybridize the target analyte in a different region, as reported in electrochemical and optical sensing for signal detection or enhancements.

4. Conclusions

We described here a novel and rational approach in probe design by computational evaluation coupled with experimental validation for application to nucleic acid sensing. Optimized performances of the sensor achieved with best scored *in silico* probes, demonstrated the validity of the theoretical modelling, in affinity biosensor analysis. Our experimental results are in complete agreement with the assigned scores, validating the theoretical evaluation as an useful tool for selecting biosensor receptors. It has general validity and it can be extended, for example, to RNA analysis, like microRNA which is now of interest in cancer diagnostic or coupled to different transduction principles.

Acknowledgments

Maria Minunni, Coordinator of the project "Affinity-Based Biosensing (ABBs) for gene doping detection: a pilot study" would like to thank the World Antidoping Agency (WADA), for funding within the "Scientific Research Grant-2008, Competition topic C: Detection of Prohibited Substances/Methods: novel methodologies".

Appendix A. Supplementary data

Supplementary data associated with this article can be found, in the online version, at doi:10.1016/j.bios.2011.06.004.

References

Allara, J., Nuzzo, R.G.J., 1983. J. Am. Chem. Soc. 105, 4481–4483.
Brockman, J.M., Frutos, A.G., Corn, R.M., 1999. J. Am. Chem. Soc. 121, 8044–8051.
Buser, O., 1983. Cold Regions Sci. Technol. 8, 155–163.
Caruso, F., Rodda, E., Neil Furlong, D., Niikura, K., Okahata, Y., 1997. Anal. Chem. 69, 2043–2049.
Chen, Y., Kung, S.C., Taggart, D., Halpern, A.R., Penner, R., Corn, R.M., 2010. Anal. Chem. 82, 3365–3370.
Dell'Atti, D., Tombelli, S., Minunni, M., Mascini, M., 2006. Biosens. Bioelectron. 21, 1876–1879.
D'Orazio, P., 2003. Clin. Chim. Acta 334 (1-2), 41–69.
Eryazici, I., Prytkova, T.R., Schatz, G.C., Nguyen, S.T., 2010. J. Am. Chem. Soc. 132, 17068–17070.
Gifford, L.K., Sendroiu, I.E., Corn, R.M., Luptak, A., 2010. J. Am. Chem. Soc. 132, 9265–9267.
Healey, B.G., Matson, R.S., Walt, D.R., 1997. Anal. Biochem. 251, 270–279.
Halpern, A.R., Chen, Y., Corn, R.M., Kim, D., 2011. Anal. Chem. 83, 2801–2806.
Kaderali, L., Schliep, A., 2002. Bioinformatics 18, 1340–1349.
Kukanskis, K., Elkind, J., Melendez, J., Murphy, T., Miller, G., Garner, H., 1999. Anal. Biochem. 274, 7–17.
Letowski, J., Brousseau, R., Masson, L., 2004. J. Microbiol. Methods 57, 269–278.
Li, F., Stormo, G.D., 2001. Bioinformatics 17 (11), 1067–1076.
Lucarelli, F., Tombelli, S., Minunni, M., Marrazza, G., Mascini, M., 2008. Anal. Chim. Acta 609 (2), 139–159.
Mannelli, I., Minunni, M., Tombelli, S., Wang, R., Spiriti, M.M., Mascini, M., 2005. Bioelectrochemistry 66, 129–138.
Mulle, J.G., Patel, V.C., Warren, S.T., Hegde, M.R., Cutler, D.J., Zwick, M.E., 2010. PLoS One 5 (3), e9921.
Powdrill, T.F., 2003. Publication number: WO03057858 (A2), European: C12Q1/68B10A; Y01N6/00, Application number: WO2003US00069 20030102.
Rahmann, S., 2003. IEEE Computer Society Bioinformatics Conference (CSB'03), p. 57.
Scarano, S., Mascini, M., Turner, A.P.F., Minunni, M., 2010. Biosens. Bioelectron. 5 (25), 957–966.
Sato, Y., Fujimoto, K., Kawaguchi, H., 2003. Colloids Surf. B 27 (1), 23–31.
Sendroiu, I.E., Gifford, L.K., Luptak, A., Corn, R.M., 2011. J. Am. Chem. Soc. 133, 4271–4273.
Smith, E.A., Wanat, M.J., Cheng, Y., Barreira, S.V.P., Frutos, A.G., Corn, R.M., 2001. Langmuir 17, 2502–2507.
Tothill, I.E., 2009. Semin. Cell Dev. Biol. 20 (1), 55–62.
Tedeschi, L., Citti, L., Domenici, C., 2005. Biosens. Bioelectron. 20 (11), 2376–2385.
Teles, F.R.R., Fonseca, L.P., 2008. Talanta 2, 606–623.
Tomiuk, S., Hofmann, K., 2001. Brief. Bioinform. 2 (4), 329–340.
Wang, X., Seed, B., 2003. Bioinformatics 19, 796–802.
Wernersson, R., Juncker, A.S., Nielsen, H.B., 2007. Nat. Protoc. 2 (11), 2677–2691.
Wilson, P.K., Jiang, T., Minunni, M.E., Turner, A.P.F., Mascini, M., 2005. Biosens. Bioelectron. 20, 2310–2313.
Zuker, M., 2003. Nucleic Acids Res. 31 (13), 3406–3415.

Supplementary data

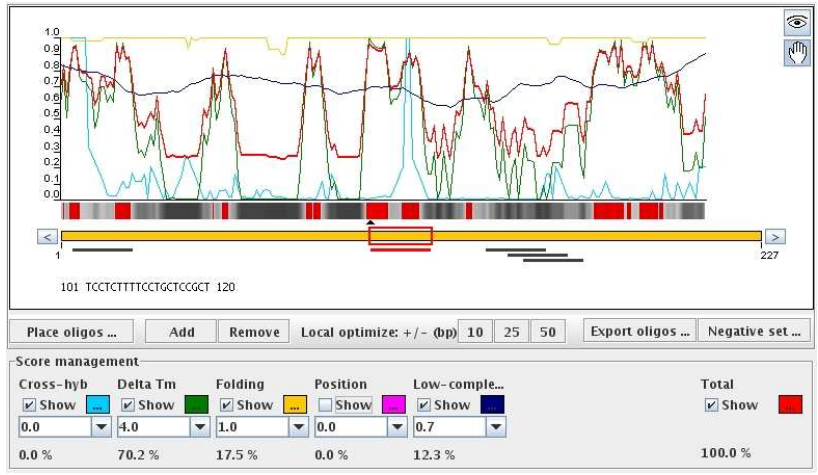

Figure S.1: Oligowiz (Wernersson *et al.*, 2007) output window in our model system. At the top, curves show scores' trends for each probe moving along the target sequence. The yellow bar represents the target sequence. The red and gray colors in the upper bar show areas on the target sequence where one can design probes with high and low score respectively. At bottom left, score management panel shows the relative weights for each parameter considered in calculation.

3.1.2 Direct Human Genomic DNA Detection

The direct detection, with no label, on non-amplified sample of genomic DNA is a challenging goal in biosensors development. In order to attain this result, here many optimization steps were studied for what concerns biosensor surface processing and genomic sample pretreatment.

Different fragmentation procedures by ultrasounds were tested on a commercial sample of human genomic DNA and each one was studied with gel electrophoresis, to evaluate the DNA fragmentation and SPRi biosensor. Among these one procedure, coupled to dsDNA thermal denaturation, resulted to be suitable for direct detection.

As a result, a label-free detection of a target gene (ABCB1) in human genomic DNA extracted from lymphocytes was performed and a calibration of the biosensor was successfully achieved down to 140 aM of target concentration.

Selectivity and specificity of the system were evidenced with a sandwich-like strategy, by using a secondary probe designed by the computational approach previously reported (see Section 3.1.1 *In Silico* Probe Design).

Furthermore, the biosensor resulted regenerable, and reusable for 20 cycles of measurements, that is one of the innovative aspects of this work.

This part of my research was reported here:

M. L. Ermini, S. Mariani, S. Scarano and M. Minunni, "Direct Detection of Genomic DNA by Surface Plasmon Resonance Imaging: An Optimized Approach", *Biosens. Bioelectron.*, **40**(1), 193-199 (2012).

Biosensors and Bioelectronics 40 (2013) 193–199

Contents lists available at SciVerse ScienceDirect

Biosensors and Bioelectronics

journal homepage: www.elsevier.com/locate/bios

Direct detection of genomic DNA by surface plasmon resonance imaging: An optimized approach

M.L. Ermini, S. Mariani*, S. Scarano, M. Minunni

Dipartimento di Chimica "Ugo Schiff" and CSGI, Università degli Studi di Firenze,Via della Lastruccia 3, 50019 Sesto F.no (FI), Italy

ARTICLE INFO

Available online 23 July 2012

Keywords:
Surface plasmon resonance imaging
Genomic
Biosensor
DNA
Nucleic acids

ABSTRACT

The direct detection of specific sequences in genomic DNA samples is very challenging in the biosensor-based approach. In this work we developed an optimized strategy for the direct detection of DNA sequences in human genomic samples by a surface plasmon resonance imaging technology. As model study, the target analyte was identified in a DNA sequence mapping the human ABCB1 gene. The computed-assisted approach was here applied for probe design. After a preliminary evaluation of the probe functioning by the complementary synthetic target, the system was applied to the direct detection of the target sequence in human genomic DNA extracted from lymphocytes. To achieve this result, several steps aimed to improve the analytical performances of the biosensor were studied and optimized. The immobilization chemistry, based on thiolated probes, was adapted here to non-amplified sequence detection. DNA sample pre-treatments, i.e. genomic fragmentation by ultrasounds and dsDNA denaturation by thermal treatment were also investigated. A sandwich-like strategy, by using a secondary probe, was also applied to understand and confirm the selectivity of the developed biosensor in detecting ABCB1 gene in genomic samples. Finally, a reliable calibration curve of ABCB1 was obtained with an experimental detection limit of 140 aM. Furthermore, the biosensor was well regenerable, assuring up to thirty cycles of effective measurements.

1. Introduction

Direct detection of a genomic DNA sample, bypassing amplification steps, is a very attractive analytical challenge, especially in biosensor-based approaches with application to molecular clinical diagnostics. The possibility of shortening the pre-analytical steps, i.e. sample pre-treatments, may lead to reduced analysis times and costs with positive impact on the detection of clinically relevant targets. In addition to key applications to the detection of genetic disorders and polymorphisms or mutations, molecular diagnostics could have important reflections also in the emerging field of theranostics. In any case, the starting point in molecular genomics is the analysis of DNA samples. Most of the reported approaches deal with amplified DNA samples and very few of them reach sensitive detection of genomic DNA avoiding sample amplification, i.e. by PCR. Different transduction principles are applied to this aim: fiber optics, surface plasmon resonance (SPR) and SPR imaging (SPRi), piezoelectric detection (Almadidy et al., 2002; Bianchi et al., 1997; Kaewphinit et al., 2010; Minunni et al., 2005; Scarano et al., 2011). Concerning SPR-based biosensors, our group reported about human, animal and plant DNA detection directly in genomic samples using BIAcore family instrumentation, also applying restriction enzymes, reaching a detection limit of 10 mg L^{-1} (Minunni et al., 2007). D'Agata et al. used a secondary amplification by gold nanoparticles on the hybridized target, revealing detectable concentrations down to and attomolar (D'Agata et al., 2011) in case of mismatch analysis and 41 zM (D'Agata et al., 2010) for full complementary sequences.

DNA amplification by PCR or other approaches undoubtedly leads to a large enrichment of the target sequences, but it also may introduce errors and it can be an additional step in the pre-analytical phase, which eventually could represent a further risk of contamination of the sample. However, some inescapable pre-analytical steps are still applied to genomic DNA analysis, i.e. DNA extraction, fragmentation, and denaturation. DNA fragmentation can be achieved by ultrasounds (D'Agata et al., 2010) or enzymatic digestion with restriction nucleases (Minunni et al., 2005; Minunni, 2012).

In any case, the extracted DNA is a double helix, in which the target sequence, complementary to the immobilized probe, is hidden. Therefore, it is mandatory that, after the fragmentation, the double-stranded DNA (dsDNA) is opened to allow the target sequence contained in it to hybridize the probe. The denaturation process, both on PCR amplified or unamplified genomic samples, can be achieved by simple thermal treatment or by alternative strategies aiming to prolong the single-stranded DNA (ssDNA) life

* Corresponding author. Tel.: +39 0554573312; fax: +39 0554573384.
E-mail address: s.mariani@unifi.it (S. Mariani).

0956-5663/$ - see front matter © 2012 Elsevier B.V. All rights reserved.
http://dx.doi.org/10.1016/j.bios.2012.07.018

time in solution by preventing the re-annealing of double strands, i.e. using small hybridizing oligonucleotide sequences (Minunni et al., 2005).

We recently demonstrated how, behind dedicated pre-analytical key steps, in DNA-based sensing the rational design of suitable capturing sequences can be strategic for improving the analytical performances of the biosensor (Ermini et al., 2011).

In this paper we reported about a DNA biosensor development for sensitive human genomic DNA (hDNA) detection, using the SPR imaging-based technology. As model study, we selected a fragment of 511 mers belonging to the human ABCB1 gene, consisting in the genomic sequence to be targeted. The human ABCB1 gene, on chromosome 7, was considered of clinical interest due to the so-called rs1045642 (C3435T) polymorphism and its possible involvement in several diseases (Campa et al., 2012; Drain et al., 2011; Jaitner et al., 2012; Kesimci et al., 2012; Penna et al., 2011; Sharma et al., 2012; Teh et al., 2012).

First, a computed-assisted design of a capturing probe (CProbe) was here applied, following our previously reported approach (Ermini et al., 2011). The hybridization reaction with the selected CProbe was then monitored and optimized by using the synthetic complementary target. For the applicability to hDNA samples, several steps were considered, i.e. suitable biochip surface treatments, hDNA fragmentation by ultrasounds, and dsDNA denaturation by thermal treatment. Finally, the system was applied to the detection of ABCB1 gene directly into genomic hDNA extracted from lymphocytes and a reliable calibration of the system was successfully obtained in the range 0.14–2.8 fM. A sandwich-like strategy, by using a secondary detecting probe (DProbe), was also applied to understand and confirm the selectivity of the developed biosensor in detecting ABCB1 gene in genomic samples. The biosensor was well regenerable, assuring up to thirty cycles of effective measurements.

2. Materials and methods

2.1. Design of DNA probes

Probes design was performed by the free software OligoWiz 2.0 (Wernersson et al., 2007). This *in silico* evaluation can be applied to select highly performing probes for biosensing applications (Ermini et al., 2011). This can be achieved starting from any given DNA target sequence by the rational setting of five parameters, here imposed as follows: cross-hyb 44.8%, delta Tm 29.9%, folding 14.9%, position 0.0% and low-complexity 10.4%. In this study the 511 mers fragment of Homo sapiens ATP binding-cassette, subfamily B (MDR/TAP) member (ABCB1) on chromosome 7 (position 87138390–87138900 of the chromosome 7, position 3673–4183 of coding sequence of the gene) was the genomic target sequence. When the sequence of the target analyte was inserted in the program, a set of scored probes normalized to values between 0 (worst probe) and 1 (best probe) was obtained. Among the ranked probes, we selected two sequences: the so-called capturing and detecting probes (namely CProbe and DProbe). Finally a DNA sequence was chosen to act as negative control: Unspecific probe, i.e. a probe designed on the Enhanced green fluorescent protein gene, not present in human genome. Detailed information about designed probes is reported in Table 1.

2.2. Solutions and reagents

Thiolated DNA probes, 10 μm in immobilization solution (IS), were covalently bound on the biochip gold surface. IS consisted of 1 M KH_2PO_4 (Merck, Italy), pH 3.8. If not otherwise specified, a solution containing 1 μm 11-mercapto-1-undecanol (MU) and 1 μm 6-mercapto-1-hexanol (MCH) was used to passivate the gold surface of biochips, for 20 h in a dark moist chamber. A solution of 300 mM NaCl, 0.02 M Na_2HPO_4, 0.1 mM EDTA, pH 7.4, 0.05% (w/v) of TWEEN® 20 (Polyethylene glycol sorbitan monolaurate) was used as hybridization solution (HS) in SPRi measurements. A solution 100 mM HCl was used to regenerate the biochip surface after each measurement cycle. PDMS (Sylgard 184 Silicone Elastomer Kit, Dow Corning, UK), was used for the micro-welled mask preparation (Scarano et al. 2011). Unless otherwise stated, reagents were purchased from Sigma-Aldrich (Milan, Italy).

All solutions were prepared in MilliQ water (Millipore Corporation, Massachusetts, USA) and filtered using vacuum filter cups (Millipore E express plus, 0.22 μm) and syringe filters (Puradisc, cellulose acetate, 0.2 μm from Whatman GmbH, Dassel, Germany). All oligonucleotides were purchased from Eurofins MWG Operon (Ebersberg, Germany); the corresponding sequences are reported in Table 1. Human genomic DNA was purchased from Novagen (Piacenza, Italy).

2.3. SPRi instrumental asset

All measurements were performed by SPRi-Lab$^+$ instrument from Genoptics-Horiba Scientific (Orsay, France). Interactions between probe and analyte were followed in real time by an optical apparatus integrated with a homemade fluidic system. The whole instrumentation asset was reported previously (Scarano et al., 2010).

2.4. Probes immobilization

A micro-welled PDMS support was used for DNA probes immobilization in array format on SF-10 glass prisms coated with gold (50 nM-thick) (SPRi-Biochip™, Genoptics-Horiba Scientific, Orsay, France) as previously described by Scarano et al., 2010. Thiolated probe solutions (0.8 μL, 10 μm in IS) were spotted in each micro-well and let immobilize on the gold surface exploiting the affinity between sulphur and gold, forming a self-assembled monolayer (SAM). Two spots were used as reference surface (only IS).

Table 1
Probes and target sequences.

Gene fragment of ABCB1 (511 mer)	5' CTCACAAGGAGGGTCAGGTGATCAGGTAAAGGTAACAA CTAACCCAAACAGGAAGTGTGGCCAGATGCTTGTATACAGGTAAGGGTGTGATTTGGTTGCTAATTTCTCTT-CACTTCTGGGAAACCAGCCCCTTATAAATCAAACTATAGGCCAGAGAGGCTGCCACATGCTCCCAGGCTGTT-TATTTGAAGAGAGACTTACATTAGGCAGTGACTCGATGAAGGCATGTATGTTGGCCTCCTTTGCTGCCCTCA-CAATCTCTTCCTGTGACACCACCCGGCTGTTGTCTCCATAGGCAATGTTCTCAGCAATGCTGCAGTCAAACAG-GATGGGCTCCTGGGACACGATGCCCAGGTGTGCTCGGAGCCACTGAACATTCAGTCGCTTTATTTCTTTGC-CATCAAGCAGCTGAAAACAAGAGTTCACAGATCAACTTCAGGACCAGCACACTTTGAATGTAGCACAATTAA-CATCATTATTTCTTACACTGAAACTGCCAAGTTACTGTGAG 3'
CProbe	5' HS—$(CH_2)_6$—GTCACTGCCTAATGTAAGTCTC 3'
CTarget	5' GAGACTTACATTAGGCAGTGAC 3'
Unspecific probe	5' HS—$(CH_2)_6$—GAGGGCGATGCCACCTAC 3'
DProbe	5' GTGGTGTCACAGGAAGAGATT–BIO 3'

After probe spotting, the biochip was subjected to vacuum for 20 min and incubated in a moist chamber for 72 h. When required, biochip surface was finally passivated with an aqueous solution of two mercaptoalchols: 1 μm 11-mercapto-1-undecanol (MU) and 1 μm 6-mercapto-1-hexanol (MCH) (Sigma, Milan, Italy) for 24 h. Then surface was washed with water, dried and finally housed into the instrument.

2.5. SPRi measurements

Measurements with the synthetic target were performed under a constant HS flow of 6 μL min^{-1} (11 μL flow cell internal volume). The corresponding calibration was carried out by injecting 100 μL of the complementary target within the 5–250 nM range of concentration. Targets reached the flow cell about 5 min after injection, lasting for about 10 min in contact with the CProbe, and allowing to monitor the hybridization process in real-time. At the end of the injection, HS flow washed the surface, removing the analyte excess from the cell.

Injections of genomic hDNA samples were performed under a high HS flow of 6000 μL min^{-1}. After samples reached cell (1.0 s), the flow was lowered to 6 μL min^{-1} and the hybridization between the CProbe and the sample was monitored for 10 min. Finally running buffer washed the surface to remove the unbound analyte from the cell. The calibration was performed by injecting 100 μL of the pre-treated genomic hDNA in the concentration range 0.3–6.0 mg L^{-1} (0.14–2.8 fM).

During hybridization, the binding was visualized by sensorgrams showing the percentage of reflectivity variation ($\Delta R\%$) in real time (s). Moreover, digital images of the punctual variation of reflected light on the surface were collected. SPR signals were acquired as $\Delta R\%$ difference between before and after (5 min from washing) the analyte binding. The biosensor surface was regenerated by 24 μL min^{-1} for 1 min of 100 mM HCl, making probes available for consecutive measurements.

2.6. Genomic pre-treatment and electrophoresis

Genomic samples (100 μL, 2.8 fM, 6 mg L^{-1}) were fragmented by applying different protocols of ultrasonication (VC100, 100 Watt Model, Sonics, Newtown, CT, USA): ultrasonic bath and ultrasonic immersion probe. Furthermore, different amplitudes and times of sonication were tested (Table S1). Ultrasonic fragmentation of genomic hDNA was evaluated by agarose (Affymetrix, Santa Clara, CA, USA) gel electrophoresis (0.5% w/w of agarose in TAE buffer 1X) with ethidium bromide (Shelton Scientific, Romeoville, IL, USA) as intercalating agent (0.004% w/w) and 100 bp DNA ladder and λ/HindIII as molecular weight markers (Fermentas, Thermo Scientific, Milan, Italy). Electrophoretic bands and distributions were visualized by an UV transilluminator (TFX-20M, Vilber Lourmat, France) and images were captured by a digital camera. Digital images were transformed in grayscale and analyzed with the image processing software ImageJ (open source software). After ultrasonication, the dsDNA was denatured at 95 °C for 7 min in C1000 Thermal Cycler (Bio-Rad, Italy), then cooled in ice-bath for three seconds and directly injected in SPRi-Lab^{+} instrument (100 μL). The protocol for fragmentation was chosen on the basis of the magnitude and the specificity of the SPRi signal obtained experimentally.

3. Results and discussion

The *in silico* approach by OligoWiz 2.0 was here applied to define suitable probing sequences to be used for ABCB1 gene detection in non-amplified hDNA samples. The approach applied is displayed in Fig. 1.

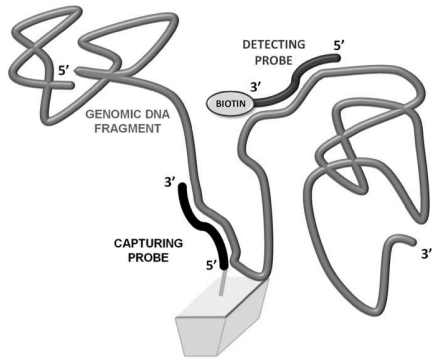

Fig. 1. Scheme of the strategy: thiolated CProbe, with estimated high performance in terms of selectivity, is immobilized on sensor surface, after incubating DNA thiolated probe 10 μM in IS on gold for 72 h in a moist chamber. This probe captures the complementary fragment in the genomic DNA sample. A secondary hybridization with DProbe on genomic DNA is performed, enhancing the signal and confirming the specificity of our strategy.

A 22 mers sequence, specific for ABCB1 gene, was selected as capturing probe (CProbe) and immobilized on the chip surface. This probe was conceived to selectively bind the target sequence on a higly conserved region of ABCB1 gene, with high specificity and selectivity. The target sequence was bound to the probe, and then exposed to the secondary hybridization with detecting probe (DProbe) to finally confirm the system selectivity in genomic DNA samples.

Key steps in sensor development were optimized to achieve sensitive and reliable genomic target conditions, i.e. sample pre-treatment (fragmentation and denaturation) and immobilization procedure.

3.1. In silico analysis

As previously reported by our group, improved analytical performances of a DNA biosensor can be achieved by the *in silico* rational design of probes (Ermini et al., 2011). Here the same computer-assisted approach was applied to design a selective strategy for the detection of a target sequence (511 mers, Table 1) on ABCB1 gene, used here as model system with potential application in theranostics. ABCB1 gene belongs to the ABC genes family, characterized by a high degree of homology. The CProbe was thus selected by OligoWiz 2.0 on the most conserved region of the 511 mers sequence, to assure a high degree of specificity, within the ABC genes. The selectivity of the CProbe was estimated by the Cross-hybridization (against the whole human genome DNA) score given by the program, resulting the highest value possible for this parameter, i.e. 1.0. Furthermore, an excellent score of 0.88 predicted high probing performances of CProbe.

To develop a sandwich-like assay, the DProbe was also selected by the program on a different region of the ABCB1 target sequence (see Fig. 1) with the aim to perform a secondary recognition, of the captured target gene. ABCB1 target sequence and nucleotidic probes are reported in Table 1.

3.2. Calibration of the biosensor with complementary target

Once selected, the capturing probe was immobilized on the gold surface of the biochip by thiol coupling, and its performance in binding the complementary synthetic target was experimentally tested by SPRi (Fig. 2).

The calibration was performed within the range of concentration 5–250 nM of synthetic complementary target, reaching signals up to $\Delta R\% = 1.38$. The sensor gave a linear response up to 25 nM, corresponding to a value of 0.45 of reflectivity variation percent. The average coefficient of variation percentage (CVav%) was here calculated as the percentage of standard deviations normalized for mean SPRi signals and averaged for all concentrations tested. This value resulted to be $< 5.8\%$ for each point of the calibration curve, demonstrating the reproducibility of the system. Unspecific probe was immobilized on the sensor surface as negative control and SPRi signals were monitored on it for all injected samples, for confirming the high selectivity and specificity of the interaction observed.

3.3. Genomic DNA detection

3.3.1. Pre-treatment optimization: ultrasonication and electrophoresis study

Genomic DNA fragmentation was achieved using two approaches. In particular, an immersion probe (dipped directly into the hDNA sample) or a sonication bath were used. The effect of amplitude frequency of ultrasounds and the sonication time applied were studied for both procedures (Table S1). Fragmentation efficiency was evaluated by agarose gel electrophoresis, obtaining a rough estimation of the fragmentation size (Fig. 3).

In particular, electrophoretic gel showed that the efficiency of fragmentation on genomic hDNA depended on the type of sonication applied. Fig. 3 shows the electrophoretical analysis, where the F1 sample was treated in an ultrasonic bath, whereas F2 and F3 samples were treated by immersing the ultrasonic probe directly in the genomic solution. The fragmented profile of each sample was compared to the untreated genomic DNA sample (lane G). F1 sample was characterized by a smear between 6557 and 23130 bp, meaning that a partial DNA fragmentation occurred respect to lane G. F2 and F3 samples showed an intermediate (100–1000 bp) and high (100–400 bp) degree of fragmentation, respectively. Therefore, only by the direct immersion of the ultrasonic probe (F2 and F3 lanes) a high DNA fragmentation was obtained. In this case, the highest amplitude applied was 20% (see Table S1), due to the rapid increase of temperature of the sample induced by the ultrasound probe. To evaluate the best protocol of sonication, fragmented hDNA samples were further thermally denatured and then tested at 2.8 fM in HS on biosensor. Among all sample tested, only F1 sample resulted to be detectable. Moreover, the F1 genomic direct hybridization on CProbe occurred only when the biochip surface was prepared with a suitable procedure (see next paragraph).

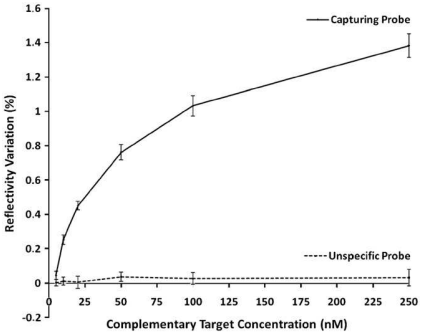

Fig. 2. SPRi signals recorded from CProbe and Unspecific probe immobilized on the biosensor surface by thiol coupling vs. different concentrations of the complementary synthetic target (from 250 nM to 5 nM). All measurement are performed under constant flux of HS (6 μl/min). Target are eluted in HS too and each injection volume is 100 μl (see Section 2). Contact time is 15 min and both dead time and washing time is 5 min.

3.3.2. Effect of alkane thiols on genomic DNA hybridization

The influence on the hybridization signal of alkane thiols used to passivate the biochip surface after probe immobilization was investigated. In particular, genomic samples were injected on biochipspassivated with thiols and on biochips not subjected to thiol passivation treatment. 2.8 fM of F1, F2 and F3 sonicated hDNA samples were injected separately on biochips modified by the two different procedures, and tested for their ability in hybridizing CProbe. No hybridization signal was obtained for the all three genomic samples (F1, F2 and F3) when the gold surface underwent thiol passivation (data not shown). Contrarily, on non-passivated biochips significant results were observed. In particular, among fragmented genomic samples, F1 gave a significant SPRi signal of 0.971 ($\Delta R\%$) on CProbe spots, and the hybridization in this condition was reproducible and specific, i.e. no interaction was recorded on bare gold, as displayed in the differential images of Fig. 4. Also the Unspecific probe (white-circled spots in Fig. 4) displayed the unexpected ability in binding the genomic samples (see next paragraph for discussion).

The different behaviors observed on passivated or not biochips could be explained by supposing that thiols may eventually modify the molecular packing of CProbe on receptor spots, leading to their reduced availability. For instance, possible disulfur superstructures of thiols could cause a reduced degree of freedom and/or a partial hindrance of the CProbe sequence.

3.3.3. Evaluation of the specificity by DProbe hybridization

In Fig. 4a, the differential image and the relative bar plot of SPRi signals obtained on F1 samples are reported. Biochip surface was modified by spotting the CProbe (6 spots), the Unspecific probe (2 spots), and two reference spots (2 spots, only IS). The Unspecific probe was chosen to be complementary to the EGFP gene, not present in the human genome. Therefore the SPRi signal obtained from the human genomic sample can be undoubtedly ascribed to unspecific interactions of the Unspecific probe. Data showed an intense signal on Unspecific probe ($\Delta R\% = 1.309$), higher than the signal on CProbe ($\Delta R\% = 0.971$). These results can be explained with the presence of fragmented genomic sequences able to hybridize Unspecific probe; contrarily, on CProbe spots, the lower signal could suggest the ability of the probe in catching selectively only fragments containing the corresponding ABCB1 target sequence.

To understand and confirm this assumption, after the hybridization on CProbe spots of F1 samples (Fig. 4a), the subsequent injection of DProbe (250 nM) was performed in a sandwich-like assay, as previously represented in Fig. 1. SPRi signals inferred from the secondary hybridization are reported in Fig. 4b. As expected, on Unspecific probe we obtained a signal enhancement of $\Delta R\% = 0.183$ whereas, on CProbe spots, a $\Delta R\% = 0.906$ was recorded. The relative intensity of the secondary hybridization

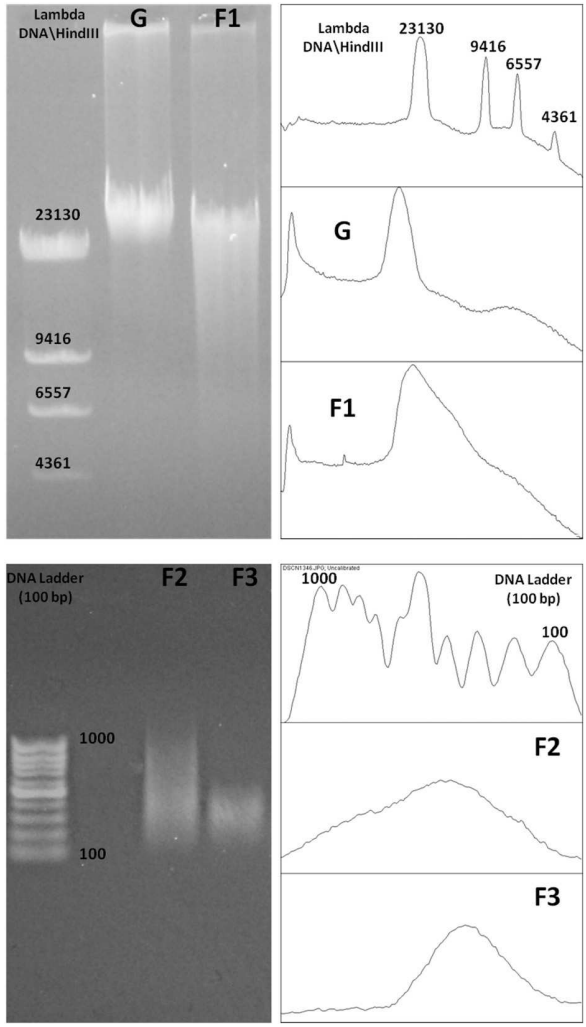

Fig. 3. Genomic DNA fragmentation for different ultrasonication procedures. Left: 0.5% agarose gel electrophoresis of genomic DNA samples. 100 bp DNA ladder and Lambda DNA/HindIII are used as markers. Right: distribution profiles of fragmentation visualized by ImageJ. Lane G is whole genomic DNA sample. Lane F1 is genomic DNA sample pre-treated in ultrasonication bath, and lane F2 and lane F3 are genomic samples pre-treated by immersing ultrasonic probe at different setups (Table S1).

indicated that the CProbe bound with high efficiency only the target sequence. In fact, DProbe was complementary to a different region of ABCB1 gene, confirming the specificity of the primary hybridization between the capturing probe and the genomic DNA fragment of interest. DProbe was previously tested in preliminary analyses on the biosensor to evaluate possible direct hybridization with immobilized probes (CProbe and Unspecific probe) even in absence of human genome. No crossing interaction was recorded among

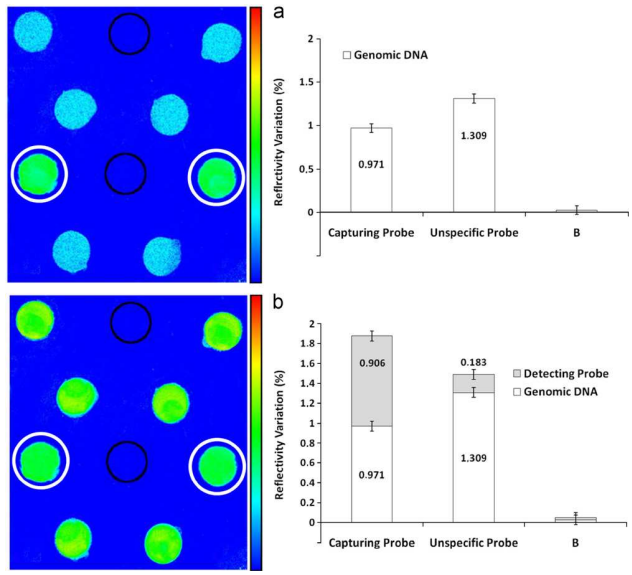

Fig. 4. Comparison between SPR signals obtained on CProbe and Unspecific probe, immobilized on the biosensor surface by thiol coupling, hybridized with pre-treated genomic F1 sample at 2.8 fM (100 μl in HS, the pre-treatment procedure is reported in Section 3.3.1) (a), and after the hybridization with DProbe (b), corresponding differential images of the spotted biochip surface are shown on the left. The bright spots represent areas where hybridization occurred between genomic DNA and capturing probe. Blank spots are circled in black and are reference spots where no probe is immobilized. Unspecific probe spots are circled in white.

probes, confirming that the sandwich-like assay carried out by using DProbe is a valid strategy to distinguish between specific and unspecific interactions possibly occurring on the sensor.

3.3.4. Calibration of the biosensor with genomic DNA

The biosensor was finally calibrated with genomic samples prepared by the same pre-treatment previously used to obtain sample F1. After thermal denaturation, genomic DNA was tested at the following concentrations: 0.14, 0.28, 0.70, 1.4, and 2.8 fM in HS. Points were fitted with a line, showing a good coefficient of determination ($R^2 = 0.990$), as reported in the upper part of Fig. 5a.

The experimental coefficient of variation %, averaged on all concentration points, resulted 17%, a very encouraging result considering the high complexity of the tested matrix and the absence of any signal amplification. The bottom part, Fig. 5b, reports the further application of the sandwich-like assay carried out with DProbe on each concentration of the genomic solutions tested. As shown in the bar plot, the SPRi signal enhancement (gray bar portion) due to the DProbe hybridization, resulted not directly correlated to the concentration of the tested DNA sample. This behavior could be due to the high variability of the lengths of fragmented DNA bound to the CProbe, and to possible intra- and inter-strand interactions among fragments. Single-stranded fragments hybridized on CProbe could actually expose their ends forming secondary structures impairing the secondary recognition with DProbe. The biosensor was successfully regenerable for up to thirty cycles of measurements (data not shown), opening encouraging perspectives in the direct detection of genomic sequences for clinical purposes by-passing PCR amplification.

The analysis time was of 30 min, considering sonication, denaturation and sample hybridization with both capturing and detecting probes.

4. Conclusions

Direct human genomic DNA detection is an attractive goal for diagnostics and theranostics, allowing faster analytical responses and cost reduction of assays, when compared with amplified DNA analysis. An optimized approach to directly detect very low concentrations (140 aM) of human genomic DNA in a multiarray SPRi biosensor was here described. As model system, the ABCB1 gene was selected and nucleic acid-based probes were selected by a computational-assisted approach. Effects of ultrasonic fragmentation on genomic DNA and of gold surface passivation after probe immobilization were studied. The best experimental conditions were found, ensuring the specific hybridization of fragmented DNA genomic sample on the specific probe. The biosensor was successfully regenerable for up to thirty cycles of measurements, foreseeing its potential application for routine analyses.

The developed biosensor allows the immobilization of a number of specific probes in a multi-array format, and could exploited for multi-analytes measurements and real time detection on whole

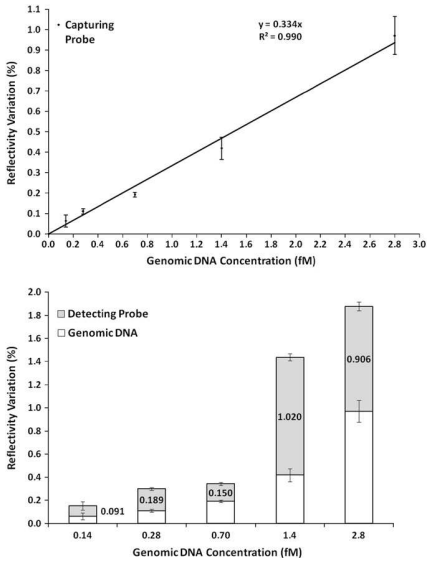

Fig. 5. Upper: SPRi signals recorded when different dilutions of the pre-treated genomic DNA flow on biosensor surface (HS flux of 6 μl/min, 100 μl injected, 15 min of contact time and both dead time and washing time is 5 min). Data are interpolated with a line with a very good correlation coefficient. Bottom: SPRi signals obtained after primary recognition of the genomic samples hybridizing with CProbe (immobilized on biochip surface by a thiol group) are coupled with signals enhancement obtained from subsequent injection of 250 nM DProbe in HS (see Section 2).

genomic samples. Moreover, the selectivity of this interaction was very well demonstrated by the use of a secondary detecting probe in a sandwich-like assay. This model strategy can be applied in the near future to the punctual detection of sequences of clinical relevance, i.e. point mutations, polymorphisms, and deletions.

Acknowledgments

The authors would like to thank the Fondazione ARPA progetto Dolore for financial support (coordinator Prof. Roberto Barale, Dip. di Biologia, Univeristà di Pisa, Italy).

Appendix A. Supplementary information

Supplementary data associated with this article can be found in the online version at doi:10.1016/j.bios.2012.07.018.

References

Almadidy, A., Watterson, J., Piunno, P.A.E., Raha, S., Foulds, I.V., Horgen, P.A., Castle, A., Krull, U., 2002. Analytica Chimica Acta 461, 37–47.
Bianchi, N., Rutigliano, C., Tomassetti, M., Feriotto, G., Zorzato, F., Gambari, R., 1997. Clinical and Diagnostic Virology 8 (3), 199–208.
Campa, D., Sainz, J., Pardini, B., Vodickova, L., Naccarati, A., Rudolph, A., Novotny, J., Försti, A., Buch, S., von Schönfels, W., Schafmayer, C., Völzke, H., Hoffmeister, M., Frank, B., Barale, R., Hemminki, K., Hampe, J., Chang-Claude, J., Brenner, H., Vodicka, P., Canzian, F., Xiong, M., 2012. PloS One 7 (3), e32784.
D'Agata, R., Corradini, R., Ferretti, C., Zanoli, L., Gatti, M., Marchelli, R., Spoto, G., 2010. Biosensors and Bioelectronics 25, 2095–2100.
D'Agata, R., Breveglieri, G., Zanoli, L.M., Borgatti, M., Spoto, G., Gambari, R., 2011. Analytical Chemistry 83 (22), 8711–8717.
Drain, S., Flannely, L., Drake, M.B., Kettle, P., Orr, N., Bjourson, A.J., Catherwood, M.A., Alexander, H.D., 2011. Leukemia Research 35 (11), 1457–1463.
Ermini, M.L., Scarano, S., Bini, R., Banchelli, M., Berti, D., Mascini, M., Minunni, M., 2011. Biosensors and Bioelectronics 26, 4785–4790.
Jaitner, J., Morath, T., Byrne, R.A., Braun, S., Gebhard, D., Bernlochner, I., Schulz, S., Mehilli, J., Schomig, A., Koch, W., Kastrati, A., Sibbing, D., 2012. Circulation: Cardiovascular Interventions 5 (1), 82–88.
Kaewphinit, T., Santiwatanakul, S., Promptmas, C., Chansiri, K., 2010. Sensors 10, 1846–1858.
Kesimci, E, Engin, A.B., Kanbak, O., Karahalil, B., 2012. Gene 493 (2), 273–277.
Minunni, M., Tombelli, S., Fonti, J., Spiriti, M.M., Mascini, M., Bogani, P., Buiatti, M., 2005. Journal of the American Chemical Society 127 (22), 7966–7967.
Minunni, M., Tombelli, S., Mascini, M., 2007. Analytical Letters 40 (7), 1360–1370.
Minunni, M., 2012. Piezoelectric-based sensing for sensitive nucleic acid detection. In: Spoto, G.; Corradini, R. (Eds.), Detection of Non-Amplified Genomic DNA. Springer.
Penna, G., Allegra, A., Alonci, A., Aguennouz, M., Garufi, A., Cannavò, A., Gerace, D., Alibrandi, A., Musolino, C., 2011. Medical Oncology 28 (4), 1549–1554.
Scarano, S., Scuffi, C., Mascini, M., Minunni, M., 2010. Biosensors and Bioelectronics 26, 1380–1385.
Scarano, S., Ermini, M.L., Spiriti, M.M., Mascini, M., Bogani, P., Minunni, M., 2011. Analytical Chemistry 83 (16), 6245–6253.
Sharma, V., Kaul, S., Al-Hazzani, A., Prabha, T.S., Rao, P.P., Dadheech, S., Jyothy, A., Munshi, A.J., 2012. Neurological Sciences 315 (1–2), 72–76.
Teh, L.K., Mohamed, N.I., Salleh, M.Z., Rohaizak, M., Shahrun, N.S., Saladina, J.J., Shia, J.K., Roslan, H., Sood, S., Rajoo, T.S., Muniandy, S.P., Henry, G., Ngow, H.A., Hla, U.K.T., Din, J., 2012. APPS Journal 14 (1), 52–59.
Wernersson, R., Juncker, A.S., Nielsen, H.B., 2007. Nature Protocols 2 (11), 2677–2691.

3.1.3 Discrimination of Single Nucleotide Polymorphism on Human Genomic DNA after Whole Genomic Amplification

The aim of this work was to find a suitable strategy for detecting a single nucleotide variation in the ABCB1 gene's sequence on blood sample enriched by whole genomic amplification (WGA). This kind of amplification, in contrast to classical PCR treatment, amplifies all sequence present in blood sample, changing the amount of DNA present in the sample but not preselecting a specific sequence. It is easy, fast and a routine standard procedure.

Our approach for SNPs detection consisted first in *in silico* probe design, second in the developing a strategy to detect SNP (rs1045642), *i.e.* carrying various steps of optimization of the experimental conditions in terms of probe length, position of SNP along sequence and sequence functionalization. Third, finally the strategy was tested directly on random amplified genomic samples from human blood.

It was demonstrated that this method allows discriminating between full match and mismatching samples, guaranteeing successful detection of the polymorphism on the ABCB1 gene, in this case.

This part of my research was reported here:

M. L. Ermini, S. Mariani, S. Scarano, D. Campa, R. Barale and M. Minunni, "Single Nucleotide Polymorphism Detection by Optical DNA-Based Sensing Coupled to Whole Genomic Amplification", *Anal. Bioanal. Chem.*, In press. DOI:10.1007/s00216-012-6345-4

Anal Bioanal Chem
DOI 10.1007/s00216-012-6345-4

ORIGINAL PAPER

Single nucleotide polymorphism detection by optical DNA-based sensing coupled with whole genomic amplification

M. L. Ermini · S. Mariani · S. Scarano · D. Campa · R. Barale · M. Minunni

Received: 20 June 2012 / Revised: 1 August 2012 / Accepted: 8 August 2012

Abstract The work presented here deals with the optimization of a strategy for detection of single nucleotide polymorphisms based on surface plasmon resonance imaging. First, a sandwich-like assay was designed, and oligonucleotide sequences were computationally selected in order to study optimized conditions for the detection of the rs1045642 single nucleotide polymorphism in the gene *ABCB1*. Then the strategy was optimized on a surface plasmon resonance imaging biosensor using synthetic DNA sequences in order to evaluate the best conditions for the detection of a single mismatching base. Finally, the assay was tested on DNA extracted from human blood which was subsequently amplified using a whole genome amplification kit. The direct detection of the polymorphism was successfully achieved. The biochip was highly regenerable and reusable for up to 20 measurements. Furthermore, coupling these promising results with the multiarray assay, we can foresee applying this biosensor in clinical research extended to concurrent analysis of different polymorphisms.

Keywords Surface plasmon resonance imaging · Whole genome amplification · DNA-based sensing · Pharmacogenomics · Single nucleotide polymorphism · *ABCB1*

Published in the special issue *Analytical Science in Italy* with guest editor Aldo Roda.

Electronic supplementary material The online version of this article (doi:10.1007/s00216-012-6345-4) contains supplementary material, which is available to authorized users.

M. L. Ermini · S. Mariani · S. Scarano · M. Minunni (✉)
Dipartimento di Chimica, Università di Firenze,
Via della Lastruccia 3,
50019 Sesto Fiorentino, Italy
e-mail: maria.minunni@unifi.it

S. Scarano · M. Minunni
Consorzio per lo Sviluppo dei sistemi a Grande Interfase (CSGI),
Via della Lastruccia 3,
50019 Sesto Fiorentino, Italy

D. Campa
Genomic Epidemiology Group,
German Cancer Research Center DKFZ,
Im Neuenheimer Feld 280,
69120 Heidelberg, Germany

R. Barale
Dipartimento di Biologia, Università di Pisa,
Via Derna 1,
56126 Pisa, Italy

Published online: 06 September 2012

Introduction

The detection of single nucleotide polymorphisms (SNPs) in target genes is an attractive goal for diagnostics and pharmacogenomics. A SNP is a DNA sequence variation of a single nucleotide. SNPs represent 90 % of all human polymorphisms and they are present in the population with allelic frequencies of 1 % or greater [1]. Most of these variations in the human genome are neutral (i.e., they have no effect on gene expression, regulation, or function). In some cases, SNPs that are present in coding sequences or gene regulatory regions can alter gene functions and change individual characteristics. For example, they could confer increased susceptibility to a particular disease or might elicit different responses to drugs [2]. For this reason, applied research on SNPs may be of relevance for clinical practice.

Different approaches concerning DNA-based sensing for detection of SNPs based on different transduction principles have been reported in the literature [3–8]. Interesting strategies have been reported for optical sensing and, in particular, surface plasmon resonance (SPR) transduction. Both nucleic acids and peptide nucleic acids have been used as a recognition element, either immobilized on a chip or used in

a sandwich-like assay [9]. In some works, specific proteins such as DNA mismatch repairing proteins [10–14] or enzymes [15] were used to achieve mismatch recognition. In the methods developed, attention was focused on sample pretreatment, which consists of extraction of DNA, in the case of amplification of the target fragment, and its subsequent dissociation to obtain single-stranded DNA that is able to hybridize the probe immobilized on the sensing surface. In some cases, denaturing agents, such as formamide, were used [16]. To increase the SPR signal intensity, many works attempted signal-enhancing strategies, aiming to achieve the detection of the target sequence directly in nonamplified genomic DNA, where the target analyte is found at femtomolar to attomolar concentrations.

In most of the published works, nanostructures were applied in the design of sandwich-like assays, using nanoparticles as mass enhancers or to obtain plasmon coupling. Zanoli et al. [17] recently reported interesting advances in DNA-sensing strategies using functionalized gold nanoparticles (AuNPs).

More recently, the application of SPR imaging (SPRi)-based sensing has been reported for the detection of target sequences in real samples of genomic DNA from plant and human blood samples in sandwiched AuNP-based assays [18]. In both cases, streptavidin-modified nanoparticles carrying specific biotinylated nucleotide sequences were used. In particular, marker sequences of transgenosis in genomic DNA samples carrying different amounts of genetically modified (GM) sequences (Roundup Ready soybean [18] were detected. The system was able to selectively identify the GM target sequence down to zeptomolar concentrations in solutions containing GM and GM-free genomic DNA at attomolar concentrations, even in the presence of a large excess of noncomplementary DNA [18].

The same approach was used for the detection of SNPs in human genomic DNA samples extracted from lymphocytes. In particular, the mismatch studied occurs in the globin gene and leads to thalassemia. The detection of targets or control DNAs was obtained by a sandwich hybridization strategy, using AuNPs conjugated to an oligonucleotide sequence complementary to the final tract of the DNA target not involved in the hybridization on the sensor surface. As sensing probes, peptide nucleic acids [19] were used and discrimination between fully matched and single-base-mismatched sequences was achieved down to 1 fM.

This challenging investigation opens up new possibilities for real applications of SPRi-based sensing. However, some room is left for SPRi-based sensitive detection of SNPs by exploring new assay designs by coupling an in silico computationally assisted approach for probe design, i.e., in silico selection, with suitable sample pretreatment.

In this report we aim to demonstrate the applicability of SPRi to the detection of SNPs in DNA extracted from human lymphocytes. We used a combination of an optimized computer-assisted design of the probes and sample pretreatment, consisting in the enrichment of the whole genomic material, which was extracted from the human lymphocytes to be analyzed. Usually in affinity-based sensing, when dealing with samples with a limited amount of DNA derived from a source, a standard PCR preamplification of the target gene or sequence is commonly performed before bioanalysis. In particular, so-called whole genome amplification (WGA) is an interesting alternative to conventional gene amplification approaches, and may potentially bypass some limiting factors when using genomic samples directly. It basically consists in a nonenzymatic fragmentation of the genetic material of the sample, followed by an amplification using universal primers. WGA is able to perform the amplification of the whole genome contained in a real sample, thus increasing the amount of DNA. A high-quality sample can be amplified one-million-fold while maintaining accurate loci and allele representation. Thus, it is evident that WGA is a promising tool to obtain a sufficient quantity of DNA from samples with a limited starting amount [20]. It is possible to apply WGA to samples collected from several years in order to study archived patient DNA. WGA can be useful when access to patient cells is limited, as in the case of samples obtained by needle biopsies and by laser capture microdissection from cancer patients [21].

As a consequence, WGA is expected to find new applications in biomedical research as a combined process of total nucleic acid amplification.

The SNP used here as a case study was rs1045642, which occurs in the gene *ABCB1* [ATP-binding cassette, subfamily B (MDR/TAP), member 1] at position 87138645 of chromosome 7. *ABCB1* is a key gene in pharmacogenomics and the rs1045642 SNP is related to the incidence of many diseases: aspirin resistance ischemic stroke and its subtypes [22], cancer risk [23], response to paroxetine in Japanese major depression [24], multidrug resistance in plasma cell myeloma [25], response and toxic effects of drugs in patients with advanced renal-cell carcinoma [26], and susceptibility to viral hepatitis A infection in Mexican Americans [27]. This wide spectrum of diseases indicates the reason for the interest in its detection.

In particular, here computationally selected probes were immobilized on an SPRi biochip surface in order to study optimized conditions for the detection of the rs1045642 SNP in the *ABCB1* gene. The SPRi biosensor was first developed using standard solutions to evaluate the best conditions for the detection of a single mismatching base. Probe characteristics were studied and optimized for the position of the polymorphic site along the DNA sequence, the length of the DNA probe, and its functionalization. First, synthetic DNA sequences were used to test and optimize the

assay, and then the strategy was tested on human DNA extracted from human blood and amplified by WGA.

Materials and methods

In silico analysis: rational probe selection and assay design

The DNA probes that were used for all the steps of the assay were selected both for immobilization on the biosensor surface and for polymorphism detection. Expected performances were evaluated and chosen by OligoWiz 2.0 [28], a software program with verified capacities for predicting the performances of probes in biosensing applications [29]. A score between 1 (maximum) and 0 (minimum) was assigned to nucleic acid sequences to represent the computationally estimated performances in hybridizing the target. This protocol provided recommendations on the design and offered the possibility to evaluate probe characteristics, allowing optimization of the working conditions of the assay.

Solutions, reagents, probes, and targets

Immobilization solution was used for immobilization of the probes on the gold chip surface; it was a 1 M aqueous solution of KH_2PO_4, pH 3.8. Hybridization solution was used as a running solution; it was an aqueous solution of 300 mM NaCl, 20 mM Na_2HPO_4, 0.1 mM EDTA, pH 7.4 with 0.05 % poly (ethylene glycol) sorbitan monolaurate (TWEEN® 20). Thiolic solution was used to passivate the biochip surface and it consisted of a 1 μM 11-mercapto-1-undecanol and 1 μM 6-mercapto-1-hexanol solution. All reagents were purchased from Sigma-Aldrich (Milan, Italy). All solutions were prepared in Milli-Q water (Millipore, Billerica, MA, USA) and filtered using vacuum filter cups (Millipore E express plus, 0.22 μm) and syringe filters (Puradisc, cellulose acetate, 0.2 μm from Whatman, Dassel, Germany).

Probes and targets were purchased from Eurofins MWG Operon (Ebersberg, Germany) and the corresponding sequences are reported in Table 1.

SPRi instrumentation and biochip preparation

An SPRi-Lab$^+$ instrument, from Genoptics-Horiba Scientific (Orsay, France), was used to test hybridization between probes and targets. Interactions were followed in real time by an optical apparatus, and a digital image of the biochip surface was shown displaying the interactions occurring on it. The whole instrumentation setup was previously reported [30].

Thiolated DNA probes were covalently immobilized on the gold chip with the help of a polydimethylsiloxane mask to obtain a removable microwelled support for deposition of the probes.

Probes (0.8 μL, 10 μM in immobilization solution) were incubated for 72 h after deposition. DNA targets were prepared in hybridization solution. Hybridization solution was also used as a running buffer for the SPRi instrument. Thiolic solution was used to saturate the gold surface.

Whole genome amplification

Genomic DNA was extracted from blood using a DNeasy 96 blood and tissue kit from QIAGEN. WGA was performed with Illustra GenomiPhi HY DNA amplification kits from General Electric, and genotyping was performed with TaqMan® SNP genotyping assays from Life Technologies/Applied Biosystems. Each injection of WGA samples was 100 μL of 6 ppm of amplified genome in hybridization solution, preheated for 7 min at 95° C. The genotype selected to assess the validity of the method was the C/C allele (the hypothesized ancestral allele).

The WGA sample was quantified using the fluorescent dye PicoGreen® (Molecular Probes, Eugene, OR, USA) with a TD-700 fluorimeter (Turner Biosystems, Milan, Italy). To calibrate the fluorimeter, five known concentrations of a standard double-stranded DNA from lambda phage (lambda DNA from Fermentas, Milan, Italy) were prepared and used as standards. Their fluorescence intensities were measured in the calibration range from 0 to 500 ppb. For quantification, the WGA sample was diluted in a buffer composed of 10 mM tris(hydroxymethyl)aminomethane hydrochloride and 1 mM EDTA, pH 7.5.

Results and discussion

The work presented here describes the optimization of a strategy for detection of SNPs in DNA sensing based on SPRi technology. First, the assay was designed by choosing DNA sequences by a computationally assisted approach; then the detection strategy was optimized for synthetic DNA sequences for the position of the polymorphic site along the DNA sequence, the length of the DNA probe, and its functionalization. The strategy developed was then tested on WGA samples obtained from human blood.

In silico analysis: rational probe selection and assay design

The first and crucial aspect to take into account when designing a DNA biosensor is the selection of the probe. In this work, the in silico design of the probes for SNP rs1045642 in the gene *ABCB1* was achieved. Probes were designed on a 511-mer fragment of the *Homo sapiens ABCB1* gene on chromosome 7 (from position 87138390 to position 87138900 of chromosome 7, from position 3673 to position 4183 of the coding sequence of the gene).

Table 1 Probes and target sequences

CProbe(5′thiol) (22-mer)	5′ HS-$(CH_2)_6$-GTCACTGCCTAATGTAAGTCTC 3′
CProbe(3′thiol) (22-mer)	5′ GTCACTGCCTAATGTAAGTCTC-$(CH_2)_6$-SH 3′
CTarget (22-mer)	5′ GAGACTTACATTAGGCAGTGAC 3′
Target 84 (84-mer)	5′GAGACTTACATTAGGCAGTGACTCGATGAAGGCATGTATGTTGGCCTCCTTTGTGCCCTCACAATCTCTTCCTGTGACACCAC 3′
DProbe END 21 (21-mer)	5′ HS-$(CH_2)_6$-GTGGTGTCACAGGAAGAGATT 3′
DProbe INT 21 (21-mer)	5′ HS-$(CH_2)_6$-TCACAGGAAGAGATTGTGAGG 3′
Target END 21 FM (21-mer)	5′ AATCTCTTCCTGTGACACCAC 3′
Target END 21 BIO FM (21-mer)	5′ BIO-AATCTCTTCCTGTGACACCAC 3′
Target END 21 MM (21-mer)	5′ GATCTCTTCCTGTGACACCAC 3′
Target END 21 BIO MM (21-mer)	5′ BIO-GATCTCTTCCTGTGACACCAC 3′
Target INT 21 FM (21-mer)	5′ CCTCACAATCTCTTCCTGTGA 3′
Target INT 21 BIO FM (21-mer)	5′ BIO-CCTCACAATCTCTTCCTGTGA 3′
Target INT 21 MM (21-mer)	5′ CCTCACGATCTCTTCCTGTGA 3′
Target INT 21 BIO MM (21-mer)	5′ BIO-CCTCACGATCTCTTCCTGTGA 3′
DProbe END 15 (15-mer)	5′ HS-$(CH_2)_6$-TCACAGGAAGAGATT 3′
DProbe END 12 (12-mer)	5′ HS-$(CH_2)_6$-CAGGAAGAGATT 3′
DProbe END 9 (9-mer)	5′ HS-$(CH_2)_6$-GAAGAGATT 3′
UProbe (18-mer)	5′ HS -$(CH_2)_7$-GAGGGCGATGCCACCTAC 3′
DProbe END 15 BIO MM (15-mer)	5′ TCACAGGAAGAGATT-BIO 3′
DProbe END 15 BIO FM (15-mer)	5′ TCACAGGAAGAGATC—BIO 3′

CProbe (5′ thiol) and CProbe(3′ thiol) are the same sequences used with 5′ and 3′ immobilization sites, respectively

Underlined polymorphic site, *END* polymorphic site in terminal position, *INT* polymorphic site in internal position, *DProbe* discriminating probe (sequence used for single nucleotide polymorphism detection), *UProbe* unspecific probe, *BIO* biotinylated

Considering the prediction by the software, we designed the assay as reported in Fig 1.

Three DNA sequences were chosen as follows: a capturing probe (score 0.88) estimated to be highly specific for the *ABCB1* gene. This probe was modified with a thiol group at the 5′ end CProbe(5′thiol) or at the 3′ end CProbe(3′thiol). Two other sequences were selected on the polymorphic site in order to find the best discriminating probe for SNP recognition. These discriminating probes mapped the polymorphic site within the sequence (DProbe INT 21, score 0.48) and at the 3′ end (DProbe END 21, score 0.55). They were chosen to be as similar as possible in terms of estimated binding performances (evaluated in silico) in order to ensure that any difference in the SPRi signal could be ascribed to the position of the polymorphism.

Mimicking WGA fragment hybridization with Target 84: primary response

Target 84 (Table 1) was used as a "simulator" fragment to mimic the target sequence of the *ABCB1* gene containing the SNP of interest. This target had the first 22 bases (5′ end) fully complementary to the capturing probe (selected with OligoWiz 2.0) and the polymorphic site at position 64 (see the assay scheme in Fig. 1).

CProbe(5′thiol) and CProbe(3′thiol) (same sequence but functionalized with a thiol group at the 5′ end and 3′ end, respectively) were preliminarily tested in order to establish which one provided the highest SPRi signal in hybridizing Target 84. Their performances were evaluated by testing a 250 nM solution of Target 84 in hybridization solution (see Fig. S1). This concentration was chosen for the good performances and reproducibility in terms of the SPRi signal (see Fig. 2), in particular using CProbe(5′ thiol). Figure S1 shows that the best signal was recorded for CProbe(5′thiol); thus, this was chosen for further hybridizations and for calibration of Target 84 on the SPRi biosensor. Signals obtained from hybridizations of different concentrations of Target 84 were recorded for CProbe(5′thiol) and the relative calibration curve was plotted (Fig. 2a).

The measurements were highly specific and no interaction was recorded on the gold surface (passivated by thiolic solution) or on blank reference spots (treated with immobilization solution and without probes). This is evidenced by the differential image of the interacting biochip shown in Fig. 2b. All modifications that occurred at the biochip surface are visualized with a color scale, with red corresponding to the highest signal. Target 84 hybridized with immobilized CProbe (five bright spots) but not with the control probe (UProbe, spot U in Fig. 2b). No interaction was recorded with the blank spot (control spot, spot B in Fig. 2b) or with the gold surface (blue area surrounding the spots). The reproducibility, expressed as

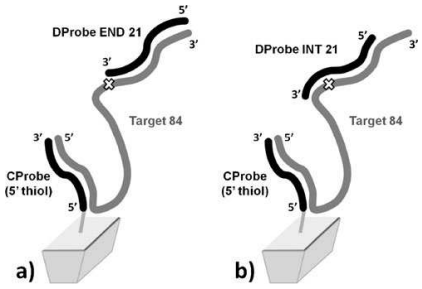

Fig. 1 The designed assay in the case of a discriminating probe carrying the polymorphic site at the end of the sequence (DProbe END 21, **a**) and in the case of the discriminating probe carrying the polymorphic site inside the sequence (DProbe INT 21, **b**). The capturing probe, designed to selectively capture the Target 84 fragment and designed for the *ABCB1* gene, was immobilized on the biochip surface

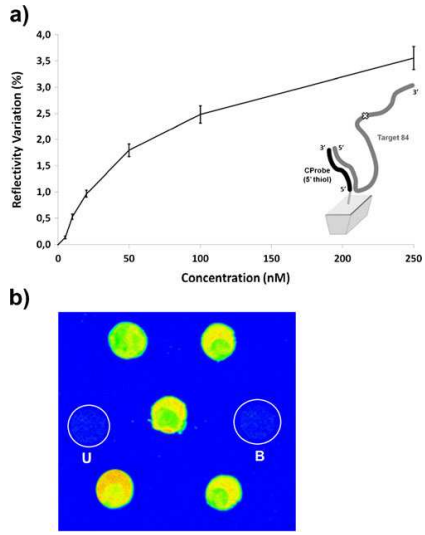

Fig. 2 **a** Variation of surface plasmon resonance imaging (SPRi) signals for CProbe(5′thiol) versus different Target 84 concentrations between 5 and 250 nM. For each point of the curve, the standard deviation was calculated and reported, resulting in a coefficient of variation of less than 9 %. **b** A differential image of the interaction between Target 84 (250 nM) and CProbe is shown. The *dark-blue area*, i.e., the area where no interactions occurred, is the gold on the chip surface (passivated by thiolic solution). *Bright areas* represent the spotted surface where immobilized CProbe interacts with Target 84. *U* indicates the unspecific probe spot and *B* indicates the blank spot for reference

the percent coefficient of variation (CV) was excellent, being less than 9 %.

Optimization of discriminating probe features for SNP detection

Step 1: influence of the position of the polymorphic site along the discriminating probe sequence

The aim of this step was to verify whether the position of the polymorphic site along the probes could influence the ability of the probe to discriminate the SNP. We chose two probes carrying the polymorphic site in a position within the sequence (DProbe Int 21) and at its 3′ end (DProbe End 21), respectively. Both probes were immobilized on the biochip surface. Calibration curves of both probes with the corresponding fully complementary targets are shown in Fig. S2.

In this optimization step, SPRi signals relative to the hybridization of probes with both the fully complementary targets (Target INT 21 FM and Target END 21 FM) and the single base mismatching targets (Target INT 21 MM and Target 21 END MM) were evaluated, using both biotinylated and nonbiotinylated target sequences. All combinations tested are reported in Fig. 3a. No significant differences in signals were recorded between matching and mismatching targets with nonbiotinylated sequences (details are provided in Fig. S3a). This finding is probably because the presence of one mismatching base did not significantly modify the stability of the duplex formed. Conversely, in case of biotinylated targets, significant differences between fully complementary targets (Target INT 21 BIO FM and Target END 21 BIO FM) and single base mismatching targets (Target INT 21 BIO MM and Target END 21 BIO MM) (Figs. 3, S3b) were found.

Considering all the combinations performed (summarized in Fig. 3a), we noticed that only one probe, carrying the mutation at the end of the sequence, could differentiate between fully matching and single base mismatching hybridization. Furthermore, biotinylated target sequences played a key role. Only by hybridizing biotinylated targets with an internal polymorphic site (Target INT 21 BIO FM and Target INT 21 BIO MM) on the probe carrying the terminal polymorphic site (DProbe END 21) was it possible to have significant discrimination for the SNP. To explain these findings, we believe that here, where fewer nucleotides (15-mers) are involved in the hybridization, the stability of the hybrid can be more easily affected by the presence of one mismatch than in a longer sequence. Furthermore, it seems that in our assay, biotin could play a key role in mismatch discrimination. Hence, from these results, biotin seems to enhance the influence of a single base mismatch on the stability of the duplex structure.

Step 2: influence of the length of the discriminating probe

The influence of probe length on the ability to detect a single mismatching base was also studied. Probes of

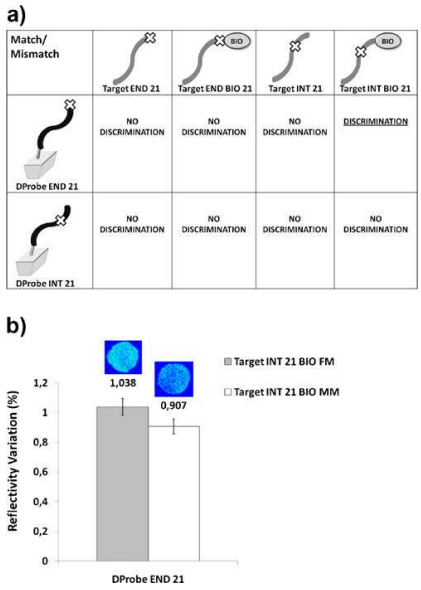

Fig. 3 Optimization of discriminating probe features for single nucleotide polymorphism detection: influence of the position of the polymorphic site along the sequence and the presence or absence of the biotin modification. **a** The ability to discriminate between a fully matching target and a single base mismatching one is reported for each probe–target combination tested. **b** SPRi values and differential images recorded from the only combination able to differentiate fully matching hybridization from mismatching hybridization, i.e., DProbe END 21 hybridized with Target INT BIO 21

different length were immobilized on the gold biochip surface: DProbe END 21 and other three probes, i.e., DProbe END 15, DProbe END 12, and DProbe END 9, obtained by shortening DProbe END 21 at the 3′ end.

Biotinylated and unmodified targets of 21-mers with the polymorphic site within the sequence were tested for hybridization, and SPRi signals were evaluated both for match and mismatch conditions. The results are shown in Fig. 4.

No signals were recorded with DProbe END 9. The other probes, 21-mers, 15-mers, and 12-mers, were all able to discriminate between matching and mismatching targets. Shortening the sequence can help to enhance the effect of the mismatching base, but a too short sequence is not able to hybridize, i.e., DProbe END 9. Very low signals were recorded from DProbe END 12, and the best ratio between full matching and mismatching signals was found for DProbe END 15. From these results we concluded that DProbe END

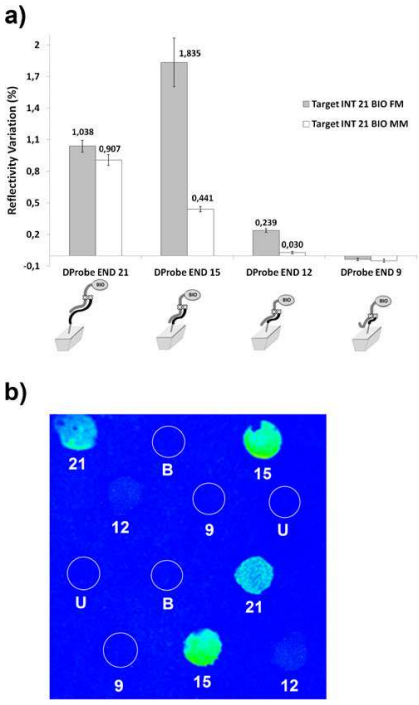

Fig. 4 **a** Reflectivity variation recorded for probes differing in length when they hybridize the fully complementary biotinylated target (*gray bars*) and the single base mismatching one (*white bars*). **b** Differential image for the fully matching target. The numbers *21*, *15*, *12*, and *9* indicate spots for DProbe END differing in length (21-mers, 15-mers, 12-mers, and 9-mers, respectively), *U* indicates the unspecific probe spots and *B* indicates blank spots for reference

15 was, among the probes tested, the one that could ensure good hybridization with targets and the highest difference in signals between the fully matching target and the mismatching one, giving the best performance in discriminating the SNP.

Mimicking the complete assay for the discrimination of SNP on Target 84

After the optimization of the probe, we found that the best conditions were ensured by a 15-base sequence modified with biotin at one end. We proceeded further to test the complete assay on the SPRi sensor (Fig. 1). DProbe END 15, with its optimal features, was tested on Target 84, which mimics the genomic sample in the assay. In this case we mimicked a sample of homozygote DNA with both alleles with the same sequence in the *ABCB1* gene. CProbe(5′thiol) was immobilized on the sensor surface and DProbe END 15 was used in a secondary hybridization for the discrimination of the SNP. The ability of the system to discriminate between match and mismatch was evaluated. Then, the results with the optimized probe were compared with those with an unmodified one (no biotin modification) to confirm if the biotin could play a key a role in the discrimination of the SNP on Target 84 (Fig. 5).

Biotinylated probes gave a signal difference corresponding to $\Delta\Delta R$=0.508 %; no signal was recorded from DProbe END 15 BIO MM on Target 84 (Fig. 5). Unmodified DProbe END 15 FM (ΔR=0.397 %) and DProbe END 15 MM (ΔR= 0.286 %) gave a lower but still significant difference in signals ($\Delta\Delta R$=0.111 %). Hence, biotinylated DProbe END 15 BIO FM and DProbe END 15 BIO MM were chosen for SNP discrimination on WGA samples.

Discrimination of SNPs in WGA samples from human blood

The assay, optimized as described already, was finally tested on WGA samples obtained from blood with the aim of

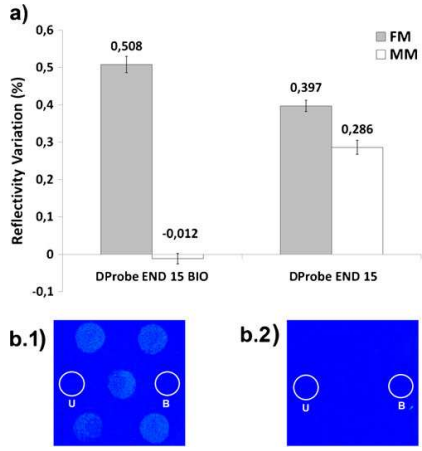

Fig. 5 SPRi signals from the secondary hybridization between the biotinylated discriminating probe (DProbe, *left*) and the unmodified one (*right*) on precaptured Target 84 (*a*). Signals for the fully matching (*FM*) DProbe (*gray bars*) are compared with those for the single base mismatching (*MM*) DProbe (*white bars*). The relative differential images of the interaction between captured Target 84 and DProbe END 15 BIO are reported for fully matching DProbe (*b.1*) and for single base mismatching DProbe (*b.2*)

verifying the possibility to discriminate the presence of the SNP also in samples containing a whole human genome. In fact, WGA allowed us to enrich a genomic sample, human in this case, from nanograms to micrograms. The final product corresponds to the whole starting genome and was composed of long fragments of random length. As proof of principle, we chose to analyze the putative ancestral allele, i.e., the homozygote C/C genotype of the SNP rs1045642. This sample was obtained from blood and genotyped as reported in "Materials and methods." This genotype was used here as a positive standard to assess the assay developed. Therefore, in this case the strands that will bind CProbe on the biochip will carry a guanine residue (complementary to the ancestral C nucleotide). On this basis, the assay was based on two hybridization steps, as represented in Fig. 6: in the first step the direct binding of the WGA sample and its detection was accomplished; then, by injecting the two discriminating probes (DProbe END 15 BIO FM and DProbe END 15 BIO MM) on the prehybridized WGA, we achieved discrimination. In particular, genotype detection was realized by comparing signals relative to the fully complementary sequence, DProbe END 15 BIO FM, containing a terminal guanine residue, with those relative to the mismatching one, DProbe END 15 BIO MM, containing a terminal thymine residue.

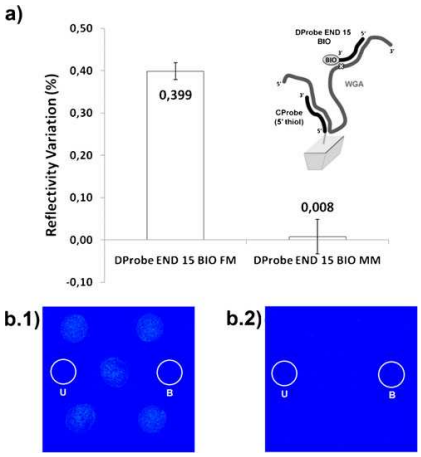

Fig. 6 SPRi signals recorded from secondary hybridization on the captured whole genome amplification (*WGA*) sample. Signals were compared for DProbe END 15 BIO FM and, after regeneration and the new binding of the WGA sample, DProbe END 15 BIO MM. The relative differential images of the interaction are reported for the fully complementary (*b.1*) and for the mismatching discriminating (*b.2*) probe, respectively

Before injection, the WGA sample (6 ppm) was thermally pretreated to dissociate the double-stranded DNA strands, allowing surface hybridization of the appropriate strand to the CProbe. The first result obtained was the direct detection of the WGA sample, giving a very good SPRi signal of ΔR=0.809 % with an excellent reproducibility among spots (CV=2 %). Moreover, the specificity of the detection on the genomic sample was confirmed by control spots, i.e., no significant signal was observed with the WGA sample: ΔR=(0.022±0.043)%. This result was relevant per se, considering the nature of the sample tested, i.e., a whole genome sequence. Furthermore, it confirms the goodness of the selected capturing probe (CProbe) selected by the in silico approach applied.

After the WGA hybridization, the secondary amplification was recorded by injecting in series the fully matching DProbe END 15 BIO FM and, after regeneration and the new binding of the WGA sample, the mismatching DProbe END 15 BIO MM.

As reported in Fig. 6, the averaged signals of the secondary hybridizations with the discriminating probes clearly gave the expected result: SPRi signals were recorded only when the full match was formed by addition of DProbe END 15 BIO FM, giving ΔR=0.399 %, with CV=5 %. In contrast, when DProbe END 15 BIO MM was injected on the prebound WGA, no signal was recorded. Moreover, the specificity of this recognition was confirmed by testing the unspecific probe (UProbe), designed with the purpose of not interacting with the WGA sample, which gave no significant signal: ΔR=(0.015±0.022)%. Finally, the sandwich-like structure obtained was highly regenerable and the sensor was able to work for up to about 20 measurement cycles (Fig. S4).

With this final assay we successfully tested the ability of the strategy developed to discriminate a single base mismatch in a genomic sample, but also confirmed the genotype of the sample, i.e., C/C. In fact, since the discriminating probe (DProbe END 15 BIO MM), containing a terminal thymine residue, did not bind the sample, the presence of an adenine residue can be excluded. This result opens up the possibility of recognizing the ancestral genotype in a fast and single-sample analysis in a real-time and label-free manner.

Conclusions

We have reported SPRi-based sensing applied to detection of SNPs. In particular, as proof of principle, the rs1045642 SNP was selected on the *ABCB1* gene. The measurement conditions were optimized in terms of the rational selection of probe sequences and their length, the position of the polymorphic site, and functionalization (with biotin in the

case of the discriminating probe). We first used a model system based on a synthetic DNA fragment, Target 84, to develop the strategy to be used further on WGA samples derived from human blood. The analytical parameters were evaluated in terms reproducibility, and resulted in an averaged CV<9 %. Finally, the sensor was applied to genomic samples extracted from blood and enriched by the WGA procedure. We clearly demonstrated, using a genotyped sample, that this method allows one to discriminate between full match and mismatch samples, allowing successful detection of the polymorphism on the *ABCB1* gene, homozygote C/C in this case. This approach has general validity and can be transferred to other genotypes of the rs1045642 SNP, as well as other SNPs.

In conclusion, these promising results can be seen as the starting point for future work oriented toward the direct detection of SNPs in real samples. Moreover, the possibility to perform measurements in a multiarray assay by the SPRi technique allows us to foresee the possible simultaneous analysis of several SNPs in the same genomic sample. To this aim, different probes specific for a number of genes could be immobilized on the sensor to screen different SNPs. Furthermore, the heterozygosis degree at the polymorphic site could be evaluated by the system, making use of sequential analysis with suitable discriminating probes. The system is label-free and regenerable, which are two key features for application of biosensors in clinical diagnostics. These findings, combined with the WGA technique, will allow the application of SPRi-based sensing also to analytical research fields for which the limiting factor is the scarce amount of DNA samples for direct biosensing assays.

Acknowledgment The authors thank Fondazione ARPA 2010, with "Progetto Dolore", for financial support.

References

1. Schafer AJ, Hawkins JR (1998) Nat Biotechnol 16:33–39
2. Savonarola A, Palmirotta R, Guadagni F, Silvestris F (2012) Pharmacogenomics J. doi:10.1038/tpj.2012.28
3. Su X, Robelek R, Wu Y, Wang G, Knoll W (2004) Anal Chem 76:489–494
4. Wang J, Rivasa, Cai X, Chicharro M, Parrado C, Dontha N, Begleiter A, Mowat M, Palecek E, Nielsen PE (1997) Anal Chim Acta 344:111–118
5. Nakayama M, Ihara T, Nakano K, Maeda M (2002) Talanta 56:857–866
6. Healey BG, Matson RS, Walt DR (1997) Anal Biochem 251:270–279
7. Wu ZS, Jiang JH, Shen GL, Yu RQ (2007) Hum Mut 28(6):630–637
8. Kelley SO, Boon EM, Barton JK, Jackson NM, Hill MG (1999) Nucleic Acids Res 27(24):4830–4837
9. Gambari R, Borgatti M, Bezzerri V, Nicolis E, Lampronti I, Dechecchi MC, Mancini I, Tamanini A, Cabrini G (2010) Biochem Pharm 80:1887–1894
10. Baum L, Ng A, Keung Leung W (2005) Mol Cell Probes 19:163–168
11. Wilson PK, Jiang T, Minunni ME, Turner APF, Mascini M (2005) Biosens Bioelectron 20:2310–2313
12. Babic I, Andrew SE, Jirik FR (1996) Mut Res 372:87–96
13. Gotoh M, Hasebe M, Ohira T, Hasegawa Y, Shinohara Y, Sota H, Nakao J, Tosu M (1997) Gen Anal Biom Eng 14:47–50
14. Behrensdorf HA, Pignot M, Windhab N, Kappel A (2002) Nucleic Acids Res 30(14):e64
15. Goodrich TT, Lee HJ, Corn RM (2004) Anal Chem 76:6173–6178
16. Kin Lao AI, Su X, Aung KMM (2009) Biosens Bioelectron 24:1717–1722
17. Zanoli LM, D'Agata R, Spoto G (2012) Anal Bioanal Chem 402:1759–1771
18. D'Agata R, Corradini R, Ferretti C, Zanoli L, Gatti M, Marchelli R, Spoto G (2010) Biosens Bioelectron 25:2095–2100
19. D'Agata R, Breveglieri G, Zanoli LM, Borgatti M, Spoto G, Gambari R (2011) Anal Chem 83(22):8711–8717
20. Balogh MK, Børsting C, Sanchez-Diz P, Thacker C, Syndercombe-Court D, Carracedo A, Morling N, Schneider PM (2006) Int Congr Ser 1288:725–727
21. Frumkin D, Wasserstrom A, Itzkovitz S, Harmelin A, Rechavi G, Shapiro E (2008) BMC Biotechnol 20:8–17
22. Sharma V, Kaul S, Al-Hazzani A, Prabha TS, Rao PPKM, Dadheech S, Jyothy A, Munshi A (2012) J Neurol Sci 315(1–2):72–76
23. Wang J, Wang B, Bi J, Li K, Di J (2012) J Cancer Res Clin Oncol 138(6):979–989
24. Kato M, Fukuda T, Serretti A, Wakeno M, Okugawa G, Ikenaga Y, Hosoi Y, Takekita Y, Mandelli L, Azuma J, Kinoshita T (2008) Progr Neuropsychopharmacol Biol Psychiatr 32(2):398–404
25. Drain S, Flannely L, Drake MB, Kettle P, Orr N, Bjourson AJ, Catherwood MA, Alexander HD (2011) Leuk Res 35(11):1457–1463
26. Garcia-Donas J, Esteban E, Leandro-Garcia LJ, Castellano DE, del Alba AG, Climent MA, Arranz JA, Gallardo E, Puente J, Bellmunt J, Mellado B, Martinez E, Moreno F, Font A, Robledo M, Rodriguez-Antona C (2011) Lancet Oncol 12(12):1143–1150
27. Zhang LN, Yesupriya A, Hu DJ, Chang MH, Dowling NF, Ned RM, Udhayakumar V, Lindegren ML, Khudyakov Y (2012) Hepatology 55(4):1008–1018
28. Wernersson R, Juncker AS, Nielsen HB (2007) Nat Protoc 2 (11):2677–2691
29. Ermini ML, Scarano S, Bini R, Banchelli M, Berti D, Mascini M, Minunni M (2011) Biosens Bioelectron 26:4785–4790
30. Scarano S, Scuffi C, Mascini M, Minunni M (2010) Biosens Bioelectron 26:1380–1385

Analytical and Bioanalytical Chemistry

Electronic Supplementary Material

Single nucleotide polymorphism detection by optical DNA-based sensing coupled with whole genomic amplification

M.L. Ermini, S. Mariani, S. Scarano, D. Campa, R. Barale and M. Minunni

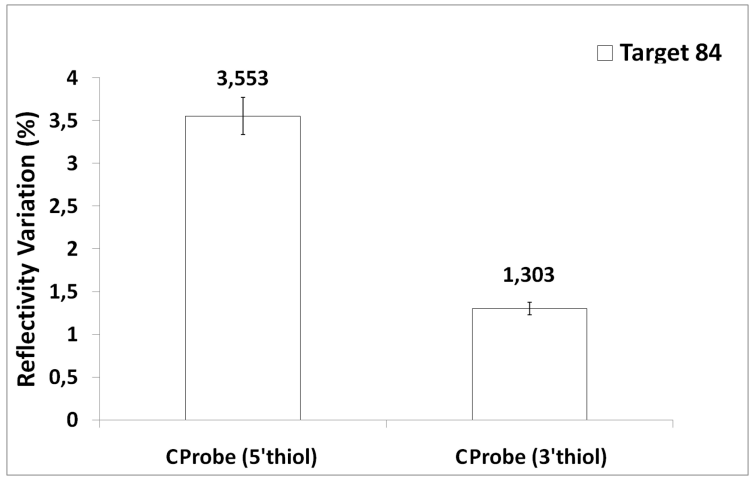

Fig S.1 SPR-I signals from the Target 84 hybridized with CProbe (5'thiol) and CProbe (3'thiol) are compared.

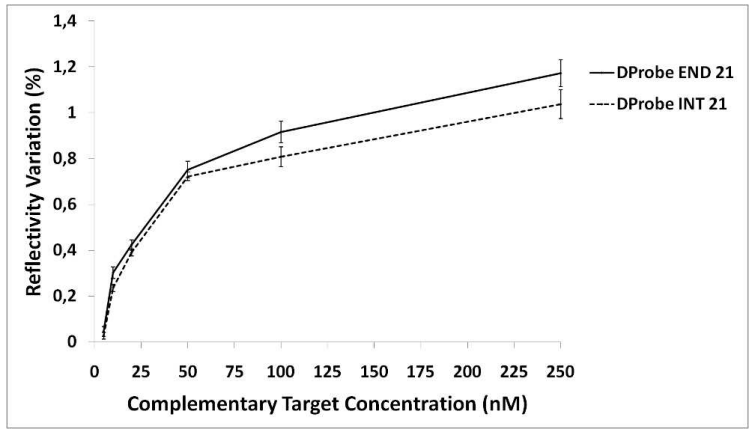

Fig S.2 SPR-i signals relative to discriminating probes immobilized on the gold surface and their hybridization with fully complementary targets (Target INT 21 FM and Target END 21 FM) evaluated by the binding curve.

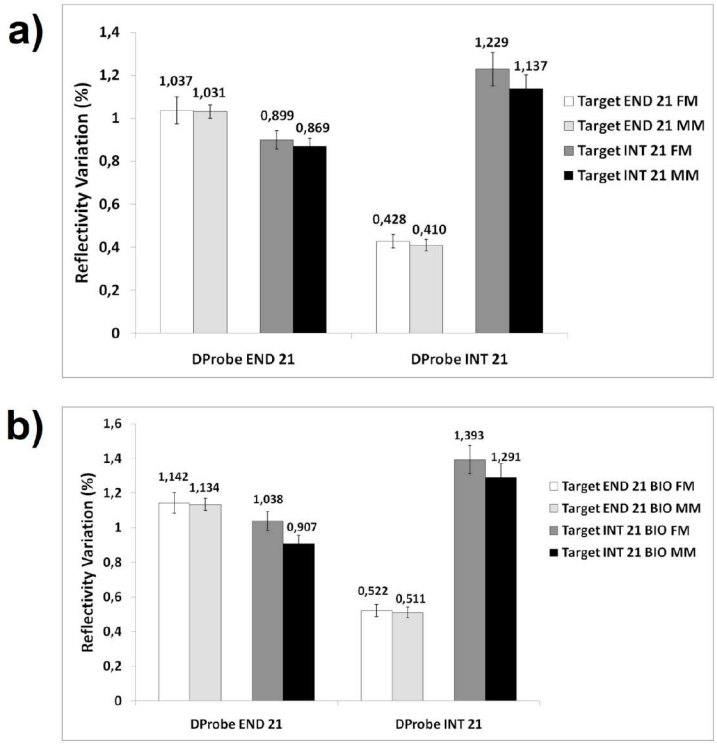

Fig S.3 SPRi signals for all the probe-target combination reported in Fig. 3. Reflectivity variation percent is reported for the discriminating probes DProbe END 21 and DProbe INT 21 hybridized with unmodified (a) and biotinylated (b) target with the polymorphic site inside the sequence and at one end.

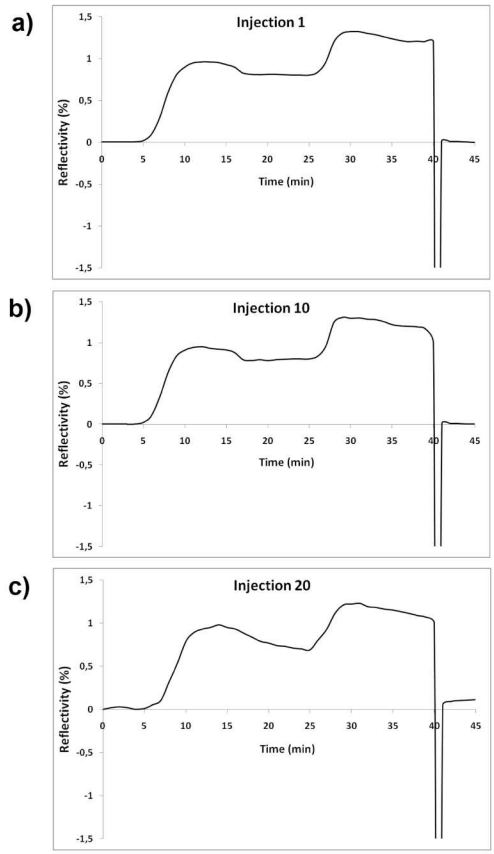

Fig S.4 SPRi signals vs time for the same interaction: CProbe immobilized, hybridized with 6 ppm WGA sample, followed by full matching DProbe hybridization. Sensorgrams (blank subtracted) were here reported for the first (a), the tenth (b) and the twentieth injection (c) during the entire biochip lifetime. Regeneration step and the new obtained baseline were reported for each of the three injections too.

Comparing the sensorgrams, it is possible to note that the reflectivity difference percent was not affected in the first ten injections, since there was no difference in signal between the first and the tenth injection. On the other hand, after twenty injections the sensorgram displayed reduced hybridization performances, meaning that the surface started to ruin and thus the SPRi signal resulted to be significantly different from the other injections.

3.1.4 Discrimination of Single Nucleotide Polymorphism on Purified Blood Samples - Preliminary Results

After the optimizations of the condition of SNPs discrimination on WGA amplified samples, the biosensor ability to detect mismatch in DNA extracted from blood from patients was investigated. Measurements were here performed directly on the DNA obtained from patient blood, after pretreatments previously selected. This kind of sample is more relevant from a clinical point of view and the possibility to perform SNP analysis directly on it could permit a possible application of the biosensor in the design of patient therapies. In particular the direct detection was successfully accomplished with the same procedure used for the commercial genomic sample[63] as reported in Fig. 3.1.

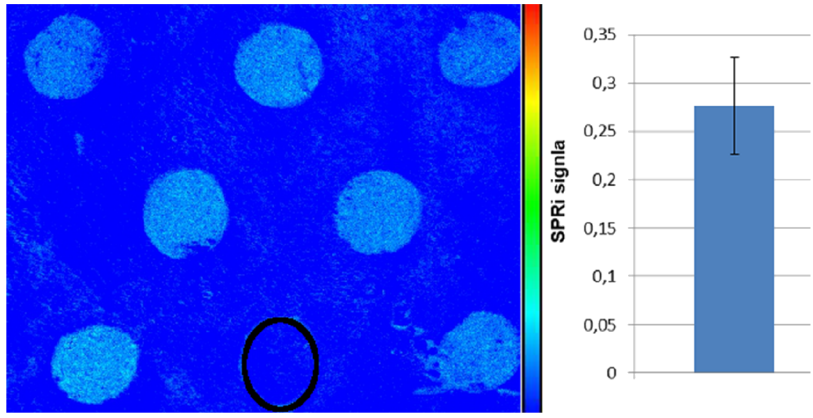

Figure 3.1: Differential image (left) and SPRi signal form the direct detection of DNA extracted from patient blood, 100 μl 6 ppm diluted in Hybridization buffer (300 mM NaCl, 20 mM Na_2HPO_4, 0.1 mM EDTA, pH 7.4 with 0.05% poly (ethylene glycol) sorbitan monolaurate (TWEEN® 20). Blank spot, *i.e.* negative control, is circled in black. Bright areas represent probe interacting with the complementary sequence in the genomic DNA.

Then the different discriminating probes were injected and tested for hybridization with captured DNA extracted from blood (*i.e.* from human Lymphocytes). From the previous results, it expected that only

fully complementary probes will hybridize, while the single mismatching will not give signal. From these, with three subsequent injections (G is not naturally found in this SNP) it should be possible to establish the kind of polymorphism of the patient. Results are shown in Fig. 3.2.

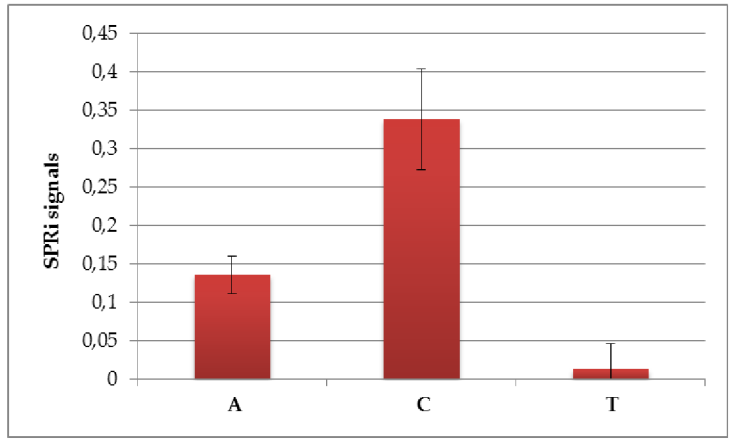

Figure 3.2: SPRi signals from Discriminating probes hybridized on fragmented DNA extracted from patient blood previously catch by Capturing probe. Probes only differing in the base present in the polymorphic site were injected (50 μl 250 nM diluted in Hybridization buffer (300 mM NaCl, 20 mM Na_2HPO_4, 0.1 mM EDTA, pH 7.4 with 0.05% poly (ethylene glycol) sorbitan monolaurate (TWEEN® 20)).

Actually, work is in progress for confirmation of these results by sequencing the DNA sample tested on SPRi.

3.2 Signal Enhancement with Nanoparticles

3.2.1 Biosensor Surface Nanostructuring

One of the possible approaches for improving the SPRi performances is to functionalize the surface of the gold chip with nanoparticles. Creating a nanostructure on the biochip surface as first layer onto anchor DNA probes could, in principle, give the possibility to increase the biosensor performances mainly for two different reasons.

First, covering a flat surface with a nanostructure increases the available area for thiols and creates a distribution of orientation of anchored probes, resulting in a change in the potential availability to interact with the target.

Second, surface plasmons of gold biochip could induce the resonance of plasmons of NPs increasing biosensor sensitivity. To test this effect different NPs were obtained. In particular, gold nanospheres, silica/gold nanoshells and silver nanoprisms (different in material, size and shape) were synthesized and immobilized through dithiol layer on gold biochip surface and further functionalized with thiolated DNA probe. All Plasmon curves and microscopy images (SEM and AFM) were studied to assess the presence of the nanostructure. Further, the influence of the nanostructure in SPRi signal was evaluated in hybridization with complementary oligonucleotide. Improved performances were found below 50 nM of target concentration using silver nanoprisms.

These studies were reported recently in a paper:

S. Mariani, M. L. Ermini, S. Scarano, F. Bellissima, D. Berti, M. Bonini and M. Minunni, "Nanotechnology Coupled to Biosensing: Looking for Improved Analytical Performances with Application to DNA-Based Sensing", Submitted to *J. Phys. Chem. C.*

Nanostructures for surface plasmon resonance imaging: looking for improved performances with application to DNA-based sensing

S. Mariani, M. L. Ermini, S. Scarano, F. Bellissima, M. Bonini, D. Berti, M. Minunni**

Department of Chemistry "Ugo Schiff" and CSGI, University of Florence, Via della Lastruccia 3, 50019 Sesto F.no (FI), Italy

AUTHOR INFORMATION

Corresponding Authors

*bonini@csgi.unifi.it, phone: +390554573014, fax: +390554573036

*maria.minunni@unifi.it, phone: +390554573314, fax: +390554573384

ABSTRACT. Surface Plasmon Resonance imaging (SPRi) is an advanced optical technology in the field of affinity biosensors. The improvement of the analytical performances of SPRi systems applied to DNA sensing is currently an open issue and, in this framework, nanoparticles (NPs) play a forefront role in signal enhancement strategies. This work reports on the nanostructuring of a commercially available SPRi gold biochip with different kinds of NPs, i.e. gold nanospheres, silica-coated Au nanoshells, and silver nanoprisms. The NPs were tethered on the chip surface and further functionalized with a DNA probe, to assess their effect on the analytical performances. The influence of different tethering conditions and different nanostructures on the SPRi signal was finally evaluated by performing hybridization assays with the corresponding complementary oligonucleotide. Results highlight the crucial role of the optical properties of the nanoparticles, showing that coupling between surface plasmon resonances of substrate and nanostructure is a prerequisite to SPRi signal enhancement: in fact, among the different nanostructures investigated, silver nanoprisms showed the best results in terms of potential improvement of the SPRi signal.

KEYWORDS. Nanoparticles, Surface Nanostructuring, Analytical performances, DNA sensors, Optical Sensors, Surface Plasmon Resonance imaging.

INTRODUCTION. Biosensors are innovative analytical devices based on the close integration between a biological receptor and a transducer. The bioreceptor is immobilized on the surface of the transducer and it is responsible for the selectivity of the system. The receptor recognizes the analyte in solution and binds it, generating an event sensed by the transducer. Different receptors coupled to a variety of transduction principles are available. Among receptors, we can distinguish between enzymes, leading to catalytic sensors, and receptors based on affinity interactions. Antigen-antibody reactions (immunoreactions), nucleic acids binding (DNA and/or RNA), aptamers and their ligands, lead all to Affinity-Based Biosensors (ABBs). About the detection of the event, transduction can be electrochemical, gravimetric, optical, thermometric, etc. Therefore, different combinations among receptors and transduction principles result in a wide variety of possible analytical applications.[1–4]

Since 20 years Surface Plasmon Resonance (SPR) has been applied to a variety of problems related to biochemistry, molecular biology, drug development, and analytical chemistry.[5,6] Conventional SPR and its most recent advancement, SPR-imaging (SPRi), are more and more exploited for advanced applications aiming at fast, label-free, real-time multiplexed analysis of bio-interactions for clinical diagnostic as well as anti-doping analysis, where high sample throughput and fast analysis time are mandatory.[7] In particular, SPRi technique results to be a suitable asset for developing versatile DNA affinity biosensors: in fact, as we recently reported,[8] SPRi has been used in a variety of affinity systems, including DNA/DNA, DNA-binding protein, DNA and RNA aptamers/protein, antibody-antigen and carbohydrate/protein interactions. SPRi can eventually contribute to support membrane related studies.[9]

Among the analytical challenges behind SPR biosensing, increased sensitivity is of crucial importance. Recently, some authors have reported interesting improved detection limits by using

catalytic activity of enzymes.[10] Alternatively, improved analytical performances in SPR based-sensing are obtained when using nanoparticles to enhance SPR signal.[11,12] Metallic Nanoparticles (NPs) are nanoscale materials that possess optical and electronic properties opening new perspectives in the strategies for detections of biomolecules such as DNA, RNA, and proteins. Different approaches have been pursued to obtain higher sensitivity in optical SPR-based sensing. Most of them deal with nanostructures incorporated within sandwich-like assays, using NPs as mass enhancers or to obtain plasmon coupling. Interesting advances on the use of functionalized Au NPs in DNA biosensing strategies have been recently summarized.[13] Particular attention has been devoted to ultra-sensitive DNA detection, aiming at DNA sequence detection directly in genomic, unamplified samples, bypassing Polymerase Chain Reaction (PCR). Behind this work, excellent reviews that have given comprehensive summaries of updated processes involving DNA sensors and DNA microarrays have been also published.[14–18] Quantum dots were also used in SPRi immunosensors.[19]

More recently, applications of SPRi-based sensing have been reported for the detection of target sequences in real samples of genomic DNA from plants and human blood, in sandwiched gold NPs-based assays.[20] NPs were coated with streptavidin and further modified with biotinylated probes. In particular, a marker sequence of transgenosis was detected in genomic DNA samples carrying different amounts of genetically modified (GM) sequences (Roundup Ready soybean, RR).[21] The same assay scheme was used for the detection of single nucleotide polymorphism (SNP), meaning the difference in one nucleotide, in samples from human genomic DNA extracted from lymphocytes to detect a mutation present in the globin gene, involved in thalassemia.[22]

Our group has recently explored the possibility to use NPs for improving analytical performances of SPRi-based sensing. In particular nanorods,[23] spherical and prismatic NPs were used both to obtain surface nanostructuring of gold biochips and/or as labels in sandwich–like assay[24] for supramolecular architectures. In this work, different nanostructures were introduced in a SPRi biochip to be used in DNA sensing. In particular gold nanoparticles, silica-coated Au nanoshells and silver nanoprisms were synthesized and immobilized on gold surfaces and the efficiency in the amplification of the analytical signal was evaluated.

First, NPs were synthesized and then covalently linked *via* dithiols on the gold chip surface, which was then functionalized with thiolated-DNA probes. The nanostructured surfaces have been characterized by scanning electron microscopy (SEM) and atomic force microscopy (AFM). Finally, hybridization experiments between the immobilized probe and its specific complementary target sequence in solution were performed and the relative sensor performances were evaluated, with the final aim of finding the best NP structure for improving the analytical performances of the sensor.

EXPERIMENTAL METHODS.

Immobilization experiments. Immobilization Solution (IS) was a water solution 1 M KH_2PO_4 (pH 3.8). Hybridization Solution (HS) was a water solution of 300 mM NaCl, 20 mM Na_2HPO_4, 0.1 mM EDTA, 0.05% TWEEN®20 (Polyethylene glycol sorbitan monolaurate), pH 7.4. Solutions were prepared in MilliQ water. Reagents were purchased from Sigma Aldrich (Milan, Italy). All synthetic oligonucleotides were purchased from Eurofins MWG Operon (Germany). Nucleotide sequences were: TProbe (Testing Probe) 5' HS-$(CH_2)_6$-GTGGTGTCACAGGAAGAGATT 3' and the complementary TTarget (Testing Target) 5'

5

AATCTCTTCCTGTGACACCAC 3'. The TProbe sequence at its 3 end maps the rs1045642 single nucleotide polymorphism (position 87138645 of the chromosome 7 on human ABCB1 gene), a variation in human genome related to the incidence of many diseases[25,26] and drug resistance.[27,28]

An unspecific sequence was used as Negative control: 5' HS-$(CH_2)_6$-GAGGGCGATGCCACCTAC 3'. The TTarget was removed from the hybrid with immobilized TProbe using a regeneration solution (RS) consisting in 100 mM HCl in MillQ water.

Nanoparticles. Silver nanoprisms: trisodium citrate (>99%), poly(sodium styrene sulfonate), sodium tetrahydridoborate (>99%) and silver nitrate (>99%) were purchased from Sigma Aldrich (Milan, Italy). Solutions were prepared in milliQ water. Silica-coated Au nanoshells: Ammonium hydroxide (30%) and sodium hydroxide pellets (>98%) were from PanreacQuimica (Spain). Tetraethylorthosilicate (TEOS) (>99%), ethanol ultrapure p.a., milliQ water 18,2 MW/cm, tetrachloroauric acid (>99,9%), tetrakis(hydroxymethyl)phosphonium chloride (THPC, 80% solution in water), (3-Aminopropyl)trimethoxysilane ATPS (97%), hydrochloric acid (37%), formaldehyde (37% w/w) were all from Sigma Aldrich-Fluka (Milan, Italy). Pentane (96%) was from Riedel de Haen (Milan, Italy), potassium carbonate p.a. was from Merck (Darmstadt, Germany). Gold nanoparticles: tetrachloroauric acid (>99,9%) and trisodium citrate dehydrate (>99%) were purchased from (Sigma Aldrich-Fluka, Italy). All solutions were prepared in MilliQ water.

Thiols and dithiols: 11-mercapto-1-undecanol (MU), 6-mercapto-1-hexanol (MCH), 1,8 Octanedithiol (ODT) and 1,4-Benzenedimethanethiol (BDMT) were purchased from Sigma (Milan, Italy).

SPRi setup. Lab$^+$-SPRi instrument was from GenOptics-Horiba Scientific (USA). The opto-

mechanical part of the instrument consisted in a light source emitting at 635 nm. Biochip were housed in a cell integrated with a fluidic system (PEEK tubing, Restek corporation, 1/16" OD x 0.01" ID) equipped with a Rheodyne valve (50 µl loop volume) and the continuous flow of HS was generated by a peristaltic pump (Miniplus 3, Gilson Inc., USA) using accurate tubing from Elkay Laboratory Products (UK) orange/black, 0.015 cc/min.

NP synthesis. Three different types of nanoparticles were synthesized: gold nanospheres, gold nanoshells and silver nanoprisms. Gold nanospheres were synthesized according to the Turkevich method.[29] Gold nanoshells have been grown on silica spheres.[30] Silver nanoprisms were synthesized with a seed-based method.[31] Details about the synthesis of the nanostructures are given in the supporting information, together with respective UV-vis absorption spectra.

NP and surface characterization. All nanoparticles suspensions were characterized by UV-Vis spectrophotometry using a Perkin Elmer Lambda 900. Gold nanospheres were 15 nm in diameter, the total diameter of the nanoshells were 150 nm and silver nanoprisms side was 40 nm. Nanostructured gold surfaces of SPRi biochips were characterized by SEM (Scanning Electron Microscope) and AFM (Atomic Force Microscope). Scanning Electron microscopy experiments were carried out with a ZEISS Sigma FEG-SEM. Atomic force microscopy images were collected by means of a PSIA XE-100 microscope in non-contact mode (NCHR probes, radius of curvature < 10 nm).

Chip surface nanostructuring. NPs were immobilized onto the gold surface of SPRi biochips through a dithiol linker. To this aim, two different dithiols were tested 1,8-Octanedithiol (ODT) and 1,4-Benzenedimethanethiol (BDMT). Dithiols immobilization was carried out by applying a pre-punched PDMS mask to obtain a removable micro-welled (1 mm in diameter) support for the deposition of dithiols (concentration: 1 mM in MilliQ water, 0.8 µL/micro-well). After the

deposition of the drops, the chip was placed into a moist chamber to which vacuum was applied for about 20 minutes to eliminate air bubbles from micro-wells and left into the moist chamber for 20 hours, avoiding the drying of the immobilization solution. Finally, drops in micro-wells were aspired with micro-syringe and micro-wells were washed with MilliQ water. Control spots, where the unspecific sequence was immobilized, and blanks (bare gold) were also prepared on the biochip.

Nanoparticles suspensions were eluted in MilliQ water to a certain density ensuring the total coverage of the spot area (1 mm in diameter each). NPs were also alternatively diluted in 20%vol/vol ethanol or 5% vol/vol ammonium hydroxide water solutions (pH~10). After that, silver nanoprisms, gold-silica core-shell NPs and gold nanospheres were covalently immobilized on the gold chip by depositing 0.8 µL onto different dithiolated micro-wells.

DNA probe immobilization on nanostructured SPRi biochips. Thiolated DNA probes (TProbe) were immobilized onto nanostructured surfaces, exploiting the affinity of sulphur for gold and silver. A 10 µM TProbe solution was prepared in IS and 0.8 µL were deposited in each micro-well and let react in the moist chamber for 20 hours. Finally, after the removal of the PDMS mask, the prism was immersed in a Passivation Solution PS (1 µM 11-mercapto-1-undecanol, MU, and 1 µM 6-mercapto-1-hexanol, MCH, in MilliQ water) for 20 hours to passivate the rest of the gold surface. Finally, the chip surface was rinsed with MilliQ water and housed in the instrument cell.

SPRi measurements on nanostructured surfaces. Calibration curves were obtained by injecting 100 µl of the complementary TTarget in HS, within the range of concentration 5 nM - 250 nM. The immobilized TProbe was then regenerated from the hybridized TTarget after each measurement by RS solution for 30 seconds. All measurement cycles were performed at fixed

angle of incident light (maximum slope of plasmon curve), and the variation of intensity of reflected light due to the target interaction was monitored as SPRi signal.

RESULTS AND DISCUSSION

In this work commercially available SPRi biochips were modified with different nanostructures and tested for their potential use in enhancing the sensitivity of a SPRi-based DNA biosensor. The basic idea was to functionalize the gold layer of biochips with NPs through the covalent linking offered by dithiols. To this aim, the most suitable dithiol was selected and the nanostructures obtained with different NPs were studied. DNA sequences were immobilized on the obtained three nanostructured chip surfaces and the hybridization reactions with the complementary target sequence were evaluated by SPRi sensing. The rationale of this approach was based on the occurrence of two phenomena: i.e. the increase of the surface area available for sensing (due to the functionalization of the chip surface with nanostructures) and the electronic properties of the nanostructured surface. The nanostructuring of a flat surface, such as the one of the chip, takes to an increase of the surface area that could enhance the amount of immobilized DNA. At the same time, the presence of structures on top of the chip gold surface could result in non-optimized instrumental conditions, which are eventually re-established by adjusting the source-sample impinging angle. On the other hand, the sensitivity of SPRi biosensor could take advantage of the coupling between the plasmon resonances of NPs and gold surface. Recently, this approach has been successfully exploited in the functionalization with noble metal NPs of the interacting surface of a gold SPRi biochip.[32]

Nevertheless, many aspects are still to be optimized when introducing nanostructure onto the surface of commercial biochips. For this reason we decided to investigate the effect of the

plasmon resonance wavelength of the nanostructures in relation to that of the chip gold surface, especially in terms of improvement performance. To this aim, the gold surface was therefore functionalized with three different nanostructures.

Silver nanoprisms were selected because of their surface plasmon resonance peak at 633 nm, almost matching the wavelenght of the instrumental light source (635 nm).

On the other hand, the resonance of the plasmon of the gold nanospheres (Abs_{max}= 528 nm) is well separated from the resonance of the chip surface, while gold nanoshells (Abs_{max} = 588 nm) were selected as an intermediate case.

Nanostructuring procedures were optimized in terms of the best dithiol and solutions to be used to immobilize the NPs, *i.e.* MilliQ water, ethanolic, or ammonia solution. Nanostructured surfaces were compared to bare gold surface in terms of stability under HS flow and of the plasmon curves.

In order to choose the best linker for the NPs, two different dithiols, BDMT and ODT, were tested. After NPs immobilization, plasmon curves relative to different dithiol/NP combinations were compared. Nanostructures built on ODT dithiol did not show significant shifts in the minimum resonance angle, contrary to BDMT. The shift observed in the case of BDMT is reasonably due to the aromatic ring, which could promote the optical coupling between the surface plasmons of biochip gold and NPs.[33] Thus, BDMT could enhance the resonance effect and was chosen as the linker to be used to immobilize NPs.

Gold nanospheres and silica-coated Au nanoshells were successfully deposited by simply adding their water dispersions on top of the BDMT layer. The nanostructured biochip surface resulted stable under HS flow: in fact, no change in the plasmonic curves was recorded by the real-time

CCD image of the spots after 48 hours of continuous flow of HS (data shown in the supporting information). This is consistent with the high affinity between sulphur and gold.

Nanostructuring with water dispersions of silver nanoprisms reflected the lower affinity between silver and sulphur, resulting damaged after 8 hours of exposure to HS. The stability of the silver nanoprism layer was improved both with 20% ethanol and with 5% ammonium hydroxide (pH~10) dispersions. Ethanol was used to ease Ag-BDMT coupling thanks to the destabilization of silver nanoprisms dispersions, while ammonia should promote dithiol deprotonation, favoring the covalent binding with the nanoprisms. Ammonia suspensions resulted the most effective in stabilizing the nanostructured surface: in fact, the nanostructuring was lost after 48 hours of flow, as highlighted by the disappearance of the shift of the resonance angle (see Figure 1) and were therefore selected for the immobilization of the nanoprisms.

In Table 1 all the optimized nanostructuring conditions for the different NPs tested and their relative shifts in terms of resonance angle are summarized. Among the studied nanostructures, nanostructuring with silver nanoprisms displayed the largest shift, highlighting the coupling between the plasmon resonances of NPs and chip. These results showed that the position of the plasmon resonance peak of nanoparticles represented a useful parameter when designing a nanostructured biochip for SPRi.

The nanostructured SPRi biochip surfaces were investigated by SEM (Scanning Electron Microscopy) and AFM (Atomic Force Microscopy). In Figure 2, the images relative to the three different nanostructured spots are reported, together with bare gold spots as reference.

Gold nanospheres and silica-coated Au nanoshells appeared irregularly distributed on the dithiolated surface, forming large aggregates which could take to a loss of sensitivity of the SPRi biochip, possibly because of the distance from the sensing surface (due to aggregate thickness)

and/or because the irregular distribution of the DNA probe immobilization, affecting the hybridization of the complementary TTarget. On the other hand, a homogeneous coverage was obtained with silver nanoprisms on dithiolated surface. The platelet-like shape of nanoprisms and their reduced thickness was of great help in the formation of a homogeneous and thin coating, which from a structural point of view, made nanoprisms the best candidate among the tested nanostructures in the design of highly sensitive SPRi biochips.

Once covalently bound to the chip surface, nanostructures were functionalized by coupling the thiolated TProbe on their surface. The effect of the different nanostructures was evaluated through the study of hybridization signals obtained by injecting the complementary TTarget onto nanostructured spots modified with TProbe, compared with those obtained from the same TProbe directly bound to the unmodified gold biochip surface. Signal intensities of the observed interactions were evaluated at different TTarget concentrations for the all three nanostructures. Negative control oligonucleotides solution was also assayed giving no significant signal.

The results are summarized in Figure 3. Both gold nanospheres and silica-coated Au nanoshells caused a loss of sensitivity of the system. In particular, nanoshells produced the strongest decrease on SPRi hybridation signals, probably because of the large distance between the probe and the sensing surface. Nanoshells were characterized by a diameter of about 150 nm, making the biochip surface insensitive (from the plasmonic point of view) to the hybridization taking place on the surface of the nanoshells. In the case of gold nanospheres, their size should not represent a problem, as long as a monolayer (or few layers) of NPs is deposited onto the chip surface. Unfortunately, as highlighted by the microscopy results, large aggregates were present on the surface, indicating that an accurate control of the deposition step is a prerequisite for the preparation of an efficient system. Finally, silver nanoprisms showed a significant improvement

over the conventional approach for target concentrations lower than 50 nM (see Figure 3): in fact, an enhancement up to 50% in SPRi signals was recorded at 20 nM (see Figure 4).

The increased sensitivity could be explained by the analysis of the plasmon curves (reflectivity vs. angle of incident light) of TProbe directly bound on gold and the corresponding tethered on the silver nanostructure (Figure 5). In the case under study, the nanostructure produced a sharper plasmon curve than the control spot one (probe on bare gold). As a consequence, for the same interaction on the sensing surface, variations of the resonance angle, corresponded to a greater variation of intensity of reflected light.

Finally, the biosensor resulted to be usable with an excellent reproducibility (CV%<10) within the first 10 measurements cycles (TProbe-TTarget interaction and hybrid denaturation by TProbe regeneration with RS).

CONCLUSIONS

The surface of a commercial SPRi biochip was functionalized with nanostructures differing in terms of composition, dimension, and shape, but all showing a surface plasmon resonance peak in the visible range. In particular, the peaks range from 633 nm (nearly matching the light source of the instrument, *i.e.* 635 nm) to 528 nm. Immobilization conditions were optimized by using different tethering agents (dithiols) and dispersing the nanoparticles in different solutions. Nanostructuring was investigated by microscopy (SEM and AFM) and in terms of shifts in SPR angle, showing that silver nanoprisms are well suited for our scope. Finally, nanostructured surfaces were functionalized with DNA probe and the hybridization reaction between the immobilized probe and the complementary target DNA in solution was studied. A significant improvement of the SPRi sensitivity was achieved at target concentrations below 50 nM, when

silver nanoprisms where used. These results show that the morphology of the nanostructured coating, the tethering conditions and the electronic properties of the nanostructures employed are all crucial factors when seeking an improvement in the performances of commercial SPRi biochips. In particular, this contribution highlights an important guideline in the engineering of nanostructured SPRi, showing that coupling between surface plasmon resonances of substrate and nanostructure is an effective approach to SPRi signal enhancement. Further enhancement of the analytical performances could be achieved by optimizing these aspects. This would allow a more sensitive direct detection of DNA, possibly bypassing DNA amplification, i.e. the PCR step, and reducing time and cost of DNA analysis.

ACKNOWLEDGMENTS

This work was supported by CSGI and MIUR. M.B. acknowledges the EU for financial support (FP7-PEOPLE-2009-RG, project SUPRACRYST).

ASSOCIATED CONTENT

Supporting Information Description. Details about the synthesis of the tested nanostructures and UV-vis absorption spectra of nanostructure dispersions, real-time CCD images of the spots on the nanostructured biochip surface under continuous HS flow. This material is available free of charge via the Internet at http://pubs.acs.org.

REFERENCES

(1) Iliuk, A. B.; Hu, L.; Tao, W. A. *Anal. Chem.* **2011**, *83*, 4440–4452.

(2) Kimmel, D. W.; LeBlanc, G.; Meschievitz, M. E.; Cliffel, D. E. *Anal. Chem.* **2012**, *84*, 685–707.

(3) Paleček, E.; Bartošík, M. *Chem. Rev.* **2012**, *112*, 3427–3481.

(4) Marx, K. A. *Biomacromolecules* **2003**, *4*, 1099–1120.

(5) Homola, J. *Analytical and Bioanalytical Chemistry* **2003**, *377*, 528–539.

(6) Homola, J. *Chem. Rev.* **2008**, *108*, 462–493.

(7) Scarano, S.; Ermini, M. L.; Spiriti, M. M.; Mascini, M.; Bogani, P.; Minunni, M. *Anal. Chem.* **2011**, *83*, 6245–6253.

(8) Scarano, S.; Mascini, M.; Turner, A. P. F.; Minunni, M. *Biosensors and Bioelectronics* **2010**, *25*, 957–966.

(9) Wang, Z.; Wilkop, T.; Han, J. H.; Dong, Y.; Linman, M. J.; Cheng, Q. *Analytical Chemistry* **2008**, *80*, 6397–6404.

(10) Zhou, W.-J.; Chen, Y.; Corn, R. M. *Anal. Chem.* **2011**, *83*, 3897–3902.

(11) He, L.; Musick, M. D.; Nicewarner, S. R.; Salinas, F. G.; Benkovic, S. J.; Natan, M. J.; Keating, C. D. *J. Am. Chem. Soc.* **2000**, *122*, 9071–9077.

(12) Lee, H. J.; Wark, A. W.; Corn, R. M. *Langmuir* **2006**, *22*, 5241–5250.

(13) Zanoli, L. M.; D'Agata, R.; Spoto, G. *Analytical and Bioanalytical Chemistry* **2011**, *402*, 1759–1771.

(14) Rosi, N. L.; Mirkin, C. A. *Chemical Reviews* **2005**, *105*, 1547–1562.

(15) Sassolas, A.; Leca-Bouvier, B. D.; Blum, L. J. *Chem. Rev.* **2008**, *108*, 109–139.

(16) Cosnier, S.; Mailley, P. *The Analyst* **2008**, *133*, 984.

(17) Song, S.; Qin, Y.; He, Y.; Huang, Q.; Fan, C.; Chen, H.-Y. *Chemical Society Reviews* **2010**, *39*, 4234.

(18) Teles, F. R. R.; Fonseca, L. P. *Talanta* **2008**, *77*, 606–623.

(19) Malic, L.; Sandros, M. G.; Tabrizian, M. *Anal. Chem.* **2011**, *83*, 5222–5229.

(20) Spoto, G.; Minunni, M. *J. Phys. Chem. Lett.* ***2012****, 3,* 2682–2691.

(21) D'Agata, R.; Corradini, R.; Ferretti, C.; Zanoli, L.; Gatti, M.; Marchelli, R.; Spoto, G. *Biosensors and Bioelectronics* **2010**, *25*, 2095–2100.

(22) D'Agata, R.; Breveglieri, G.; Zanoli, L. M.; Borgatti, M.; Spoto, G.; Gambari, R. *Anal. Chem.* **2011**, *83*, 8711–8717.

(23) Ermini, M. L.; Scarano, S.; Minunni, M. In *Proceedings of the International Workshop on Biophotonics*; Parma, Italy, 2011.

(24) Ermini, M. L.; Mariani,, S.; Bellissima, F.; Scarano, S.; Bonini, M.; Minunni, M. In *Proceedings of Convegno Nazionale Sensori: Innovazione, attualità e prospettive*; Rome, Italy, 2012.

(25) Wang, J.; Wang, B.; Bi, J.; Li, K.; Di, J. *Journal of Cancer Research and Clinical Oncology* **2012**, *138*, 979–989.

(26) Campa, D.; Sainz, J.; Pardini, B.; Vodickova, L.; Naccarati, A.; Rudolph, A.; Novotny, J.; Försti, A.; Buch, S.; von Schönfels, W.; Schafmayer, C.; Völzke, H.; Hoffmeister, M.; Frank, B.;

Barale, R.; Hemminki, K.; Hampe, J.; Chang-Claude, J.; Brenner, H.; Vodicka, P.; Canzian, F. *PLoS ONE* **2012**, *7*, e32784.

(27) Sharma, V.; Kaul, S.; Al-Hazzani, A.; Prabha, T. S.; Rao, P. P. K. M.; Dadheech, S.; Jyothy, A.; Munshi, A. *J. Neurol. Sci.* **2012**, *315*, 72–76.

(28) Drain, S.; Flannely, L.; Drake, M. B.; Kettle, P.; Orr, N.; Bjourson, A. J.; Catherwood, M. A.; Alexander, H. D. *Leukemia Research* **2011**, *35*, 1457–1463.

(29) Turkevich, J.; Stevenson, P. C.; Hillier, J. *Disc. Faraday Soc.* **1951**, *11*, 55–75.

(30) Rasch, M. R.; Sokolov, K. V.; Korgel, B. A. *Langmuir* **2009**, *25*, 11777–11785.

(31) Aherne, D.; Ledwith, D. M.; Gara, M.; Kelly, J. M. *Advanced Functional Materials* **2008**, *18*, 2005–2016.

(32) Jung, J.; Na, K.; Lee, J.; Kim, K.-W.; Hyun, J. *Analytica Chimica Acta* **2009**, *651*, 91–97.

(33) Liu, N.; Mukherjee, S.; Bao, K.; Brown, L. V.; Dorfmüller, J.; Nordlander, P.; Halas, N. J. *Nano Lett.* **2012**, *12*, 364–369.

TABLES

Table 1. Optimized nanostructuring conditions and shifts of the resonance angle for the different nanostructures.

Nanostructure	Dithiol (Conc.)	Medium of suspension	Shift*
Gold nanospheres	BDMT (1 mM)	MilliQ water	0.31°
Gold nanoshells	BDMT (1 mM)	MilliQ water	0.42°
Silver nanoprisms	BDMT (1 mM)	Ammonia in MilliQ water (pH~10)	0.51°

* calculated as the difference of the resonance angle with respect to the reference spot.

FIGURE CAPTIONS

Figure 1. CCD images and shifts in angle of minimum reflection (respect to bare gold surface) recorded after different times of HS flux for different spots on the SPRi biochip.

Figure 2. Representative SEM and AFM images of the nanostructured surfaces. SEM images were taken with a Zeiss Sigma FEG-SEM. AFM images were taken with a PSIA XE-100 microscope.

Figure 3. Reflectivity variation for different concentrations of DNA target recorded from DNA probes immobilized on different functionalized surfaces.

Figure 4. Reflectivity variation percent for 20 nM DNA target, recorded from DNA probes immobilized on different functionalized surfaces.

Figure 5. Reflectivity vs. angle of incident light recorded for bare gold and gold functionalized with silver nanoprisms.

FIGURES

Figure 1

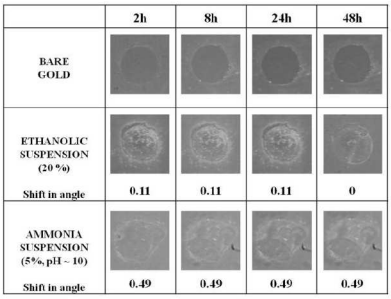

Figure 2

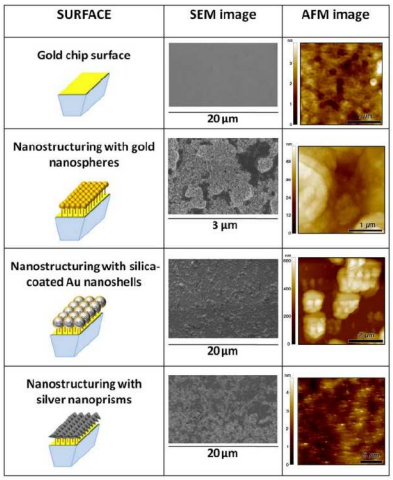

20

Figure 3

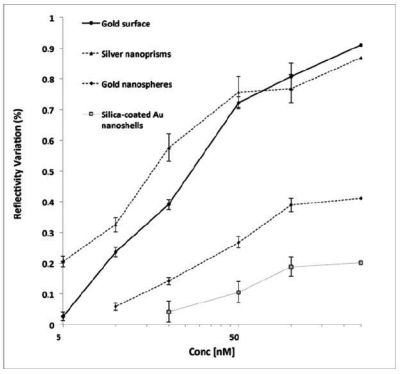

Figure 4

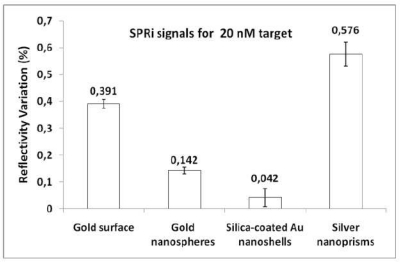

21

Figure 5

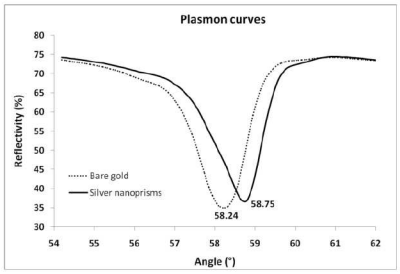
Plasmon curves
Reflectivity (%)
Angle (°)
Bare gold
Silver nanoprisms
58.24
58.75

22

TABLE OF CONTENTS IMAGE.

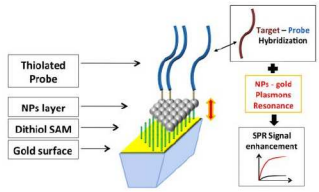

SUPPORTING INFORMATION

Nanostructures for surface plasmon resonance imaging: looking for improved performances with application to DNA-based sensing

S. Mariani, M. L. Ermini, S. Scarano, F. Bellissima, M. Bonini, D. Berti, M. Minunni**

Synthesis of Gold Nanoparticles.

Gold nanoparticles were prepared according to the procedure described by Turkevich et al.[1] 5 ml of a 1 mM tetrachloroauric acid solution in MilliQ water were added in a flask under magnetic stirring. The solution was brought to the boiling point and 0.25 ml of a 40mM citrate solution were added, still under magnetic stirring. Below the UV-vis absorption spectrum of the obtained dispersion of NPs is shown together with a picture of the dispersion of the nanostructures. The results are consistent with the formation of NPs with a radius of 10 nm.[2]

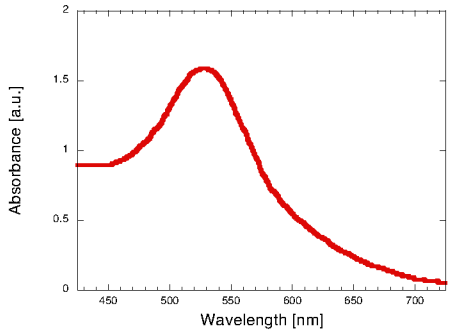

2

Synthesis of Gold Nanoshells.

Gold nanoshells synthesized were prepared by coating silica colloidal particles (average diameter of 150 nm) with a gold shell according to the method developed by Rasch.[3] Monodisperse silica colloids (150 nm in diameter) were prepared according to the Stöber process through the hydrolysis of TEOS (Tetraethyl orthosilicate).[4] Obtained silica particles were washed by absolute ethanol, dried in oven at 100 °C for 2 hours, and redispersed in ethanol. 0.10 mL of 30% NH_4OH (aq) solution was added to 10 mL of a 1 mg/mL dispersion of silica particles under magnetic stirring and 0.5 mL of 10% v/v of APTES (aminopropyltriethoxy silane) solution in ethanol was added dropwise to the dispersion. The dispersion was during for 24 hours and the nanoparticles were precipitated by adding 40mL of hexane and collected by centrifugation at 3000 rpm for 1 h. After discarding the supernatant, the particles were suspended in 5mL of ethanol by means of sonication. This precipitation is repeated twice, after which the particles are re-dispersed through sonication in MilliQ water. In a way to protonate the amine of APTES, the pH was adjusted to ~3 with concentrated HCl. Gold seeds were prepared by adding an aqueous solutions of sodium hydroxide (0.2 M, 1.5 mL), an aqueous solution of the reducing agent (THPC, 1 mL, 70mM), and an aqueous solution of tetrachloroauric acid (2 mL**,** 25 mM) to 45.5 mL of MilliQ water under stirring. As a result, an orange-brown hydrosols of gold is formed.[5] A gold hydroxide solution was also prepared: 25 mg of potassium carbonate were dissolved in 100 mL of MilliQ water, followed by the addition of 1.5 mL of a 1.0% w/w tetrachloroauric acid solution. After stirring for 30 minutes the solution is colorless, indicating that hydrolysis of $HAuCl_4$ has taken place. This gold hydroxide solution is then stored for 24 h in the dark and then used for the formation of the gold shell. APTES-functionalized silica particles were sonicated for 20 min to ensure dispersion and then 2.5mL of the dispersion were added to 5.0 mL of the gold seed dispersion. The pH was eventually readjusted to 3.0 with concentrated HCl and the dispersion was mildly shaken for 2 min before storing it in the dark overnight at 4°C. The resulting particles were isolated by centrifugation at 2500 rpm for 3 h.

3

Supernatant was discarded and the precipitate re-dispersed through sonication in 2.5 mL of MilliQ water. This dispersion (2.5 mL) was added to 4 mL of the gold hydroxide solution. The pH was adjusted to 8.0 by adding NH_4OH (aq, 30% w/w) and formaldehyde (10 µl) was immediately added. Dispersion changes from colorless to blue over the course of about 10 min. Nanoshells were isolated by centrifugation at 2500 rpm for 1 h. After discarding the supernatant, Au nanoshells were re-dispersed in MilliQ water through sonication. The UV-vis absorption spectrum is reported in the figure below, showing a maximum at 595 nm, together with a picture of the dispersion of the nanostructures.

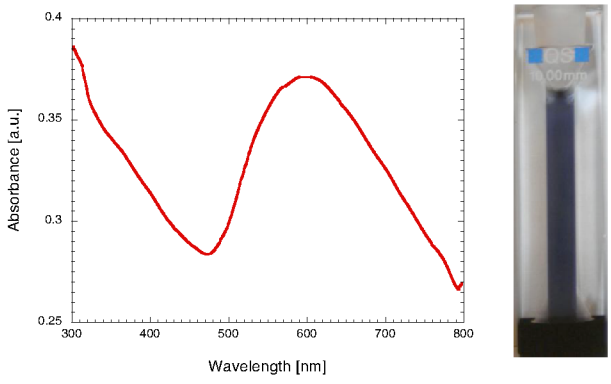

4

Synthesis of Silver Nanoprisms.

Silver nanoprisms were prepared according to a procedure reported in literature,[6] in a way to tune the absorption peak as close as possible to the laser wavelength used within the SPRi apparatus. The method involves silver seed production and nanoprism growth. Silver seeds are produced by combining aqueous trisodium citrate (5 mL, 2.5mM), aqueous poly(sodium styrene sulphonate) (PSSS; 0.25 mL, 500 mg/L; 1,000 kDa) and aqueous $NaBH_4$ (0.3 mL, 10mM, freshly prepared) followed by the addition of aqueous $AgNO_3$ (5 mL, 0.5mM) at a rate of 2mL/min. Nanoprisms were then produced by combining 5mL of MilliQ water, aqueous ascorbic acid (75 µL, 10mM) and 160 µl of seed dispersion, followed by the addition of aqueous $AgNO_3$(3 mL, 0.5mM) at a rate of 1mL/min. After synthesis, aqueous trisodium citrate (0.5 mL, 25 mM) is added to stabilize the particles and the sample is diluted with MilliQ water as desired. The synthesis is complete after the 3 minutes required for addition of the $AgNO_3$ during which the color of the solution changes as the SPR red-shifts as a consequence of nanoprism growth. The UV-vis spectrum is reported below, showing a maximum absorption at 633 nm, together with a picture of the dispersion of the nanostructures.

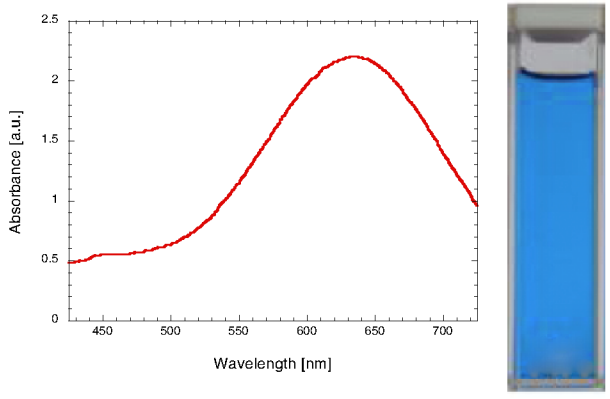

5

Real time CCD images.

CCD images of the spots on the nanostructured biochip surface under continuous HS flow at different times, showing that the nanostructuring is stable over the investigated time.

	2 h	48 h
Silica-coated Au nanoshells	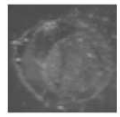	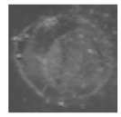
Au nanospheres	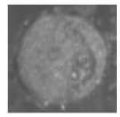	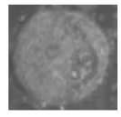

6

References.

(1) Turkevich, J.; Stevenson, P. C.; Hillier, J. *Discussions of the Faraday Society* **1951**, *11*, 55.
(2) Kimling, J.; Maier, M.; Okenve, B.; Kotaidis, V.; Ballot, H.; Plech, A. *J. Phys. Chem. B* **2006**, *110*, 15700–15707.
(3) Rasch, M. R.; Sokolov, K. V.; Korgel, B. A. *Langmuir* **2009**, *25*, 11777–11785.
(4) Ibrahim, I. A. M.; Zikry, A. A. F.; Sharaf, M. A. *J American Sci* **2010**, *6*, 985–989.
(5) Duff, D. G.; Baiker, A.; Edwards, P. P. *Langmuir* **1993**, *9*, 2301–2309.
(6) Aherne, D.; Ledwith, D. M.; Gara, M.; Kelly, J. M. *Advanced Functional Materials* **2008**, *18*, 2005–2016.

3.2.2 DNA Functionalized Nanoparticles for Signal Improvement

Much of the research involving the use of gold nanoparticles in SPR biosensors incorporates them as labels, enhancing the limit of detection compared to direct detection[32;62;64]. NPs labeled methods can be of great use in developing advanced SPR biosensing devices[62;65;66;67;68;69]. It has been shown that this approach can significantly increase detection sensitivity for a variety of analytes[68;70]. Gold films modified with colloidal Au were first shown to provide an enhanced signal for biosensing purposes by Lyon *et al.*[71] and from there, research widely moved to this direction.

The improvement of analytical performances was here tested combining the use of NPs with SPRi DNA biosensing. Signal enhancement was here studied through the building of molecular architecture in a sandwich-like assay (Fig. 3.3). NPs differing in size, shape and material were synthesized, functionalized and characterized. In particular here two kinds of NPs were applied having different plasmonic absorption characteristics: silver nanoprisms used in previous work (see Section 3.2.1) and silica spheres having no absorption. Both were functionalized with thiolated DNA sequences and tested in a sandwich like assay on the SPRi biochip.

Nanoparticles synthesis, characterization and functionalization

Silver nanoparticles were synthesized as previously reported by Aherne *et al.*[72], reducing silver nitrate with sodium tetrahydroborate and growing formed seed.

Silver seeds are produced by combining aqueous trisodium citrate (5 mL, 2.5 mM), aqueous poly(sodium styrene sulphonate) (PSSS; 0.25 mL, 500 mg/L; 1,000 kDa) and aqueous $NaBH_4$ (0.3 mL, 10 mM, freshly

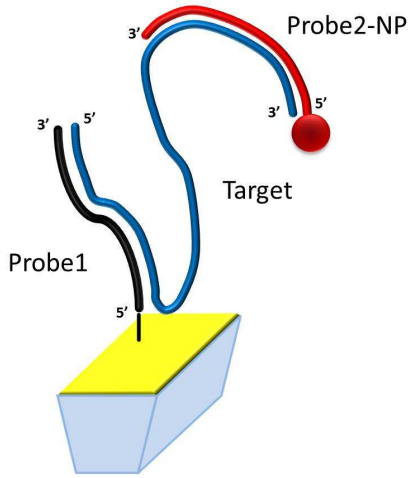

Figure 3.3: Schematic representation of the DNA structure built on the sensing surface of the SPRi biochip. The two extremities of Target are complementary to two the different probes: Probe1, immobilized on gold, and Probe2 functionalized with NP and added in solution, after the hybridization with Target.

prepared) followed by the addition of aqueous $AgNO_3$ (5 mL, 0.5 mM) at a rate of 2 mL/min. Nanoprisms were then produced by combining 5mL of MilliQ water, aqueous ascorbic acid (75 μL, 10 mM) and 160 μl of seed dispersion, followed by the addition of aqueous $AgNO_3$ (3 mL, 0.5 mM) at a rate of 1 mL/min. After synthesis, aqueous trisodium citrate (0.5 mL, 25 mM) is added to stabilize the particles and the sample is diluted with MilliQ water as desired. The synthesis is complete after the 3 minutes required for addition of the $AgNO_3$ during which the color of the solution changes as a consequence of nanoprism growth.

Silica nanoparticles were synthesized as previously reported by Nakamura *et al.*[73] using 3.12 mM (3-mercaptopropyl) triethoxysilane (MPES) in 10 ml ethyl alcohol with 28% of NH_4OH.

NPs were characterized by microscopies: AFM measurements were carried out with a PSIA XE-100E system; SEM investigations were carried out with a Cambridge Stereoscan 360 working at 20 kV of acceleration

potential and 25 mm of working distance.

Functionalization of silver nanoparticles with Probe2 was accomplished by incubating overnight a 250 nM solution in diluted in Hybridization buffer (HB, 300 mM NaCl, 20 mM Na_2HPO_4, 0.1 mM EDTA, pH 7.4 with 0.05% poly (ethylene glycol) sorbitan monolaurate (TWEEN® 20)) (Fig. 3.3).

Functionalization of Silica NPs with Probe2 was accomplished by adding 5 μl 0,5 μM of 1,4-di(maleimido)butane in a 250 nM solution of Probe2 in HB together with NPs (1/100 dilution) (Fig. 3.4).

Functionalized NPs were studied with Dynamic light scattering (DLS) and Zeta Potential measurements were carried out by means of a Brookhaven 90 Plus instrument. Light source was a 633 nm laser, while the scattered photons were collected at 90C. Samples were properly diluted with MilliQ water to optimize the scattering signal. Zeta potential was calculated according to the Smoluchowski model.

Sequences used in this work are reported in Table 3.1. UProbe was a control sequence immobilized on the sensor in order to assess the specificity of the interactions.

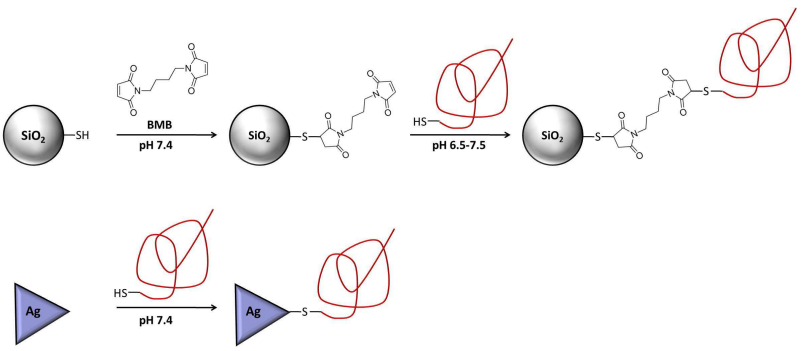

Figure 3.4: Scheme of procedures for nanoparticle functionalization with Probe2 sequence.

Probe1	5′ HS-$(CH_2)_6$-GTCACTGCCTAATGTAAGTCTC 3′
Target	5′ GAGACTTACATTAGGCAGTGACTCGATGAAGGC ATGTATGTTGGCCTCCTTTGTGCCCTCACAATCTCT TCCTGTGACACCAC 3′
Probe2	5′ HS-$(CH_2)_6$-GTGGTGTCACAGGAAGAGATT 3′
ProbeU	5′ HS-$(CH_2)_6$-GAGGGCGATGCCACCTAC 3′

Table 3.1: DNA sequences.

Results

Silica NPs and silver nanoprisms were functionalized with the same probe (Probe2) and tested in a sandwich-like assay.

First, silica NPs were characterized by AFM and SEM images reported in Figs. 3.5 and 3.6. From these it was possible to estimate that the NPs size was about 100 nm and furthermore NPs were all homogeneous in size.

Silver NPs were characterized in our previous work (see Section 3.2.1). Both NPs were further functionalized with thiolated DNA. For verifying the occurred conjugation between NPs and DNA, dynamic light scattering measurements were performed. In particular, for each NPs type, the Zeta potential of a solution of DNA functionalized NPs was compared with the Zeta potential of a solution of not-functionalized NPs.

Changes in Zeta potential are correlated to changes in surface charge of the NPs. It is expected that DNA functionalization carries to a variation of the surface charge of the NPs, thus it can be seen by Zeta potential measurements. Results are reported in Table 3.2.

Non-functionalized Ag nanoprisms showed a negative potential (around -7.6 mV), reasonably due to the effect of trisodium citrate physisorbed on their surface to stabilize the dispersion. Once the probe was in-

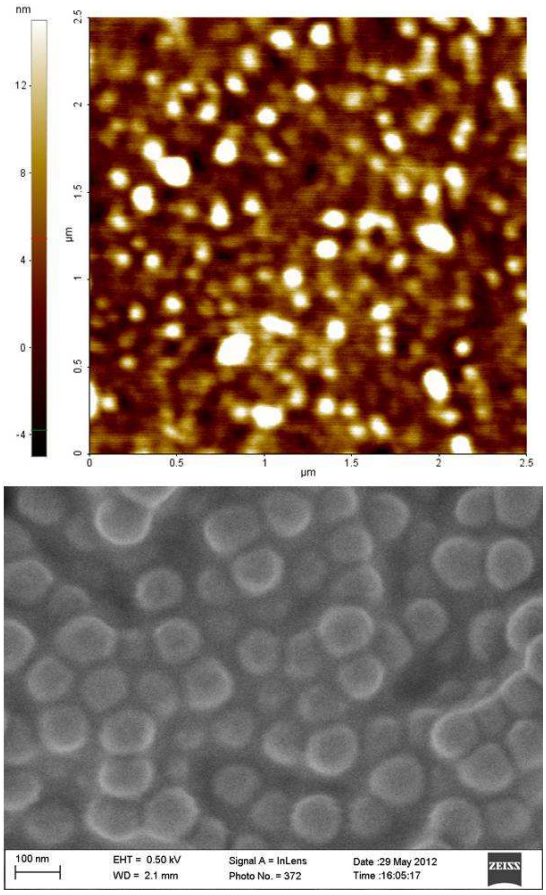

Figure 3.5: AFM image of silica NPs. It is possible to estimate that the size of the NPs is about 100 nm. AFM measurements were carried out with a PSIA XE-100E system; SEM images of silica NPs. SEM investigations were carried out with a Cambridge Stereoscan 360 working at 20 kV of acceleration potential and 25 mm of working distance.

Nanoparticle	Zeta potential (mV)
Ag nanoprisms	-7,61
Probe2 - Ag nanoprisms	-5,18
SiO_2 nanospheres	-46,52
Probe2 - SiO_2 nanospheres	-22,88

Table 3.2

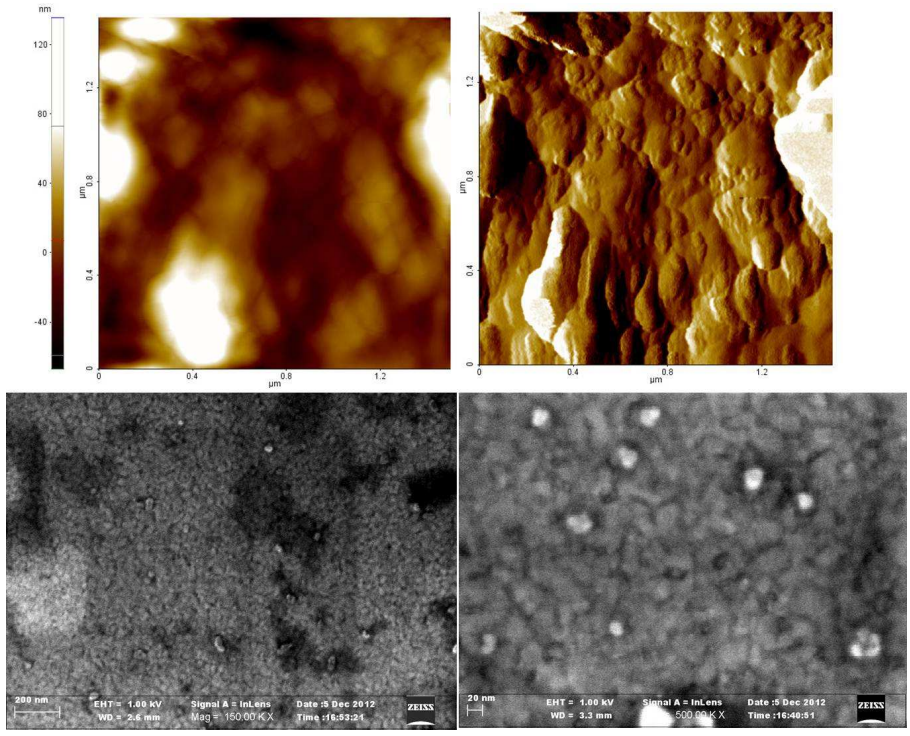

Figure 3.6: AFM image (topography and error signal images) of silver NPs. It is possible to estimate that the size of the NPs is about 20 nm. AFM measurements were carried out with a PSIA XE-100E system; SEM images of silver NPs. SEM investigations were carried out with a Cambridge Stereoscan 360 working at 20 kV of acceleration potential and 25 mm of working distance.

troduced, a significant change in the Zeta potential was found. The absolute value of the Zeta potential decreased, consistently with the reaction of the probe with the nanoprism surface. The fact that the potential was still negative was due to the phosphate groups of the probe.

Bare SiO_2 NPs showed a strongly negative Zeta potential, consistently with the reaction conditions: in fact, NPs were stabilized through the negative charges generated by the alkaline medium during their synthesis. Similar to the case of Ag nanoprisms, when the probe was coupled

to the surface of SiO_2 NPs, the potential displayed a clear decrease (in absolute value). Taking into account that the surface of SiO_2 NPs consists only partially of thiol groups, it is not surprising that also after the functionalization SiO_2 NPs still have a strong negative charge.

Once NPs were characterized, the influence of the NPs on the SPRi signal was evaluated in comparison to the same probe interaction, but without NPs.

NPs were chosen for their properties for what concerns plasmon absorption and dimension. The idea was to evaluate the influence on the SPRi signal of different aspects: size only, *i.e.* variation of refractive index for silica nanoparticles and optical properties for silver NPs.

SPRi signals for hybridizations between NPs functionalized with Probe2 and Target were recorded when silver nanoprisms or silica spheres were used (Fig. 3.7). In our experimental setup, Target was first recognized by Probe1 (Figs. 3.7a and 3.7a'), and then the intensities of the enhanced signals were recorded with the Probe2 bound to NPs. The SPR signals recorded after Probe2 hybridization for the two different NPs (Figs. 3.7b' and 3.7c') were compared both with the one from not-functionalized Probe2 interaction (Fig. 3.7a'). A signal enhancement was observed with both NPs. In Figs. 3.7b and 3.7c, differential images clearly evidence a very specific recognition, *i.e.* no interaction occurred with control surfaces (blank: B spot; not specific probe, *i.e.* negative control: U spot). Silver nanoprisms-Probe2 gave a higher SPRi signal with respect to silica spheres-Probe2. This is evidenced both from the image visual analysis and from the reflectivity variation signals as reported in Fig. 3.7b' and Fig. 3.7c'.

In SPR transduction, the intensity of signal directly depends on how much the surface modifications shift the plasmon resonance conditions. In our instrumental setup, *i.e.* working at fixed angle and fixed source wavelength for a fixed gold thickness, resonance conditions depends on

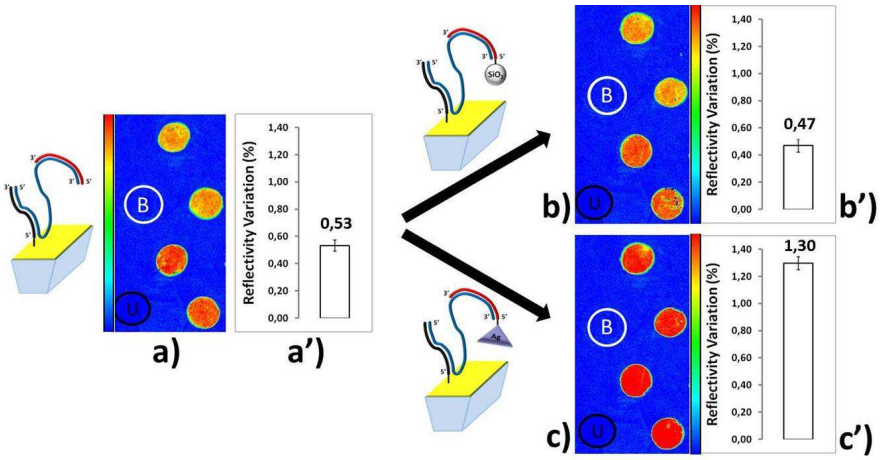

Figure 3.7: SPRi results when the sandwich structure is built on biosensor surface. Differential image (a) and SPRi signal (a') for Probe1-Target interaction (Target concentration: 250 nM). Differential images (b,c) and SPRi signals (b',c') from Target-Probe2 interaction respectively when silica nanospheres or silver nanoprisms are used. B spot, circled in white, are surface area taken as control (no probe immobilized). U spots are surface area where a not-complementary DNA probe (ProbeU) is immobilized.

the variation of the refractive index of the medium in contact with the gold surface. Referring to our case of study, both NPs generated a significant variation of the refractive index at the gold interface, however the signal intensities obtained for silica and silver NPs was very different. It could be supposed for silver nanoprisms an effect, not occurring with silica NPs, which led to a greater shift of resonance condition: plasmon coupling. This is supported by the fact that silver nanoprisms evidenced a peak of absorption in the same range of the source wavelength, thus it is possible to suppose that somehow plasmon of gold surface interacted with silver, exciting its plasmons. The resonance between gold and silver plasmons could generate a big variation of intensity of reflected light and hence a bigger SPRi signal enhancement effect.

Conclusions

Despite many applications of NPs on SPR platform for signal enhancement are being developed, there is still a lack in guidelines about the rational choice of suitable NPs characteristics. As demonstrated in this work, the influence of the kind of NPs on this application is of impact. Selecting the NPs to use on the basis of their characteristics, in terms of material and plasmon absorption, could carry to the exploitation of the enhancement possibility. In our asset we had an increase in SPR signal higher than 200 percent with silver nanoparticles and no enhancement with bigger silica nanospheres, meaning that NPs choice can dramatically have a repercussion on the sensibility of the system. In this work, using silver nanoparticles the detection limit moved down to 500 pM of Target (84-mer), ten-fold lower compared to detection without NPs. At this concentration of Target, the direct detection is not possible in our asset. Only with silver NPs we were able to specifically detect the analyte.

M. L. Ermini *et al.*, "DNA Functionalized Nanoparticles for Surface Plasmon Resonance Signal Improvement". In preparation for *Adv. Funct. Mater.*

4

Conclusions

A strategy for SNPs detection was developed starting from the rational design of the probes to be used as receptor, coming to the application of the optimized strategy on treated blood samples. These promising results can be seen as the starting point for future work oriented toward the direct detection of SNPs in real samples. In principle, using four different discriminating probes, each bearing a different base in the polymorphic site, the genotype of the sample can be determined. It is possible to foresee the simultaneous analysis of several SNPs in the same genomic sample: different probes specific for a number of genes could be immobilized on the sensor in order to screen different SNPs. The heterozygosis degree at the polymorphic site could be evaluated by the system, making use of sequential analysis with suitable discriminating probes.

Furthermore, the system is regenerable after each interaction (up to 20 times), which is not so commonly found in biosensor applied to complex samples, but it represent a key feature for application in clinical diagnostics.

The studies performed with nanoparticles, suggested that a focused selection of nanoparticles can have great impact on SPRi biosensor perfor-

mances. The improvement can be reached when suitable nanoparticles and condition are found. From the results obtained, it could be interesting to couple the enhancement effects gained from the two approaches, studying the possibility to have the addition of the two effects.

Finally, it could be certainly attractive to couple the sandwich for SNPs detection to the sandwich enhancement with NPs: it could be possible to further explore enhanced detection limits on other real samples/different matrices coupling improved sensitivity to analysis of clinically relevant samples. This work is certainly a step forward regarding the design and the development of biosensors in clinical diagnostic. Important results have been achieved and many aspects may be of interest for future works in biosensors field.

5

Appendix

Biochip Regeneration Procedure

After about 20 cycles of measurements, each interacting surface resulted affected by the constant flux, the regeneration steps with acids and biointeractions. The experimental stress on the surface caused a detachment of probes carrying to reduced performances with complementary sequences and hence SPRi signal resulted to be lower than expected. Thiol layer and gold surface were ruined during time improving the possibility to obtain unspecific interaction. For these reasons the biochip, after its life, needs a regeneration procedure in order to be useful for a new life. The displacement of the immobilized thiols is necessary, with the destruction of biological material on the surface.

The surface was subjected to a treatment with plasma, in order to regenerate gold surface, removing thiols and biomolecules. Plasma treatment was carried out by means of a Harrick PDC-32G plasma cleaner operating at High level during 15 minutes with a Air-generated plasma.

For assessing the success of the procedure, plasma-treated surface and non-treated surface was studied by AFM and compared (Fig. 5.1).

From AFM images it is possible to appreciate a variation of the rough-

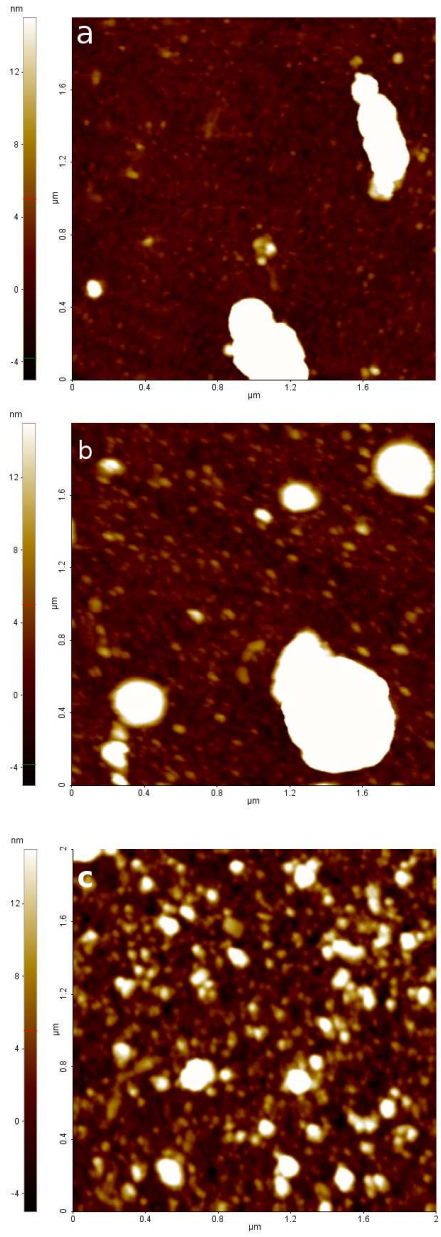

Figure 5.1: AFM images of bare gold (panel a), gold functionalized with DNA probes (panel b) and plasma treated gold surface (panel c).

ness of the surface among bare gold (Fig. 5.1a), the gold functionalized with DNA probes (Fig. 5.1b) and plasma treated gold surface (Fig.

5.1c). Roughness of the bare gold estimated with the microscopy expressed by the profile roughness parameter (Rq) was 1.2 nm. From DNA functionalized surface (Fig. 5.1b) the presence of a monolayer of thiolated DNA was evidence only by a variation in roughness (Rq = 1.9 nm), because the layer is too small to result visible from AFM images.

The plasma-treated surface showed a profile roughness parameter Rq = 4.3 nm. From the image (Fig. 5.1c) it can be noticed a rearrangement of the surface gold structure with the formation of crystals. This phenomenon seemed to be comparable to what happens when a metal film is subjected to thermal treatment. It is possible to suppose that the procedure not only removed the molecules on the surface but was also cause of a change on the surface structure of gold. Thus, the roughness becomes higher respect to other two surface studied because of the formation of these gold structures.

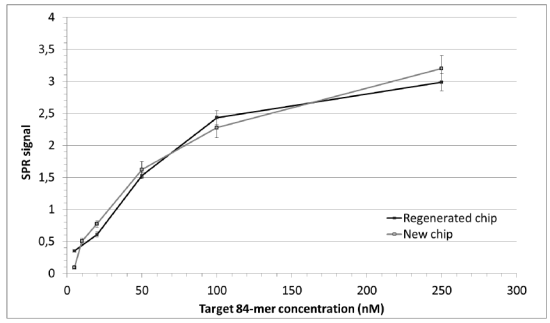

Figure 5.2: SPRi signals from Probe1 hybridizations with different concentration of 84-mer Target (see Section 3.2.2, Table 3.1). Calibrations are compared between a new chip and a regenerated chip, *i.e.* plasma-treated.

Furthermore, for testing the treated surface, it was functionalized with DNA probe (Probe1) and its hybridization with 84-mer Target (for sequence, see Section 3.2.2, Table 3.1) was followed. The SPRi signals from the renewed surface were compared with the signals from the same interaction using a new biochip (SPRi measurements were performed as reported in my previous work[74]). The SPRi measurements on this

chip are reported in Fig. 5.2.

Comparing signals from the same interaction but from new and renewed chips it is possible to verify that there are not evident different between them.

Thus it is possible to conclude that the procedure performed with plasma cleaner is suitable for giving a new life to a chip, since the optimal performances were re-established.

Bibliography

[1] B. Liedberg, C. Nylander and I. Lunström, "Surface plasmon resonance for gas detection and biosensing". *Sens. Actuators*, **4**, 299-304 (1983).

[2] I. Pockrand, J. D. Swalen, J. G. Gordon II and M. R. Philpott, "Surface plasmon spectroscopy of organic monolayer assemblies". *Surf. Sci.*, **74**, 237-244 (1978).

[3] S. Scarano, M. Mascini, A. P. F. Turner and M. Minunni, "Surface plasmon resonance imaging for affinity-based biosensors". *Biosens. Bioelectron.*, **25**, 957-966 (2010).

[4] J. Borch and P. Roepstorff, "Screening for enzyme inhibitors by surface plasmon resonance combined with mass spectrometry". *Anal. Chem.*, **76**, 5243-5248 (2004).

[5] J. Homola, "Surface Plasmon Resonance Based Sensors" in Springer Series on Chemical Sensors and Biosensors, Vol.4, 2006. Volume editor: J. Homola.

[6] G. Spoto and M. Minunni, "Surface plasmon resonance imaging: what next?". *J. Phys. Chem. Lett.*, **3**, 2682-2691 (2012).

[7] M. L. Ermini, S. Scarano, R. Bini, M. Banchelli, D. Berti, M. Mascini and M. Minunni, "A rational approach in probe design for nucleic acid-based biosensing". *Biosens. Bioelectron.*, **26**, 4785-4790 (2011).

[8] B. N. Chorley, X. Wang, M. R. Campbell, G. S. Pittman, M. A. Noureddine and D. A. Bell, "Discovery and verification of functional single nucleotide polymorphisms in regulatory genomic regions: current and developing technologies". *Mutat. Res., Rev. Mutat. Res.*, **659**, 147-157 (2008).

[9] J. Robert, V. Le Morvan, D. Smith, P. Pourquier and J. Bonnet, "Predicting drug response and toxicity based on gene polymorphisms". *Crit. Rev. Oncol. Hematol.*, **54**, 171-196 (2005).

[10] B. Rahim-Williams, J. L. Riley III, A. K. K. Williams and R. B. Fillingim, "A quantitative review of ethnic group differences in experimental pain response: do biology, psychology, and culture matter?". *Pain Med.*, **13**, 522-540 (2012).

[11] O. I. Stenina, T. V. Byzova, J. C. Adams, J. J. McCarthy, E. J. Topol and E. F. Plow, "Coronary artery disease and the thrombospondin single nucleotide polymorphisms". *Int. J. Biochem. Cell Biol.*, **36**, 1013-1030 (2004).

[12] F. Lucarelli, S. Tombelli, M. Minunni, G. Marrazza and M. Mascini, "Electrochemical and piezoelectric DNA biosensors for hybridisation detection". *Anal. Chim. Acta*, **609**, 139-159 (2008).

[13] K. Kerman, M. Saito and E. Tamiya, "Electroactive chitosan nanoparticles for the detection of single-nucleotide polymorphisms using peptide nucleic acids". *Anal. Bioanal. Chem.*, **391**, 2759-2767 (2008).

[14] S. O. Kelley, E. M. Boon, J. K. Barton, N. M. Jackson and M. G. Hill, "Single-base mismatch detection based on charge transduction through DNA". *Nucleic Acids Res.*, **27**, 4830-4837 (1999).

[15] M. Nakayama, T. Ihara, K. Nakano and M. Maeda, "DNA sensors using a ferrocene-oligonucleotide conjugate". *Talanta*, **56**, 857-866 (2002).

[16] Q. Xu, K. Chang, W. Lu, W. Chen, Y. Ding, S. Jia, K. Zhang, F. Li, J. Shi, L. Cao, S. Deng and M. Chen, "Detection of single-nucleotide polymorphisms with novel leaky surface acoustic wave biosensors, DNA ligation and enzymatic signal amplification". *Biosens. Bioelectron.*, **33**, 274-278 (2012).

[17] Y. Akagi, M. Makimura, Y. Yokoyama, M. Fukazawa, S. Fujiki, M. Kadosaki and K. Tanino, "Development of a ligation-based impedimetric DNA sensor for single-nucleotide polymorphism associated with metabolic syndrome". *Electrochim. Acta*, **51**, 6367-6372 (2006).

[18] B. Moody and G. McCarty, "Statistically significant Raman detection of midsequence single nucleotide polymorphisms". *Anal. Chem.*, **81**, 2013-2016 (2009).

[19] H. Šípovà, T. Špringer and J. Homola, "Streptavidin-enhanced assay for sensitive and specific detection of single nucleotide polymorphism in TP53". *Anal. Bioanal. Chem.*, **399**, 2343-2350 (2011).

[20] P. K. Wilson, T. Jiang, M. E. Minunni, A. P. F. Turner and M. Mascini, "A novel optical biosensor format for the detection of clinically relevant TP53 mutations". *Biosens. Bioelectron.*, **20**, 2310-2313 (2005).

[21] L. J. Blackwell, K. P. Bjornson, D. J. Allen and P. Modrich, "Distinct MutS DNA-binding modes that are differentially modulated

by ATP binding and hydrolysis". *J. Biol. Chem.*, **276**, 34339-34347 (2001).

[22] S. Nakano, T. Kanzaki, M. Nakano, D. Miyoshi and N. Sugimoto, "Measurements of the binding of a large protein using a substrate density-controlled DNA chip". *Anal. Chem.*, **83**, 6368-6372 (2011).

[23] I. Babic, S. E. Andrew and F. R. Jirik, "MutS interaction with mismatch and alkylated base containing DNA molecules detected by optical biosensor". *Mutat. Res., Fundam. Mol. Mech. Mutagen.*, **372**, 87-96 (1996).

[24] M. Gotoh, M. Hasebe, T. Ohira, Y. Hasegawa, Y. Shinohara, H. Sota, J. Nakao and M. Tosu, "Rapid method for detection of point mutations using mismatch binding protein (MutS) and an optical biosensor". *Genet. Anal.: Biomol. Eng.*, **14**, 47-50 (1997).

[25] X. Su, Y.-J. Wu, R. Robelek and W. Knoll, "Surface plasmon resonance spectroscopy and quartz crystal microbalance study of MutS binding with single thymine-guanine mismatched DNA". *Front. Biosci.*, **10**, 268-274 (2005).

[26] R. S. Lahue, K. G. Au and P. Modrich, "DNA mismatch correction in a defined system". *Science*, **245**, 160-164 (1989).

[27] K. G. Au, K. Welsh and P. Modrich, "Initiation of methyl-directed mismatch repair". *J. Biol. Chem.*, **267**, 12142-12148 (1992).

[28] S. S. Su, R. S. Lahue, K. G. Au and P. Modrich, "Mispair specificity of methyl-directed DNA mismatch correction in vitro". *J. Biol. Chem.*, **263**, 6829-6835 (1988).

[29] M. Grilley, K. M. Welsh, S. S. Su and P. Modrich, "Isolation and characterization of the Escherichia coli mutL gene product". *J. Biol. Chem.*, **264**, 1000-1004 (1989).

[30] Y. Li, A. W. Wark, H. J. Lee and R. M. Corn, "Single-nucleotide polymorphism genotyping by nanoparticle-enhanced surface plasmon resonance imaging measurements of surface ligation reactions". *Anal. Chem.*, **78**, 3158-3164 (2006).

[31] Y. Sato, K. Sato, K. Hosokawa and M. Maeda, "Surface plasmon resonance imaging on a microchip for detection of DNA-modified gold nanoparticles deposited onto the surface in a non-cross-linking configuration". *Anal. Biochem.*, **355**, 125-131 (2006).

[32] R. D'Agata, R. Corradini, G. Grasso, R. Marchelli and G. Spoto, "Ultrasensitive detection of DNA by PNA and nanoparticle-enhanced surface plasmon resonance imaging". *ChemBioChem*, **9**, 2067-2070 (2008).

[33] R. D'Agata, G. Breveglieri, L. M. Zanoli, M. Borgatti, G. Spoto and R. Gambari, "Direct detection of point mutations in nonamplified human genomic DNA". *Anal. Chem.*, **83**, 8711-8717 (2011).

[34] P. E. Nielsen, M. Egholm, R. H. Berg and O. Buchardt, "Sequence-selective recognition of DNA by strand displacement with a thymine-substituted polyamide". *Science*, **254**, 1497-1500 (1991).

[35] G. Feriotto, R. Corradini, S. Sforza, N. Bianchi, C. Mischiati, R. Marchelli and R. Gambari, "Peptide nucleic acids and biosensor technology for real-time detection of the cystic fibrosis W1282X mutation by surface plasmon resonance". *Lab. Invest.*, **81**, 1415-1427 (2001).

[36] A. I. K. Lao, X. Su and K. M. M. Aung, "SPR study of DNA hybridization with DNA and PNA probes under stringent conditions". *Biosens. Bioelectron.*, **24**, 1717-1722 (2009).

[37] R. Corradini, G. Feriotto, S. Sforza, R. Marchelli and R. Gambari, "Enhanced recognition of cystic fibrosis W1282X DNA point mu-

tation by chiral peptide nucleic acid probes by a surface plasmon resonance biosensor". *J. Mol. Recognit.*, **17**, 76-84 (2004).

[38] R. D'Agata, G. Breveglieri, L. Zanoli, M. Borgatti, G. Spoto and R. Gambari, "Surface plasmon resonance imaging (SPR-I), peptide nucleic acid (PNA) probes and nanoparticle-enhancement for PCR-free ultrasensitive detection of beta-thalassemia mutations in human genomic DNA". *Int. J. Mol. Med.*, **26**, S61 (2010).

[39] C. Ananthanawat, T. Vilaivan, V. P. Hoven and X. Su, "Comparison of DNA, aminoethylglycyl PNA and pyrrolidinyl PNA as probes for detection of DNA hybridization using surface plasmon resonance technique". *Biosens. Bioelectron.*, **25**, 1064-1069 (2010).

[40] K. Nakatani, S. Sando and I. Saito, "Scanning of guanine-guanine mismatches in DNA by synthetic ligands using surface plasmon resonance". *Nat. Biotechnol.*, **19**, 51-55 (2001).

[41] A. Kobori and K. Nakatani, "Dimer of 2,7-diamino-1,8-naphthyridine for the detection of mismatches formed by pyrimidine nucleotide bases". *Bioorg. Med. Chem.*, **16**, 10338-10344 (2008).

[42] E. Milkani, S. Morais, C. R. Lambert and W. G. McGimpsey, "Detection of oligonucleotide systematic mismatches with a surface plasmon resonance sensor". *Biosens. Bioelectron.*, **25**, 1217-1220 (2010).

[43] F. Song, F. Zhou, J. Wang, N. Tao, J. Lin, R. L. Vellanoweth, Y. Morquecho and J. Wheeler-Laidman, "Detection of oligonucleotide hybridization at femtomolar level and sequence-specific gene analysis of the Arabidopsis thaliana leaf extract with an ultrasensitive surface plasmon resonance spectrometer". *Nucleic Acids Res.*, **30**, e72 (2002).

[44] S. S. Agasti, S. Rana, M.-H. Park, C. K. Kim, C.-C. You and V. M. Rotello, "Nanoparticles for detection and diagnosis". *Adv. Drug Delivery Rev.*, **62**, 316-328 (2010).

[45] G. Doria, J. Conde, B. Veigas, L. Giestas, C. Almeida, M. Assunção, J. Rosa and P. V. Baptista, "Noble metal nanoparticles for biosensing applications". *Sensors*, **12**, 1657-1687 (2012).

[46] X.-J. Chen, B. L. Sanchez-Gaytan, Z. Qian and S.-J. Park, "Noble metal nanoparticles in DNA detection and delivery". *Wiley Interdiscip. Rev.: Nanomed. Nanobiotechnol.*, **4**, 273-290 (2012).

[47] L. M. Zanoli, R. D'Agata and G. Spoto, "Functionalized gold nanoparticles for ultrasensitive DNA detection". *Anal. Bioanal. Chem.*, **402**, 1759-1771 (2012).

[48] J. Cheon and J.-H. Lee, "Synergistically integrated nanoparticles as multimodal probes for nanobiotechnology". *Accounts Chem. Res.*, **41**, 1630-1640 (2008).

[49] X.-M. Qian and S. M. Nie, "Single-molecule and single-nanoparticle SERS: from fundamental mechanisms to biomedical applications". *Chem. Soc. Rev.*, **37**, 912-920 (2008).

[50] G. Liu and Y. Lin, "Nanomaterial labels in electrochemical immunosensors and immunoassays". *Talanta*, **74**, 308-317 (2007).

[51] J. A. Dieringer, A. D. McFarland, N. C. Shah, D. A. Stuart, A. V. Whitney, C. R. Yonzon, M. A. Young, X. Zhang and R. P. Van Duyne, "Surface enhanced Raman spectroscopy: new materials, concepts, characterization tools, and applications". *Faraday Discuss.*, **132**, 9-26 (2006).

[52] S. Petralia, T. Barbuzzi and G. Ventimiglia, "Polymerase chain reaction efficiency improved by water soluble β-cyclodextrins capped platinum nanoparticles". *Mater. Sci. Eng., C*, **32**, 848-850 (2012).

[53] L.-P. Sun, S. Wang, Z.-W. Zhang, Y.-Y. Ma, Y.-Q. Lai, J. Weng and Q.-Q. Zhang, "Interaction of gold nanoparticles with *Pfu* DNA polymerase and effect on polymerase chain reaction". *IET Nanobiotechnol.*, **5**, 20-24 (2011).

[54] L. He, M. D. Musick, S. R. Nicewarner, F. G. Salinas, S. J. Benkovic, M. J. Natan and C. D. Keating, "Colloidal Au-enhanced surface plasmon resonance for ultrasensitive detection of DNA hybridization". *J. Am. Chem. Soc.*, **122**, 9071-9077 (2000).

[55] A. N. Shipway and I. Willner, "Nanoparticles as structural and functional units in surface-confined architectures". *Chem. Commun.*, , 2035-2045 (2001).

[56] I. Willner, B. Basnar and B. Willner, "Nanoparticle-enzyme hybrid systems for nanobiotechnology". *FEBS J.*, **274**, 302-309 (2007).

[57] I. Willner, R. Baron and B. Willner, "Integrated nanoparticle-biomolecule systems for biosensing and bioelectronics". *Biosens. Bioelectron.*, **22**, 1841-1852 (2007).

[58] O. I. Wilner and I. Willner, "Functionalized DNA nanostructures". *Chem. Rev.*, **112**, 2528-2556 (2012).

[59] M. C. Daniel and D. Astruc, "Gold nanoparticles: Assembly, supramolecular chemistry, quantum-size-related properties, and applications toward biology, catalysis, and nanotechnology". *Chem. Rev.*, **104**, 293-346 (2004).

[60] C. Burda, X. B. Chen, R. Narayanan and M. A. El-Sayed, "Chemistry and properties of nanocrystals of different shapes". *Chem. Rev.*, **105**, 1025-1102 (2005).

[61] N. L. Rosi and C. A. Mirkin, "Nanostructures in biodiagnostics". *Chem. Rev.*, **105**, 1547-1562 (2005).

[62] E. E. Bedford, J. Spadavecchia, C.-M. Pradier and F. X. Gu, "Surface plasmon resonance biosensors incorporating gold nanoparticles". *Macromol. Biosci.*, **12**, 724-739 (2012).

[63] M. L. Ermini, S. Mariani, S. Scarano and M. Minunni, "Direct detection of genomic DNA by surface plasmon resonance imaging: an optimized approach". *Biosens. Bioelectron.*, **40**, 193-199 (2013).

[64] Y. Chen and W. Cheng, "DNA-based plasmonic nanoarchitectures: from structural design to emerging applications". *Wiley Interdiscip. Rev.: Nanomed. Nanobiotechnol.*, **4**, 587-604 (2012).

[65] G. A. Sotiriou, "Biomedical applications of multifunctional plasmonic nanoparticles". *Wiley Interdiscip. Rev.: Nanomed. Nanobiotechnol.*, DOI:10.1002/wnan.1190 (2012).

[66] J.-H. Lee, J.-H. Hwang and J.-M. Nam, "DNA-tailored plasmonic nanoparticles for biosensing applications". *Wiley Interdiscip. Rev.: Nanomed. Nanobiotechnol.*, DOI:10.1002/wnan.1196 (2012).

[67] X. Guo, "Surface plasmon resonance based biosensor technique: a review". *J. Biophotonics*, **5**, 483-501 (2012).

[68] T. K. Sau, A. L. Rogach, F. Jäckel, T. A. Klar and J. Feldmann, "Properties and applications of colloidal nonspherical noble metal nanoparticles". *Adv. Mater.*, **22**, 1805-1825 (2010).

[69] S. Gao, N. Koshizaki, H. Tokuhisa, E. Koyama, T. Sasaki, J.-K. Kim, J. Ryu, D.-S. Kim and Y. Shimizu, "Highly stable Au nanoparticles with tunable spacing and their potential application in surface plasmon resonance biosensors". *Adv. Funct. Mater.*, **20**, 78-86 (2010).

[70] N. J. Wittenberg and C. L. Haynes, "Using nanoparticles to push the limits of detection". *Wiley Interdiscip. Rev.: Nanomed. Nanobiotechnol.*, **1**, 237-254 (2009).

[71] L. A. Lyon, M. D. Musick and M. J. Natan, "Colloidal Au-enhanced surface plasmon resonance immunosensing". *Anal. Chem.*, **70**, 5177-5183 (1998).

[72] D. Aherne, D. M. Ledwith, M. Gara and J. M. Kelly, "Optical properties and growth aspects of silver nanoprisms produced by a highly reproducible and rapid synthesis at room temperature". *Adv. Funct. Mater.*, **18**, 2005-2016 (2008).

[73] M. Nakamura and K. Ishimura, "One-pot synthesis and characterization of three kinds of thiol−organosilica nanoparticles". *Langmuir*, **24**, 5099-5108 (2008).

[74] M. L. Ermini, S. Mariani, S. Scarano, D. Campa, R. Barale and M. Minunni, "Single nucleotide polymorphism detection by optical DNA-based sensing coupled with whole genomic amplification". *Anal. Bioanal. Chem.*, DOI:10.1007/s00216-012-6345-4 (2012).

Alla fine, sento che non è facile, nè guardarsi indietro nè andare avanti senza sentirsi pesanti. Cercherò di non essere troppo sentimentale, ma non ci riuscirò, lo so.

Innanzitutto vorrei tanto ringraziare la Prof. Maria Minunni, che durante il mio percorso non è stata solo la mia tutrice scientifica ma anche di più. Un vulcano di idee e proposte sempre in attività! Mi ha dato la possibilità di imparare indirizzandomi verso nuove esperienze e responsabilità, permettendomi di crescere anche grazie al suo esempio, ai racconti di vita. La ringrazio per avermi dato la possibilità di capire quanto possa valere il potersi dedicare alla propria ricerca senza troppi limiti.

Un grazie grosso grosso va a Simona, per essere stata sempre pronta a essere punto di confronto scientifico e non, per aver condiviso paranoie, fasi difficili, buone notizie, momenti di gioia e, non meno importante, la sua scrivania. Grazie anche per l'appoggio morale, per i nostri trip musicali (del genere: "ti dà fastidio se lascio in loop questa canzone anche per la prossima mezz'ora?"), per i coinvolgenti e improvvisi raptus di "mettotuttoaposto" e per le sessioni completamente irrazionali di design.

Vorrei ringraziare il Prof. Baglioni, la Dott.ssa Debora Berti, il Dott. Massimo Bonini e Francesca Bellissima per avermi dato la possibilità di lavorare con loro e per la disponibilità nella collaborazione. In particolare un grosso grazie a Francesca per le varie sintesi e un grazie ancora più grosso lo devo a Massimo, per tutto il tempo speso tra AFM, SEM e nanoparticelle, per la pazienza, le mille spiegazioni, le chiacchierate, i buoni consigli e le risate.

Mille e più grazie a Stefano, detto anche, tra gli altri soprannomi, S. Mariani vista la sua infinita pazienza nell'ascoltare le mie noie, paranoie e lamentele. Lavorarci insieme è stato, oltre che produttivo, bello e pure divertente. Grazie per i caffè mattutini, i consigli sulla dieta a pranzo, per il "cooooriii" e per i "tranquilla", per la schiettezza e soprattutto per essere davvero un ottimo amico.

Ringrazio babbo Marcello e mamma Fernanda, Mirko e Lorenza che,

nonostante tutto e nonostante magari non sempre io sia stata molto comprensibile ai loro occhi, mi sono stati vicini e sempre pronti a darmi una mano e tanto affetto. Un particolare ringraziamento a Riccardo perché è tanto carino e quando siamo insieme mi catapulta in un mondo meraviglioso.

Un grosso grosso enorme grazie ai miei amici valdarnesi DOC, Gaia e Stefano perché mi hanno aiutato tanto, perché anche se non siamo sempre molto vicini fisicamente in realtà lo siamo lo stesso. Grazie per il supporto pratico, morale e affettivo, grazie a Gaia che mi dice sempre di sì (ormai da più di vent'anni direi) e a Stefano, spesso compagno di paranoie.

Grazie a tutta la combriccola dei "vecchi chimici", con annessi e annesse, nessuno escluso. In particolare ringrazio Samuele, per avermi convinto a fare il dottorato e anche ovviamente per tutto il resto, Francesco, Irene, Nicola e Daniele per esserci stati, per l'appoggio, l'affetto, per aver capito e non aver giudicato e perché mi fanno capire che posso contare su di loro. Grazie a Francesco per le attenzioni, i caffè, gli sfoghi e per tutto. Grazie all'Ire per i rimpalli di paranoie, l'aiuto a riprendere il filo, l'ascolto durante gli sfoghi. Grazie a Nicola per i pianti, le cene, il vino e le risate. Grazie a Daniele per i gelidi racconti, l'affetto, l'ascolto, le bischerate e le batuttacce da toscanaccio. Grazie a Tommaso per quando c'è stato. Grazie al Comandella per la quantità di "sciocchezze" dette, il supporto, la sincerità, i film e per Mr. Wiggles. Grazie a Antonio e a Lorenza per l'affetto, le premure e l'ospitalità. Grazie a Antonio e Paolo per le infinite chiacchierate e per DT. Grazie a Paolo per l'aiuto nell'impaginazione (troppo pignolo...). Grazie al Colonnello Puzzettone, B.B., Captain Hego e tutti i loro simpatici compari che sono stati buoni con me: per avermi aiutato, tra le altre cose, a sdrammatizzare, per le infinite e interminabili boiate, per essersi messi da parte quando si vedeva che avevo più bisogno, per avermi sopportato con pazienza e per essere meravigliosi come sono (piacere di conoscerla...).

Grazie a chi c'è stato, a chi c'è e, perchè no, a chi ci sarà.